

PDF hosted at the Radboud Repository of the Radboud University Nijmegen

The following full text is a publisher's version.

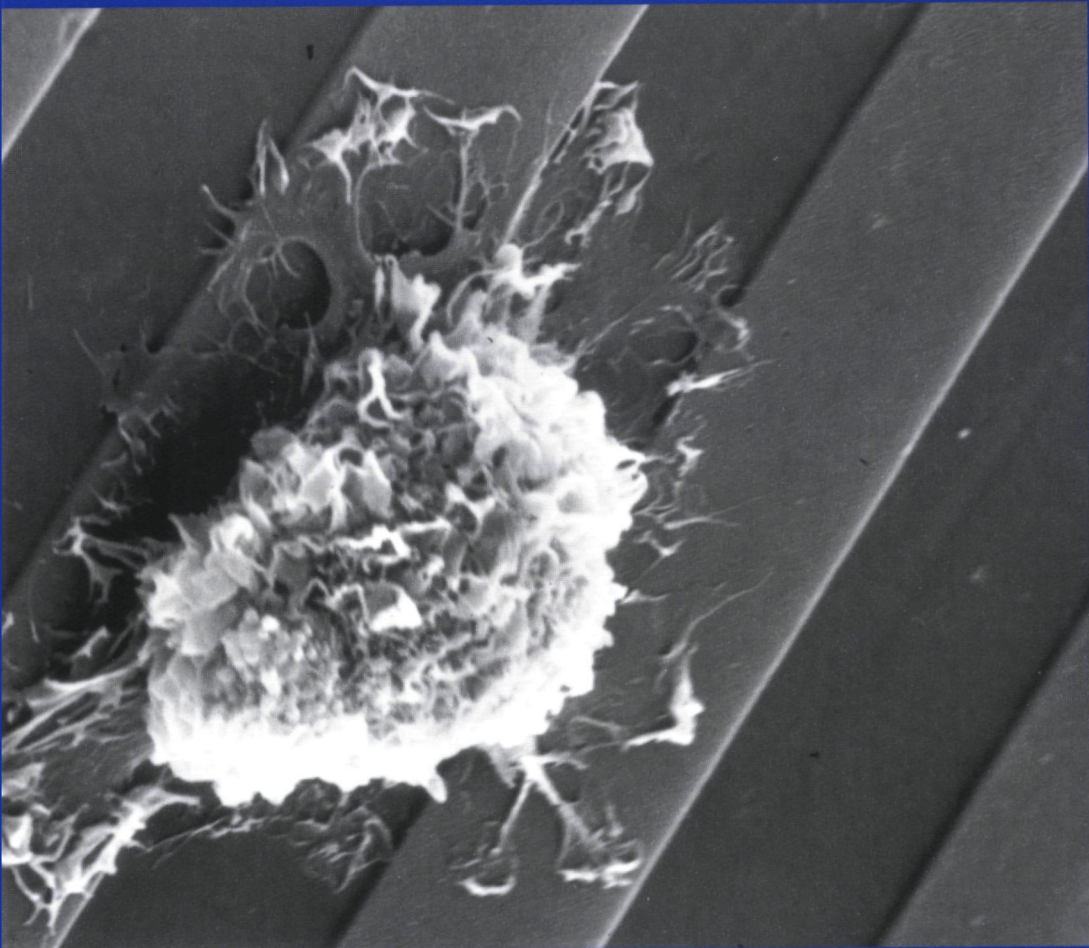
For additional information about this publication click this link.

<http://hdl.handle.net/2066/146812>

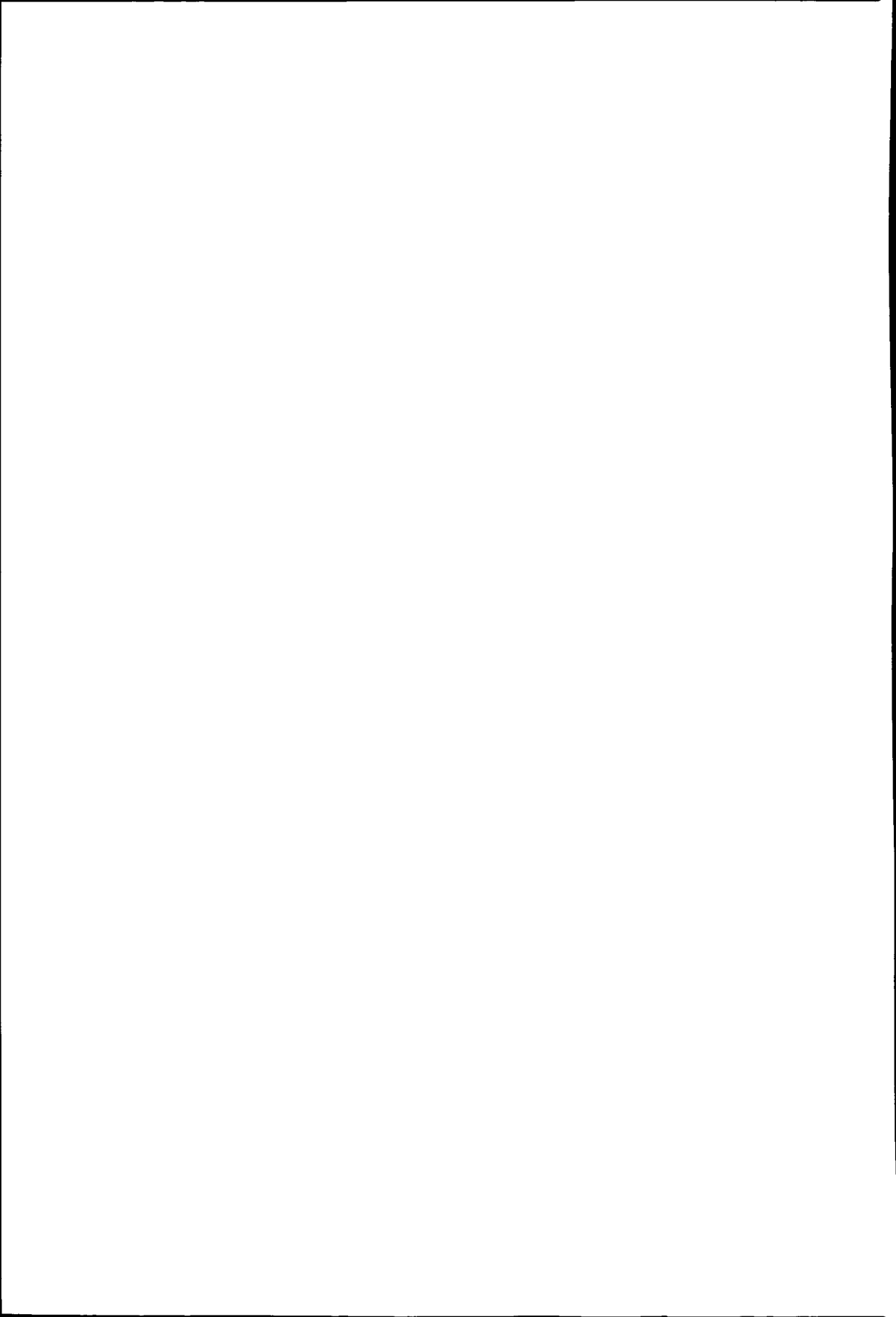
Please be advised that this information was generated on 2021-11-03 and may be subject to change.

Engineered Implant Surfaces

Modification of Cell and Tissue Response by Microgrooves



Frank Walboomers



**Engineered implant surfaces:
Modification of cell and tissue response by microgrooves**

Paranymfen. R W Wassenaar
R.J.T van der Steen

Engineered implant surfaces Modification of cell and tissue response by microgrooves / Xaverus
Franciscus Walboomers

Thesis Katholieke Universiteit Nijmegen - With ref - With summary in Dutch

ISBN 90-9013298-8

Subject headings biomaterials/ implants/ tissue engineering/ microtextures/ biologic response/
surface modifications

Engineered implant surfaces: Modification of cell and tissue response by microgrooves

Een wetenschappelijke proeve op het gebied van de Medische Wetenschappen

PROEFSCHRIFT

ter verkrijging van de graad van doctor
aan de Katholieke Universiteit Nijmegen
volgens besluit van het College van Decanen
in het openbaar te verdedigen op
donderdag 24 februari 2000
des namiddags om 3 30 uur precies

door

Xaverus Franciscus Walboomers

geboren op 15 juni 1971 te Apeldoorn

Promotoren: Prof. dr. J.A. Jansen
Prof. dr. L.A. Ginsel

Manuscriptcommissie: Prof. dr. P. Stoelinga
Prof. dr. H.H. Renggli
Prof. dr. W. Beertsen (ACTA Amsterdam)

This project was supported by the Netherlands Organization for Scientific Research (NWO), grant no. 902-35-120.

The publication of this thesis was supported financially by:

- Ortomed BV
- Nederlandse Organisatie voor Wetenschappelijk Onderzoek (NWO)
- Nederlandse Vereniging voor Biomaterialen (NVB)
- Stichting Electronenmicroscopie Nederland (SEN)

voor mijn ouders

Publications related to this thesis:

- 1) Growth behaviour of fibroblasts on microgrooved polystyrene- Walboomers, X.F., Croes, H.J.E., Ginsel, L.A., and Jansen, J.A., *Biomaterials* **19**, 1861-1868 (1998).
- 2) Microgrooved subcutaneous implants in the goat- Walboomers, X.F., Croes, H.J.E., Ginsel, L.A., and Jansen, J.A. *J Biomed Mater Res* **42**, 634-641 (1998).
- 3) Soft tissue and epithelial models- Jansen, J.A., den Braber, E.T., Walboomers, X.F., and de Ruijter, J.E. *Adv Dent Res* **13**, 57-66 (1999).
- 4) Attachment of fibroblasts on smooth and microgrooved polystyrene- Walboomers, X.F., Monaghan, W., Curtis, A.S.G., and Jansen, J.A. *J Biomed Mater Res* **46**, 212-220 (1999).
- 5) Contact guidance of rat fibroblasts on various implant materials- Walboomers, X.F., Croes, H.J.E., Ginsel, L.A., and Jansen, J.A. *J Biomed Mater Res*, **47**, 204-212 (1999).
- 6) The effect of poly-l-lactic acid with parallel surface micro groove on osteoblast-like cells *in vitro*- Matsuzaka, K., Walboomers, X.F., de Ruijter, J.E., and Jansen, J.A. *Biomaterials* **20**, 1293-1301 (1999).
- 7) Effect of microgrooved poly-l-lactic (PLA) surfaces on proliferation, cytoskeletal organization, and mineralized matrix formation of rat bone marrow cells- Matsuzaka, K., Walboomers, X.F., de Ruijter, J.E., and Jansen, J.A. *Clin Oral Impl Res*, in press (1999).
- 8) Early spreading events of fibroblasts on microgrooved substrates- Walboomers, X.F., and Jansen, J.A., *J Biomed Mater Res*, in press (1999).
- 9) Microgrooved silicone subcutaneous implants in guinea pigs- Walboomers, X.F., and Jansen, J.A., *Biomaterials*, in press (1999).
- 10) Influence of transforming growth factor β 3 on fibrous capsule formation around microgrooved subcutaneous implants *in vivo*- Gehrke, T.A.E., Walboomers, X.F., Renggli, H.H., and Jansen, J.A., *Tissue Engineering*, submitted.

CONTENTS:

1	Introduction	9
1	<i>Introduction</i>	11
2	<i>Cell structure cytoskeleton and cell attachment</i>	12
2 1	<i>Microfilaments</i>	12
2 2	<i>Intermediate filaments</i>	13
2 3	<i>Microtubules</i>	14
2 4	<i>Fibroblast attachment to substrates</i>	15
2 5	<i>Cell locomotion and the formation of focal adhesions</i>	16
3	<i>Cell adhesion to microgrooved biomaterials</i>	18
3 1	<i>Microgrooved surfaces</i>	18
3 2	<i>Production of microgrooves</i>	18
3 3	<i>Cell and tissue response to microgrooved surfaces</i>	20
4	<i>Research objectives</i>	30
2	Growth behaviour of fibroblasts on microgrooved polystyrene	35
3	Attachment of fibroblasts on smooth and microgrooved polystyrene	49
4	Contact guidance of rat fibroblasts on various implant materials	69
5	Early spreading events of fibroblasts on microgrooved substrates	85
6	The effect of microgrooved poly-l-lactic acid on osteoblast-like cells <i>in vitro</i>	105
7	Microgrooved subcutaneous implants in the goat	121
8	Microgrooved silicone subcutaneous implants in guinea pigs	134
9	Summary, adress to the aims, and closing remarks	153
	Samenvatting, evaluatie van de doelstellingen, en afsluitende opmerkingen	159
	Dankwoord	164
	Curriculum Vitae	165

Introduction

1 INTRODUCTION

An implant can be broadly defined as an artificial device, inserted (semi-)permanently into the body. In the last few decades, there has been an enormous increase in both the variety and the number of implants used in medicine and dentistry. The primary reasons for this increase are the exponential growth of the population and wealth in the western world. Implants are usually placed to aid patients that, due to a congenital defect, a trauma or a pathologic cause, have some part of the body absent, damaged, diseased, or just simply worn. In such cases an implant can be used to restore the missing function, or improve its healing or operation. Additionally, a relatively small number of implants is used for cosmetic reasons. It has to be noticed that due to the growing percentage of elderly people in the population, the number of geriatric diseases will increase, and thus the number of implants used in their treatment.

With our improved understanding of medicine, chemistry, and physics, a parallel expansion in the number of implant materials and designs has occurred. A good example of this trend is the current emphasis in biomedical research on *tissue engineering*, defined as “an interdisciplinary field in which the principles of engineering and the life sciences are applied toward the regeneration of biologic substitutes aimed at the creation, preservation, or restoration of lost organ function”¹, or in other words “the application of the principles and methods of engineering and the life sciences toward the fundamental understanding of structure/function relationships in normal and pathological mammalian tissues and the development of biological substitutes to restore, maintain, or improve functions”².

However, epidemiologic research still indicates that a number of implant procedures can be regarded as “failures”, meaning that the implantation did not result in lasting clinical performance. This often leads to so-called revision surgery. Causes for implant revision can be inherent to the patient, surgical procedure, and of course compatibility of the implant itself. It is supposed that an important factor in the final tissue-reaction towards an implanted device is the (initial) reaction of cells towards the device. Therefore, many studies performed during the last two decades have focused on understanding of the interactions between different cells and tissues of the body, and implant materials. It is of the most importance that the used implant material fits in and is functional in a living organism, in other words it has to be ‘biocompatible’. For instance, when implants are placed in the soft tissues of the body, minimal capsule formation around the implant, implant migration, or implant extrusion are desired.

This thesis will focus on the possible influence of micrometer sized groove and ridge patterns, so-called ‘microgrooves’, on the biocompatibility of implant materials. First the structure and behaviour of cells will be described. After this, microgrooves and previous experiments on this subject will be regarded.

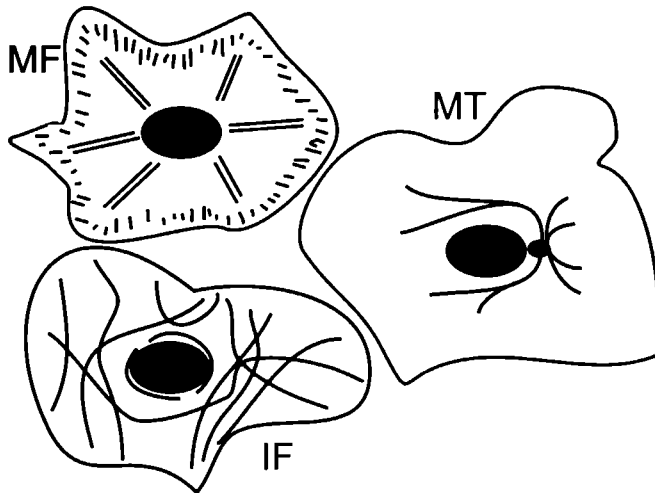


Figure 1: Schematic representation of microfilaments (MF), intermediate filaments (IF), and microtubules (MT) in a cell

2 CELL STRUCTURE: CYTOSKELETON AND CELL ATTACHMENT

All living organisms consist of cells. The shape, internal organization, and motility of these cells are determined by two structural elements. First, the cells' internal framework: the cytoskeleton. Second, the attachments of the cell to its environment. The cytoskeleton of animal cells consists merely of three groups of protein-based structures: microfilaments, intermediate filaments, and microtubules (Figure 1). Continuous breakdown and assembly of pieces of the cytoskeleton and cell attachments allow the cell to change its shape, to move, to divide, and to respond on its micro-environment. Besides this 'mechanical' responsibility, the cytoskeleton and attachments have another important function. They controls the spatial location of the cell's components, and provide a communication pathway between cellular protein complexes and organelles, like the nucleus, mitochondria or Golgi-apparatus³.

2.1 Microfilaments

The microfilaments are a group of proteins consisting of actin, myosin, and several associated proteins. Actin is the most abundant protein in many cells. In actively motile fibroblasts up to 15% of the total protein can be actin. Actin monomers are globular proteins (G-actins) with a 375 amino acids long sequence, with a molecular weight of 43 kDa. Above a critical concentration the monomers self-assemble into flexible 8 nm thick filaments. This filamentous form is called F-actin. In an actin filament the monomers are packed into a single tight helix with about two monomers each turn. This

gives the polymer the misleading appearance of a double helix twisting around each 37 nm (Figure 2) In a fibroblast usually about 50% of the actin is filamentous and 50% is free or bound to the actin-binding protein profilin, which sequesters free actin monomers in the cytoplasm, and thereby serves as a pool of stored actin The actin filaments are joined together, to form an extensive gel-like framework by cross-linking proteins, especially filamin-dimers When exposed to a short period of mechanical stress, the network will not change its formation When exposed to a long period of mechanical force, however, the cross-linkers will dissociate and re-associate, thereby irreversibly changing the shape of the network Next to the filamentous actin in the cytosol, actin filaments are also especially abundant just beneath the plasma membrane, forming an organelle-free cellular cortex This cortex prevents organelles from touching the inner cellular membrane

There are many associated proteins that influence the structure and functionality of the actin-framework The main associated protein is myosin, which is responsible for the sliding of actin-filaments Myosin molecules, when correctly aligned with the polarity of actin filaments, are able to bind to these actins Then, myosin can move along the actin strand This process is adenosine triphosphate (ATP)-dependent, the required energy is obtained by metabolism of ATP into adenosine diphosphate (ADP) When one actin-bound myosin binds to another actin-bound myosin molecule, movement of one or both myosins results in movement of the entire actin network

The other actin-associated proteins have various functions Gelsolin is capable of fragmenting filaments into smaller ones when the cellular calcium concentration is higher than 10^{-7} M Therefore, it seems to be involved in the rearrangement of the actin skeleton Tropomyosin binds actin filaments in order to strengthen them Fimbrin and α -actinin bundle filaments into fibers Minimyosin is capable of transporting various vesicles along actin-filaments Spectrin attaches the sides of filaments to the plasma membrane Finally, cap-proteins cap one side of the filament and are involved in the attachment to the plasma membrane

2.2 Intermediate filaments

The intermediate filaments were named 'intermediate' because they are larger than the actin microfilament, but smaller than the myosin microfilament, about 1 e 8-10 nm in diameter Intermediate filaments are usually divided into four types, on basis of homology in their amino acid sequence Type I are the keratins, that are present in epithelial cells Type II consists of vimentin (in cells of

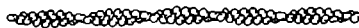


Figure 2 The arrangement of globular actin molecules in an actin filament The molecules are packed into a single tight helix This arrangement may give the appearance of two helical strands ³

mesenchymal origin, like fibroblasts and osteoblasts), desmin (in muscle cells), and glial fibrillary acidic protein (in glial cells) Type III are the neurofilament proteins, found in neurons Finally, type IV are the nuclear lamins, present around the cell nucleus The subunits of intermediate filaments are dimer-forming filamentous proteins from 40-130 kDa Dimers line up side by side to form so-called protofilaments, which associate in a staggered manner to form filaments

As mentioned above, fibroblasts contain nuclear lamins, that line the inner membrane of the nucleus Further, fibroblasts possess vimentin-filaments, a 52 kDa large protein It has to be noted that this type of filament is also regularly seen in other cultured cells, due to the dedifferentiation *in vitro* of differentiated cell-types towards a fibroblast-like phenotype Staining of vimentins shows that they are present into the fibroblast as a network that surrounds the nucleus and extends across the cytoplasm Presence of intermediate filaments is not necessary for the survival of cells, but it provides mechanical support for the cell and its nucleus

2.3 Microtubules

Microtubules consist of vast numbers of tubulin-molecules Tubulin is a heterodimer, formed from two subunits α - and β -tubulin Each subunit is about 450 aminoacids long and 50 kDa in weight Tubulins self-assemble into microtubules, with the α -subunit of one tubulin touching the β -subunit of another Microtubules are very labile cylindrically shaped structures with an inner-diameter of 14 nm and an outer-diameter of 25 nm When a cross-section of a tubule is made, it can be seen that 13 tubulins are present Microtubules are polar structures They have a fast growing (plus) end, while the other end (minus) tends to lose subunits if not stabilized This minus end is stabilized by embedding in the microtubule organizing center (MTOC) called the centrosome, which is located next to the nucleus near the center of a cell This centrosome contains two centrioles and is surrounded by a cloud of a yet uncharacterized amorphous material The plus ends of microtubules are extending outward from the centrosome

Similar to actin, there are various associated proteins, which can influence the behaviour of microtubules These associated proteins are involved in linking the tubule to other parts of the cytoskeleton, or in transporting organelles along a microtubule Antibody-staining shows that

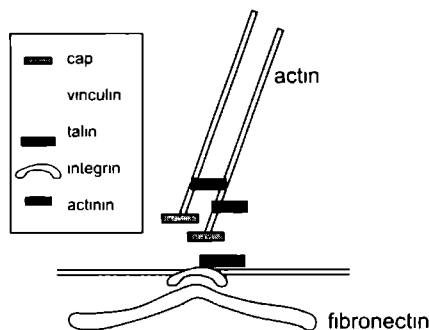


Figure 3 Arrangement of a number of proteins involved in a focal adhesion

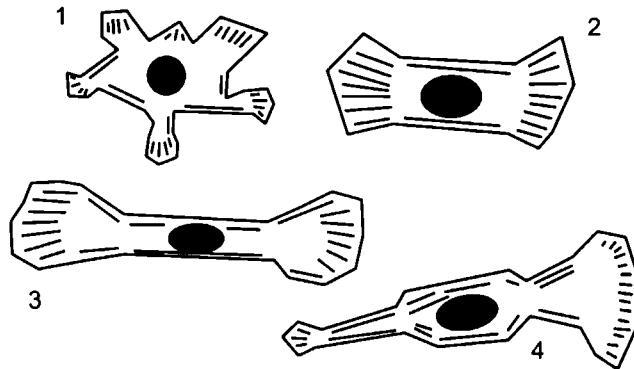


Figure 4: Shapes of cells and distribution of cortical actin filaments during various stages of cellular movement.
 1=nonpolarized cell, 2=bipolar cell, 3=stretched cell, 4=unipolar cell³.

microtubules are lying co-linear with parts of the intermediate filament framework. Removal of the tubules causes the collapse of the intermediate filament network into a perinuclear cap. From such experiments is concluded that microtubules organize the intermediate filament network. Microtubules were also shown to be associated with the determination of the orientation of actin-filaments, and location of endoplasmatic reticulum and Golgi-apparatus in the cell. It is known that organelles can be transported along microtubules. In this ATP-dependent transport along microtubules two proteins are involved: kinesin and dynein. Kinesin moves an organelle to the plus end of a microtubule, dynein to the minus end³.

2.4 Fibroblast attachment to substrates

When cells are cultured, they adhere to each other and to the substratum they are growing on. Adhesions from cells to a certain substratum can be divided into three groups, on the basis of a morphologic criterion, i.e. the size of the separation between the plasma membrane and substratum⁴. The first group, extracellular matrix (ECM) contacts, show a separation of ± 100 nm between the membrane and the substratum. This space is filled with strands and cables of ECM material, connecting membrane and substratum. Second, close contacts have a separation of 30-50 nm. These contacts exhibit submembraneous densities parallel to the plasma-membrane, and can be compared to one half of a particular cell-cell junction: the zonula adhaerens. The third and last group are focal adhesions, who show a 10-20 nm gap between membrane and substratum. They can be compared to one half of another particular cell-cell junction: the zonula occludens.

At focal adhesions filamentous components of the cytoskeleton are bound to ECM proteins, with the help of transmembrane proteins. More specific: the end of an actin filament is connected to an integrin. An integrin is a transmembrane glycoprotein that can bind to ECM components, like fibronectin, vitronectin, or laminin. An integrin is built as a noncovalently associated complex of two high-molecular-weight polypeptides: the α - and β -chain. The integrins are divided in three families according to their β chain. Though there are at least 14 different α -chains and at least 8 β -chains, not

all heteromers are possible. Matrix proteins often contain a RGD sequence, i.e. a sequence of the aminoacids arginine, glycine and aspartic acid. This sequence is the part of the matrix protein that is bound by the integrin⁵⁻⁷.

In the connection between actin-filaments and integrin several proteins play a role: amongst others cap-proteins, α -actinin, vinculin, tallin (see Figure 3), tenuin, and paxillin. Tenuin strengthens the binding of vinculin to actinin. Paxillin is capable of binding vinculin and is thought to be involved in the control of focal adhesion organization. The attachment sites are well positioned to act as signal-transducing centers to report on changes in the cell's immediate environment. Recent findings indicate that such signals are in part mediated through the activation of tyrosine kinases concentrated at the sites of adhesion. Changes in the phosphotyrosine content of paxillin accompanying this elevation in kinase activity suggest that paxillin may be an important intermediary in these pathways^{5,8-10}.

2.5 Cell locomotion and the formation of focal adhesions

The cytoskeleton and attachment sites of a cell are involved in cellular movement. In *in vitro* experiments, cytochalasins can be used to break actin filaments down. Besides, phalloidin can be used to stabilize filaments. If cytochalasins are administered to a cell, locomotion, phagocytosis, cytokinesis and production of microspikes and lamellopodia are paralyzed. If phalloidin is injected into a cell, it blocks cell migration. Such experiments underline that changes in cell morphology and cell movements are actin-based events, rather than dependent on other cytoskeletal components³.

When cell movement is studied microscopically the following observations can be made.

Before movement starts, a cell has thin extensions in all directions: the lamellopodia. In these lamellopodia, short filamentous pieces of actin are present: the microspikes (Figure 4, no. 1). When two opposing lamellopodia become strongly engaged, they cause the cell to become bipolar (no. 2). At the organelle-free periphery of a cell, actin-filaments are oriented along the membrane. This inhibits the outgrowth of other lamellopodia. The opposite forces then cause a cell to become stretched (no. 3). Subsequently, cell movement can propagate to real cell locomotion. One end of the cell becomes rather quiet, whereas the other side, the leading edge, shows enlargement of the lamellopodium, with extensive microspikes (no. 4). In an electron-micrograph the leading edge is visible as a ruffled membrane. In the leading edge new cell adhesions are formed, after which the cortical actin-meshwork contracts. This causes the cell to move on in the direction of the new adhesion. On the other end of the cell, old adhesions are abandoned. When this happens cells usually leave behind complete integrins, i.e. including cytoplasmatic and transmembrane domains^{11,12}.

When the lamellopodium of a spreading fibroblast is observed in more detail, it can be seen that it is 200-300 nm in thickness. Actin monomers diffuse, or are transported, to the front edge of the lamellopodium. Subsequently, they attach to the many present short microspikes. In this way, the growing end of the spikes abut the front edge of the lamellopodium. In this process, possibly also a 'motor protein' is involved. This could be either myosin itself, or a myosin-like protein. In the extending lamellopodium, the new focal adhesions of a cell are formed, from precursor contacts. These precursor contacts are made in two steps. The first step in the formation of a precursor contact is a non-specific approach of the cell membrane to the substrate surface, based on electrostatic and Van der Waals powers. The second stage is the specific binding of integrin membrane-receptors to proteins on

the substratum-surface. After the pushing of the lamellopodium by the microspikes has come to a halt, the microspikes start moving in a lateral way, searching for suitable attachment sites. It is proposed that in this process also microtubules are involved. When a single or several microspike(s) reach a newly formed precursor contact, this contact is stabilized. Vinculin and other proteins accumulate, and the adhesions will eventually mature into a complete focal adhesion, a cluster of integrins. From this focal adhesion the further formation of the actin stress fiber into the cytoplasm takes place (Figure 5). The formation of new focal adhesions can be established very quickly, with times reported varying from 1 to 30 minutes. Recently it has been proven that immediately after ECM-integrin binding, mRNAs and ribosomes are relocated to the newly formed focal adhesions¹⁴. In this way, specialized regions in the cell are created, where mechanical forces on the integrins can immediately be reflected in protein production.

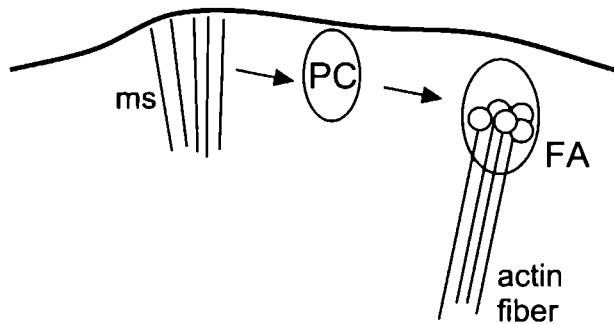


Figure 5: The formation of a new focal adhesion. Microspikes (ms) abut the edge of the lamellopodium. When the propagation stops, microspikes move laterally, until they encounter a precursor contact (PC). Then specific proteins accumulate and the contact matures into a full focal adhesion (FA). From this focal adhesion actin stress fibers are formed¹³

3 CELL ADHESION TO MICROGROOVED BIOMATERIALS

The engineering scope of current implant systems is focused on the development of so-called 'smart' biomaterials, which can be defined as man-made materials which have been designed to induce a specific biological response. Such materials actively influence the surrounding wound healing processes. In general, wound healing around implants is influenced by four material-related factors ¹⁵:

- 1- Physico-chemical properties of the implant material
- 2- Mechanical properties of the implant
- 3- Surface-topography of the material: i.e. the macrotopography and microtopography
- 4- Overall shape and design of the implant

As mentioned in section 1, this thesis will deal with the influence of a certain microtopography, i.e. microgrooves, on the behaviour of cells and tissues. Consequently, the next paragraphs will first describe the manufacturing of microgrooved surfaces. Subsequently, previous experiments performed by our and other research groups with such surfaces will be reviewed.

3.1 Microgrooved surfaces

Material surface topography can be divided into roughness and texture. With 'roughness' non-standardized discontinuities, and with 'texture' a standardized and controlled pattern is meant. It is already known since the beginning of this century that surface topography can influence cell behaviour. During that time, it was noticed ¹⁶ that cells *in vitro* migrated along spider web filaments. This regulation of cell behaviour, called 'contact guidance', was rediscovered about twenty-five years ago by Rovinsky ¹⁷, who saw fibroblast aligning themselves to 40 µm deep triangle-shaped grooves with a 200 µm pitch. Recently, the microgroove principle was further explored in cell culture as well as animal studies. Many studies were performed to investigate the possible use of textured surfaces for medical and dental implants, because of their resemblance to the structure of the ECM network, or to direct specific migration or (out)growth of cells and tissue ^{18,19}.

3.2 Production of microgrooves

For the production of microtextured surfaces numeral techniques can be applied, i.e. from simple manual scratching to more controlled fabrication methods. In the last decade, with the rise of the microconductor technology photo-lithographic techniques have become available. Because these techniques are relatively fast and cheap, and also allow the texturing of surfaces of reasonable size, they seem the most promising for biomedical research and applications ^{15,20}.

Introduction

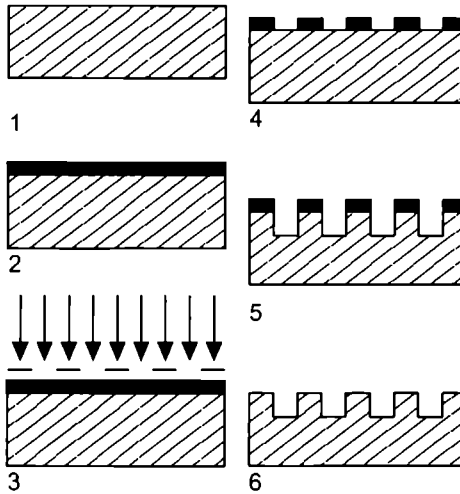


Figure 6: A schematic representation of the photo-lithographic technique. The material (1) is covered with photo resist (2). This resist layer is illuminated through a patterned mask. After this the developed resist is washed off (4), the material is etched (5), and finally the left-over resist is removed (6).

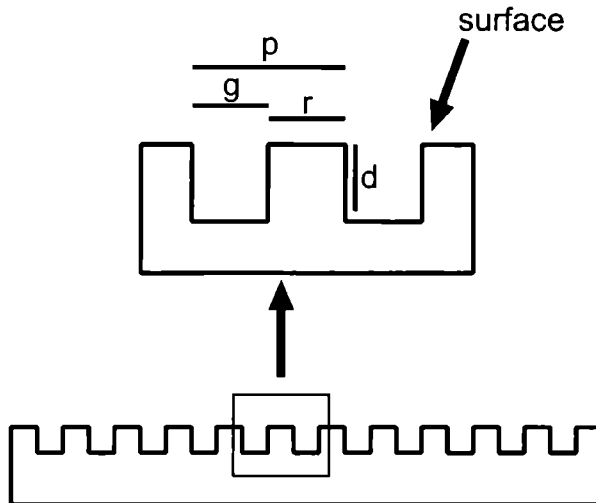


Figure 7: Dimensions of a surface groove pattern as seen in a cross-section. p =pitch, r =ridge-width, g =groove-width, d =groove-depth

In this method the material, usually silica, is first cleaned and dried with filtered air. Then the material is coated with a primer and photo-resist. The samples are patterned by exposing to light through a mask that has the desired pattern. Subsequently, the exposed resist is developed and rinsed off. In the last step, the samples are etched. This etching can be performed under wet or dry conditions. In the first situation, chemicals are used that etch the material along its crystal planes. A disadvantage of this method is that it can only be applied in crystalline materials. In the second situation, ion beams or directed ions derived from a plasma are used as etchants. This technique of physical etching allows a higher resolution than the wet technique, and is also applicable in amorphous materials. Finally, after the etching process the remaining resist is removed (Figure 6). If a substrate is provided with microgrooves, the dimensions of the applied texture are usually described in pitch (or spacing), ridge-width, depth and groove-width (Figure 7).

Apart from using the so obtained microtextured material as substrates for cell-growth, they can also be used as a template in a solvent-casting procedure for the production polymeric substrates. In this way, the photo lithographic techniques have to be performed only once, and vast numbers of identical replicas can be made in many materials.²¹⁻²³

3.3 Cell and tissue response to microgrooved surfaces

During the last years many research has been done to reveal the mechanisms by which micro-texture can influence cellular growth, migration and attachment. Recently, excellent reviews have been published by Von Recum^{18,24}, Singhvi²⁵, Brunette¹⁵, and Curtis²⁶.

In our research group, den Braber performed a series of experiments.²⁷⁻³³ To evaluate the effect of surface treatment and surface microtexture on cellular behaviour, smooth and microtextured silicone substrata were produced (width 2, 5, and 10 μm , depth 0.5 μm). Subsequently, these substrata were either left untreated or treated by ultraviolet irradiation, radio frequency glow discharge treatment (RFGD), or both. It was found that the dimension of the surface events did not influence the wettability characteristics.

When the effect of the substrata surface topography on cellular behaviour was quantified, cell counts proved that neither the presence of the surface grooves, nor the dimension of these grooves had an effect on the cell proliferation. Cells were elongated and aligned parallel to the surface grooves. The cells were capable of spanning the surface grooves on all textures. Wettability and surface free energy influence the cell growth, but play no measurable role in the shape and orientation of cells on microtextured surfaces. Analysis of grooves with a width from 1 to 10 and a depth of 0.45 or 1 μm showed that the ridge width is the most important parameter in the establishment of contact guidance. Varying the groove width and groove depth did not affect cell size, shape, or the angle of cellular orientation.

Microfilaments and vinculin containing attachment complexes, were also investigated. In addition, depositions of bovine and endogenous fibronectin and vitronectin were studied. Here, it was observed that microfilaments and vinculin aggregates on the 2 μm grooved substrata were orientated along the surface grooves, while this orientation occurred significantly less on the 5 and 10 μm grooved surfaces. In contrast, bovine and endogenous fibronectin and vitronectin were orientated along the surface grooves of all textured surfaces. These proteins did not seem to be hindered by the surface

grooves, since many groove spanning filaments were found on all microgrooved surfaces. Vinculin was located mainly on the surface ridges on all textured surfaces.

A TEM study showed that the cells attached specifically to the ridges. Only on 10 μm wide groove patterns adhesions were observed in the surface grooves. On all other textures, cell protrusions extended into the grooves, but none of these were found to contact or attach to the bottom of the microgrooves. Focal adhesions were observed on the ridges of the surface patterns.

Also, the effect of microtextured surfaces on cell behaviour was studied on gratings produced into commercially pure titanium wafers. TEM revealed that focal adhesions were wrapped occasionally around the edges of the ridges. On 5 and 10 μm wide grooves cells protruded into the grooves, and even possessed adhesions on the walls of the grooves. Comparison of these results with the observations on microtextured silicone rubber substrata suggests that material specific properties do not influence the orientational effect of the surface texture on the observed cellular behaviour. The proliferation rate of the RDFs however seemed to be much higher on titanium than on silicone rubber substrata.

Finally, an *in vivo* study was performed, using silicone rubber implants, either smooth or equipped with 2, 5, and 10 μm wide grooves. These were implanted subcutaneously in rabbits for 3, 7, 42, and 84 days. SEM observation showed fibroblasts, erythrocytes, lymphocytes, macrophages, fibrin, and collagen on all implant surfaces after 3 and 7 days. After 42 and 84 days only little collagen, a small number of fibroblasts, but no inflammatory cells, were seen on the implant surfaces. The fibroblasts were not orientated along the surface grooves on all textured surfaces. No significant differences between the thickness of the capsule surrounding the smooth and microgrooved implants were found. In contrast, lower numbers of inflammatory cells, and higher numbers of blood vessels were found in the capsules surrounding the microgrooved implants.

Reviewing these results, it was concluded that the experiments in this work did not provide a final model or explanation for the working mechanisms of cellular behaviour to microtextured surfaces. The *in vitro* studies provided new insight in the contact guidance phenomenon, but did not confirm nor reject unequivocally one of the earlier published hypotheses concerning contact guidance. Many investigators speculated on the benefits of microtextured implants, and even speculated that such an implant surface would prevent the formation of a fibrous capsule. In the *in vivo* experiment, no reduction of the fibrous capsule around the microtextured implants was found. Most likely, the depth of the groove was insufficient to facilitate mechanical interlocking of the implant.

In Table 1 the most relevant *in vitro* and *in vivo* studies to the effect of surface microtexture on cell and tissue response as reported by other research groups are listed.

Table 1: A number of previous experiments on cell growth behaviour on microtextured and patterned substrates

Cell	Substrate material	Topography (μm)	Method of production	Results	First author [ref.]
BHK	fused silica	grooves, $d=0.1-6.0$, combined with adhesive tracks	ion etching	Cells respond to multiple guidance cues Adhesiveness tracks always overrule effects of topography	Britland '96 [34]
PEC, HGF	Ti coated silicon	V-grooves, $g=70-130$, $p=80-140$	etching of silicon, coating of 50 nm Ti, sterilize in EtOH, wash in medium	Alignment (note that the groove dimensions are larger a cell)	Brunette '83 [35]
HGF, PEC	Ti coated silicon, epoxy	V-grooves, or vertical, $g=34-162$, $r=24-96$, $d=5-92 \mu\text{m}$ (a) $d=0.5-60$, $p=4.9-220 \mu\text{m}$ (b)	see Brunette '83	Alignment of cells along the grooves, TEM shows similar organization in cytoskeleton Cells are rounded and have more filopodia Little influence of groove pitch and depth	Brunette '86 a,b [36,37]
fibroblast epithelial <i>in vivo</i>	epoxy	V-grooves $d=0.5$ and up, p varying	micromachining photolithographic technique followed by epoxy replica	<i>In vitro</i> Attachment on grooved better than on smooth surface, not influenced by increased surface area Grooves direct cell migration <i>In vivo</i> around percutaneous implants the length of epithelial attachment is decreased	Brunette '88a,b [38,39]
<i>in vivo</i>	(silicone coated) versapor filters	pores 0.4-10	x	Topography of 1-2 μm allows direct fibroblast attachment and shows minimal tissue response or inflammatory reaction	Campbell '89 [40]
epithelial <i>in vivo</i>	Ti coated epoxy	V-grooves, $d=10$	micromachining	<i>In vitro</i> Cells orient and attachment increases <i>In vivo</i> 7-10 days placed percutaneous implants show shorter length of epithelial and longer length of connective tissue attachment	Chehroudi '89 [41]

epithelial <i>in vivo</i>	Ti coated epoxy	V-grooves, d=3-22, p=7-39	micromachining	Adhesion best when d=3 or 10 μm . Fibroblasts obliquely insert 22 nm grooves. Epithelial downgrowth <i>in vivo</i> inhibited by vertically placed d=10 or 22 μm . Effect d=22 caused by connective tissue reaction, effect of smaller grooves due to contact guidance	Chehroudi '90 [42]
<i>in vivo</i>	Ti coated epoxy	V-grooves, d=3-22	micromachining	In electron microscopy it was observed that epithelial cells interdigitate with 3-10 μm grooves, but not with 22 μm . Fibroblasts insert obliquely into 22 μm implant	Chehroudi '91 [43]
epithelial <i>in vivo</i>	Ti coated epoxy	V-grooves, d=19, 30	micromachining	Percutaneous implant encourages connective tissue ingrowth and inhibits apical epithelial migration	Chehroudi '92 [44]
epithelial <i>in vivo</i>	Ti coated epoxy	V-grooves and pits, d=10	micromachining	3D reconstructions are made of epithelial cells on grooved percutaneous implants. Cells are aligned along the grooves and less flattened.	Chehroudi '95 [45]
<i>in vivo</i>	Ti coated epoxy	V-grooves and pits, d=30-120	micromachining	Radiography is used as a method to evaluate bonelike tissue formation around implants. Most bonelike foci around shallow grooves and deep pits.	Chehroudi '97 [46]
endothelial cells	ECM coated islands separated by non-adhesive regions	20-3	microcontact printing of self-assembled monolayer (SAM) of alkanethiolates on gold, ECM coating	Culturing cells on smaller islands regulates a transition from growth to apoptosis. The cells shape plays a central role in cell function.	Chen, '98 [47]
RBC	poly-styrene	grooves; g=5, d=0.5, 5	not mentioned	Protein-synthesis increases.	Chesmel, '89 [21]

calvarial bone cells	poly-styrene with 0-2% styrene monomer	0.5-5 grooves	PS replica of silicon mold, 15 minutes RFGD (25V, 100 mTorr)	Uniform adsorption of proteins on surface, no influence on DNA synthesis.	Chesmel, 95a [22]
calvarial bone cells	poly-styrene with 0-2% styrene monomer	0.5-5 grooves	see Chesmel 95a	2% and 0.5 μm causes increase in collagenous protein production, 1% and 0.5 μm and all 2% surfaces cause increase in non-collagenous protein production. 1% or 0.5 μm cause increase of migration velocity.	Chesmel, 95b [23]
fibroblast	Ti	V-grooves, d=3, p=6-10	micromachining	Topography alters fibronectin mRNA level, stability, secretion, and assembly.	Chou, '95 [48]
fibroblast	Ti	V-grooves, d=3, p=6	micromachining	Topography alters the expression of metalloproteinase-2	Chou, '98 [49]
BHK, CHF, CCH, PMN	Perpex	5 grooves	photolithographic technique, followed by an oxygen-plasma surface treatment	PMNs are the only not to align. Reaction is dependent on cell-type.	Clark, '87 [50]
BHK, CEN, MDCK	Perspex	grooves; p=4-24, d=0.2-1.9	see Clark '87	Groove depth most important factor. Alignment is cell-type dependent. Cells interaction must be allowed.	Clark, '90 [51]
BHK, CEN, MDCK	Quartz	ultra fine grooves: p=260, d=100-400 nm	laser holography, photolithography, clean by sonication in acetone, then acid/peroxide	Groove depth is the most important factor determining cell alignment.	Clark, '91 [52]

BHK, MDCK	Quartz	adhesiveness patterns of 4-50	photolithographic technique, photo resist removed by rinse in acetone and water causing (hydrophobic) methyl groups to covalently adhere to quartz	BHK cells: alignment, increases in time; MDCK cells. elongation of single cells, cell colonies are unaffected.	Clark, '92 [53]
epithelial fibroblast	Ti coated epoxy	V-grooves d=3, g=40	micromachining	Grooves are used to direct confrontations between epithelial and fibroblast cells. Fibroblast movement is accelerated. Fibroblasts show contact inhibition, epithelial cells not Grooves promote the invasion of fibroblasts into epithelial sheets	Damji, '96 [54]
hepatocytes, various tumor cells	poly-styrene	g>10	photolithographic technique followed by oxygen treatment resulting in tracks of reduced hydrophobicity	Selective adhesion of collagen and cells.	Dewez, '98 [55]
CHF	Quartz	grooves, d=0.69, g=1.65-8.96, p=3-32	photolithographic technique followed by ion-milling	Alignment, ridge-width determining, F-actins and focal adhesions parallel to groove.	Dunn, '86 [56]
gingival fibroblast	Ti and Ti alloys	not mentioned	grinding	Cells have a higher density of focal adhesions at the edges of the ridges.	Eisenbarth, '96 [57]
gingival fibroblast	Ti	d=3, p=30	micromachining	Serum concentration and topography both influence the appearance of ECM protein tenascin.	Goto, '98 [58]
human fibroblast	silicone	Up (pillars) and down (wells) configurations, 1-10 μ m	photolithographic technique, silicone replica, wash in liquinox, 70% EtOH, dry under UV	2 and 5 μ m up: increased proliferation compared to down.	Green, '94 [59]

PLE	epoxy	V-grooves, d=60, p=92	micromachining	Secretion of several proteinases increases.	Hong, '87 [60]
x	various polymers	x	x	A new method for texture production is described.	Kapur, '96 [61]
HGF	Ti	polished, sand-blasted and etched surface.	etching with hydrofluoric acid, store in 99% EtOH, ultrasonical rinse 20 minutes in 99% EtOH, airdry	On polished surface cells are extremely flat, and show random orientation. On etched and sandblasted: cells round or flat with long processes. Etched alignment, sandblasted: cells grow in clusters.	Kökönen, '92 [62]
human skin fibroblast	silicone	g=2-10	photolithographic technique	Cell cycle analysis reveals some differences in proliferation between cells on various textures	van Kooten, '98 [63]
rat epithelial	quartz	cylindrical diameter 32	fused quartz fibers on microscope slide	Alignment of actins and ECM(fibronectin/laminin). The behaviour of cells changes when transformed cells are used.	Levina, '96 [64]
endothelial	glass	various	laser ablation, various chemical modification techniques	Micro cell culture chambers are studied Cells grow in a tube-like fashion Chambers could also be useful as micro reactors.	Matsuda, '94 [65]
endothelial	glass	20-130	adhesional stripes	Migration rates are not influenced by texture, only the migration direction.	Matsuda, '96 [66]
neuro blastoma	fused silica	x	self-assembled monolayers	Neuronal networks can be assembled with micro manufacturing techniques.	Matsuzawa '93 [67]
HGF	SiO ₂ layer on Si plate	g = 1.0, 1.5 and 2.0	photolithographic technique, etch in SiO ₂ layer until Si is reached. 70% EtOH, water, steam sterilize	Cells arrange parallel during adhesion, to achieve maximum contact area	Meyle, '91 [68]

HGF	Araldite	d and r =1.0, g =1 0 or 4.0	photolithographic technique, etch in SiO ₂ /Si plate, Araldite replica, disinfect in 70% EtOH	In TEM: some cells ignore grooves, some fill grooves with cytoplasm, some bridge grooves and just attach to ridges. Focal adhesions and micro-filaments are oriented: only visible in a cross section parallel to groove	Meyle, '93 [69]
5 human cell types	SiO ₂ layer on Si plate	1.0 µm deep and wide grooves	see Meyle '91	Fibroblasts align, keratinocytes and PMNs do not. Monocytes and macrophages about 20% shows alignment.	Meyle, '95 [70]
HGF	Ti	p=30, d=3	micromachining	Alignment of micro-tubules after 20 minutes, focal contacts after 40- 60 minutes Microfilaments appear at random, orient after 3 hours	Oakley, '93 [71]
HGF	Ti	p=30, d=3	micromachining	Colcemid is used to inhibit microtubule formation, cells still align.	Oakley, '95a [72]
PEC	Ti	p=30, d=3	micromachining	Single cells, pairs, and clusters are studied. Cell contacts increased cell spreading, most variability of alignment in cell clusters.	Oakley, '95b [73]
HGF	Ti	p=30, d=3	micromachining	Colcemid and cytochalasin B are used to inhibit microtubule, and microfilament formation. Still alignment occurs. Tubules seem principal, but not sole factor in alignment.	Oakley, '97 [74]
CHF, epithelial	poly- styrene, epon	p= 5-30	microtome in cell culture dish, or in brass with epon replica	Alignment, probably caused by effect on focal adhesions.	Ohara, '79 [75]
<i>in vivo</i> , rat	silicone	pillars diameter 50-500, height 100-1000	micromachining	These textures result in reduced fibrous capsule formation, and increased blood vessel proximity.	Picha, '96 [76]
calvarial osteo blast	Ti coated epoxy	V-grooves	micromachining	More cells on grooved surfaces Cells align from 20 minutes on. Bonelike nodules are formed, also in an oriented fashion.	Qu, '96 [77]

mouse macrophages, <i>in vivo</i> (rabbit)	silicone	pillars and pits, 2, 5 or 8	photolithographic technique, silicone replica. Cleaned ultrasonically, Liquinox wash, autoclaving.	<i>in vivo</i> : 2 and 5 μm events show less mononuclear cell and thinner capsule. <i>in vitro</i> . macrophages elongated, extensive pseudopods.	Schmidt, '91 [78]
CEF	glass	grooves $p=10$, $d=2 \mu\text{m}$?	Position of MTOC is dependent on substratum surface.	Schutze, '91 [79]
AtT-20, PRH	glass	grooves $g=7, 18$, $r=3, 12$, $d=3, 5 \mu\text{m}$?	On PRH: increase in DNA synthesis and albumin secretion. On AtT-20 no effect on growth and function; in transformed cell shape control is lost.	Singhvi, '92 [80]
<i>in vivo</i> , rat	PTFE	conical, height = 12 at the base and 0.1 at the tip	ion beam etching	Fibrous capsule is 30% less in thickness.	Taylor, '83 [81]
fibroblast	silicone	$d=1.7$, $g=1-6$, $r=2-6$	ion etching	Cyclic stretching of silicone leads to fibroblast orientation. Texture overrules this effect.	Wang, '95 [82]
various types nerve cells	quartz	$d=100 \text{ nm}$, $p=260 \text{ nm}$	micromachining	Some cells show no high-order F-actin cytoskeleton, still alignment occurs.	Webb, '95 [83]
BHK	silica	depth 0.5, 1, 2, 5.0 μm , width 5, 10 or 25 μm	photolithographic technique, removal of photo resist by acetone. 1 minute additional etching	After 5 minutes periodic (0.6 μm) actin/ vinculin condensation at the groove edge. Cytoskeletal poisons reduce alignment/ elongation.	Wójciak, '95a [84]
P388D1 mouse macrophage cell-line	silica	depth 0.5 and 5.0 μm width 10 μm	see Clark, '90	Pattern increase cell spreading, elongation and movement. Shallow grooves most effective	Wójciak, '95b and '96 [85,86]

fibroblast P388D1 neuronal cells	ultrathin micro-fibers	diameter 0.2-5	x	These 3D environments caused cell alignment and influenced cell movements.	Wójciak, '97 [87]
FMC	Quartz	grooves; p=1.8-7.4, d=1.1	etching, wash in chromic acid, 24 hour wash in distilled water	p is the most important factor in cell-alignment.	Wood, '88 [88]

Ti= titanium, CHF=chicken heart fibroblast, PEC=porcine epithelial cells; HGF=human gingival fibroblast, BHK=baby hamster kidney fibroblast; CCH=chick cerebral hemisphere, PMN=poly morpho nuclear cell; CEF=chick embryo fibroblast; RBC=rat bone cell; CEN=chick embryonal neuron, MDCK=Mandine-Darby canine kidney epithelial cell; PRH=primary rat hepatocyte; PLE=porcine periodontal ligament epithelial cell. All dimensions given are in μm ; for an explanation of groove-width (g), ridge-width (r), depth (d) and pitch (p) see Figure 7.

4 RESEARCH OBJECTIVES

Materials used for the manufacturing of medical and dental implants have to support the wound healing processes which occur in the direct environment of the implants. Previous studies showed that substrate surface microtexture has influence on cellular and tissue behaviour. Apparently, cells recognize the dimensions of surface configurations and react accordingly. In this process the cytoskeleton and focal adhesions of the cell play a vital role. Further knowledge and understanding of this surface topography principle would be of significant help in the improvement and development of biomaterials as used for the manufacturing of medical and dental implants.

The main working hypothesis is the following: 'Cells that are predominantly involved in tissue regeneration around surgical implants recognize and specifically respond to topographical features by cytoskeletal rearrangement and modification of focal adhesions'. Consequently, the objective of this study is to determine how surface geometry of microgroove patterns influence cellular behaviour *in vitro*, and the tissue reaction *in vivo*. Therefore, the main research questions are:

1. Does the cellular growth behaviour *in vitro* to standardized, well characterized surfaces relate to the microgeometrical properties of these surfaces?
2. Does the orientation of intra-cellular cytoskeletal components differ between cells cultured on smooth and microtextured surfaces?
3. Several scientific publications propose mechanisms for the occurrence contact guidance. Can any of these theories be proven true or denied?
4. What is the influence of the groove-depth on the response of the cells? Is groove-depth an important factor in the alignment and maximal attachment of cells?
5. Is the cellular response to microtextures the same if different substrate materials are compared?
6. How is the initial attachment behaviour of cells towards the substrate influenced by the application of microgrooves?
7. Is the response to microgrooves in the substrate dependent on cell-type?
8. Does the application of microgrooves on implant surfaces influence the healing of these implants?

REFERENCES

- 1 Vacanti, C.A ,and Mikos, A.G (1995) Letter from the editors. *Tissue Eng.* 1, 1-2.
- 2 Nerem, R.M., and Sambanis, A. (1995) Tissue engineering: from biology to biological substitutes. *Tissue Eng* 1, 3-14.
- 3 Alberts, B, Bray, D, Lewis, J Raff, M, Roberts, K and Watson, JD. "Molecular biology of the cell 3rd edition", Garland Publishing, 1995, New York, NY
- 4 Chen, W.-T. and Singer, S.J. (1982) Immunoelectron studies of the sites of cell-substratum and cell-cell contacts in cultured fibroblasts. *J Cell Biol* 95, 205-222
- 5 Luna, E.J. and Hitt, A.L (1992) Cytoskeleton-plasma membrane interactions. *Science* 258, 955-964.
- 6 Steffensen, B., Duong, A.H., Milam, S.B., Potempa, C.L., Winborn, W.B., Magnusson, V L , Chen, D., Zardeneta, G. and Klebe, R.J. (1992) Immunohistological localization of cell adhesion proteins and integrins in the periodontium. *J. Periodontol* 63, 584-592.
- 7 Schwartz, M.A., Schaller, M.D., and Ginsberg, M H (1995) Integrins: emerging paradigms of signal transduction *Annu Rev Cell Dev Biol* , 11, 549-599.
- 8 Turner, C.E., Glenney, J.R jr. and Burridge, K. (1990) Paxillin a new vinculin-binding protein present in focal adhesions. *J Cell Biol* 111, 1059-1068.
- 9 Turner, C.E. (1994) Paxillin a cytoskeletal target for tyrosine kinases. *Bioassays* 16, 47-52.
- 10 Jokush, B.M., Bubeck, P., Giehl, K, Kroemker, M., Moschner, J., and Rothkegel, M. (1995) The molecular architecture of focal adhesions. *Annu Rev Cell Dev Biol* 11, 379-416
- 11 Bray, D. (1992) Cell movements. Garland Publishing, New York, NY.
- 12 Lackie, J M (1982) Cell movement and cell behaviour. Allen & Unwin, London, UK.
- 13 Small, J V., Anderson, K., and Rottner, K. (1996) Actin and the coordination of protrusion, attachment and retraction in cell crawling. *Biosc Reports*, 16, 351-368
- 14 Chicurel, M.E , Singer, R.H , Meyer, C J , and Inber, D.E. (1998) Integrin binding and mechanical tension induce movement of mRNA and ribosomes to focal adhesions. *Nature*, 392, 730-733
- 15 Brunette, D M. (1996) Effects of surface topography of implant materials on cell behaviour in vitro and in vivo. In: Hoch, HC. (Ed.) Nanofabrication and biosystems, Cambridge University Press, Cambridge, UK.
- 16 Harrison, R G. (1912) The cultivation of tissues in extraneous media as a method of morphogenetic study *Anat Rec* 6, 181-193.
- 17 Rovensky, Y.A., Slavnaja, I.L. and Vasiliev, J M (1971) Behaviour of fibroblast-like cells on grooved surfaces. *Exp Cell Res.* 65, 193-201.
- 18 Recum, A F. von and Kooten, T.G. van (1995) The influence of micro-topography on cellular response and the implications for silicone implants *J Biomater Sci Polymer Edn* 7, 181-198.
- 19 Curtis, A S G and Clark, P. (1990) The effects of topographic and mechanical properties of materials on cell behaviour *Crit Rev Biocomp* 5, 343-362
- 20 Jansen, H.V. Gardeniers, J G E., de Boer, M J , Elwenspoek, M.E., and Fluitman, J.H.J. (1996) A survey on the reactive ion etching of silicon in microtechnology *Journal of micromechanics and microengineering*, 14-28.
- 21 Chesmel, K., Clark, C.C. and Black, J. (1989) Culture surface morphology and chemistry have a synergetic effect on bone cell protein synthesis. *Trans Ann Mtg Soc Biomat* , 1.
- 22 Chesmel, K. and Black, J (1995a) Cellular responses to chemical and morphologic aspects of biomaterial surfaces. I A novel *in vitro* model system. *J. Biomed Mat Res* 29, 1089-1099
- 23 Chesmel, K. Clark, C.C., Brighton, C T and Black, J (1995b) Cellular responses to chemical and morphologic aspects of biomaterial surfaces II The biosynthetic and migratory response of bone cell populations *J. Biomed Mat Res* 29, 1101-1110
- 24 Recum, A.F. von, Shannon, C.E., Cannon, E.C , Long, K J , Kooten, T G van, and Meyle, J (1996) Surface roughness, porosity, and texture as modifiers of cellular adhesion *Tissue Eng* , 2, 241-253

- 25 Singhvi, R., Stephanopoulos, G. and Wang, D.I.C. (1994) Review: effects of substratum morphology on cell physiology. *Biotechnol Bioeng* 43, 764-771.
- 26 Curtis, A.S.G., and Wilkinson, C (1997) Topographical control of cells. *Biomaterials*, 18, 1573-1583.
- 27 Braber, E.T. den, Ruijter, J.E. de, Smits, H.T.J., Ginsel, L.A., Recum, A.F. von and Jansen, J.A. (1995) Effects of parallel surface microgrooves and surface energy on cell growth. *J Biomed Mat Res* 29, 511-518.
- 28 Braber, E.T. den, Ruijter, J.E. de, Smits, H.T.J., Ginsel, L.A., Recum, A.F. von and Jansen, J.A. (1996) Quantitative analysis of cell proliferation and orientation on substrata with uniform parallel surface microgrooves. *Biomaterials*, 17, 1093-1099.
- 29 Braber, E.T. den, Ruijter, J.E. de, Smits, H.T.J., Ginsel, L.A., Recum, A.F. von and Jansen, J.A. (1996) Quantitative analysis of fibroblast morphology on microgrooved surfaces with various groove and ridge dimensions. *Biomaterials*, 17, 2037-2044.
- 30 Braber, E.T. den, Ruijter, J.E. de, and Jansen, J.A. (1997) The effect of a subcutaneous silicone rubber implant with shallow surface microgrooves on the surrounding tissue in rabbits. *J Biomed Mater Res*, 37, 539-547
- 31 Braber, E.T. den, Ruijter, J.E. de, Ginsel, L.A., Recum, A.F. von, and Jansen, J.A. (1998) Orientation of ECM protein deposition, fibroblast cytoskeleton, and attachment complex components on silicone microgrooved surfaces. *J Biomed Mater Res*, 40, 291-300
- 32 Braber, E.T. den, Ruijter, J.E. de, Croes, H.J.E., Ginsel, L.A., and Jansen, J.A., (1998) Transmission electron microscopical study of fibroblast attachment to microtextured silicone rubber surfaces. *Cell and Materials* 7, 31-39.
- 33 Braber, E.T. den, Jansen, H.V., Boer, M.J. de, Croes, H.J.E., Elwensproek, M., Ginsel, L.A., and Jansen, J.A. (1998) Scanning electron microscopic, transmission electron microscopic, and confocal laser scanning microscopic observation of fibroblasts cultures on microgrooved surfaces of bulk titanium substrata. *J Biomed Mater Res*, 40, 425-433
- 34 Britland, S., Morgan H., Wojciak-Stothard, B., Riehle, M., Curtis, A., and Wilkinson, C. (1996) Synergistic and hierarchical adhesive and topographic guidance of BHK cells. *Exp Cell Res* 228, 313-25.
- 35 Brunette, D.M., Kenner, G.S. and Gould, T.R.L. (1983) Grooved titanium surfaces orient growth and migration of cells from human gingival explants. *J Dent Res* 62, 1045-1048.
- 36 Brunette, D.M. (1986) Fibroblasts on micromachined substrata orient hierarchically to grooves of different dimensions. *Exp Cell Res* 164, 11-26.
- 37 Brunette, D.M. (1986) Spreading and orientation of epithelial cells on grooved substrata. *Exp Cell Res* 167, 203-217.
- 38 Brunette, D.M. (1988) The effect of implant surface topography on the behaviour of cells. *Int J Oral Maxillofac Implants* 3, 231-246.
- 39 Brunette, D.M. (1988) The effect of surface topography on cell migration and adhesion. In *Surface characterization of Biomaterials*, ed. B.D. Ratner, Elsevier Science Publishers, Amsterdam.
- 40 Campbell, C.E., and Recum A.F. von (1989) Microtopography and soft tissue response. *J Invest Surg* 2, 51-74.
- 41 Chehroudi, B., Gould, T.R.L. and Brunette, D.M. (1989) Effects of a grooved titanium-coated implant surface on epithelial cell behaviour *in vitro* and *in vivo*. *J Biomed Mat Res*. 23, 1067-1085.
- 42 Chehroudi, B., Gould, T.R.L. and Brunette, D.M. (1990) Titanium coated micromachined grooves of different dimensions affect epithelial and connective tissue cells differently *in vivo*. *J Biomed Mat Res*. 24, 1203-1219.
- 43 Chehroudi, B., Gould, T.R., and Brunette, D.M. (1991) A light and electron microscopic study of the effects of surface topography on the behaviour of cells attached to titanium-coated percutaneous implants. *J Biomed Mater Res* 25, 387-405.
- 44 Chehroudi, B., Gould, T.R.L. and Brunette, D.M. (1992) The role of connective tissue in inhibiting epithelial downgrowth on titanium-coated percutaneous implants. *J Biomed Mat Res* 26, 493-515
- 45 Chehroudi, B., Soorany, E., Black, N., Weston, L., and Brunette, D.M. (1995) Computer-assisted three-dimensional reconstruction of epithelial cells attached to percutaneous implants. *J Biomed Mater Res* 29, 371-379

Introduction

- 46 Chehroudi, B., Gould, T.R L and Brunette, D.M. (1997) The effects of micromachined surfaces on formation of bonelike tissue on subcutaneous implants as assessed by radiography and computer image processing . *J Biomed Mat. Res* 34, 279-290.
- 47 Chen, C.S., Mrksich, M., Huang, S., Whitesides, G.M., and Ingber, D.E. (1997) Geometric control of cell life and death *Science* 276, 1425-1428.
- 48 Chou, L. Firth, J.D., Uitto, V-J., and Brunette, D.M. (1995) Substratum surface topography alters cell shape and regulates fibronectin mRNA level, mRNA stability, secretion and assembly in human fibroblasts. *J Cell Sci* 108, 1563-1573
- 49 Chou, L. Firth, J.D , Uitto, V-J , and Brunette, D.M. (1998) Effects of titanium substratum and grooved surface topography on metalloproteinase-2 expression in human fibroblasts. *J Biomed Mat. Res* 39, 437-445.
- 50 Clark, P., Connoly, P. and Curtis, A S.G (1987) Topographical control of cell behaviour I: simple step clues. *Development* 99, 439-448.
- 51 Clark, P., Connoly, P. and Curtis, A.S.G (1990) Topographical control of cell behaviour II: multiple grooved substrata. *Development* 108, 635-644.
- 52 Clark, P., Connoly, P. and Curtis, A S.G. (1991) Cell guidance by ultrafine topography *in vitro* *J Cell Res* 86, 9-24.
- 53 Clark, P., Connoly, P and Moores, R (1992) Cell guidance by micropatterned adhesiveness *in vitro* *J Cell Sci* 103, 287-292.
- 54 Damji, A., Weston, L., and Brunette, D.M. (1996) Directed confrontations between fibroblasts and epithelial cells on micromachined grooved substrata. *Exp Cell Res* 228, 114-124.
- 55 Dewez, J -L., Lhoest, J -B , Detrait, E , Berger, V , Dupont-Gillain, C C , Vincent, L.M., Schneider, Y-J., Bertrand, P., and Rouxhet, P.G. (1998) Adhesion of mammalian cells to polymer surfaces: from physical chemistry of surfaces to selective adhesion on defined patterns. *Biomaterials* 19, 1441-1445.
- 56 Dunn, G.A and Brown, A F (1986) Alignment of fibroblasts on grooved surfaces described by a simple geometric transformation *J Cell Sci* 83, 313-340.
- 57 Eisenbarth, E., Meyle, J., Nachtgall W , and Breme, J (1996) Influence of the surface structure of titanium materials on the adhesion of fibroblasts. *Biomaterials* 17, 1399-1403.
- 58 Goto, T , and Brunette, D.M. (1998) Surface topography and serum concentration affect the appearance of tenascin in human gingival fibroblasts *in vitro* *Exp Cell Res* 224, 474-480
- 59 Green, A.M , Jansen, J.A , Waerden, J.P.C.M. van der and Recum, A.F. Von (1994) Fibroblast response to microtextured silicone surfaces Texture orientation into or out of the surface *J. Biomed Mat Res* 28, 647-653.
- 60 Hong, H L and Brunette, D.M. (1987) Effect of cell shape on proteinase secretion by epithelial cells. *J Cell Sci* 87, 259-267.
- 61 Kapur, R , Spargo, B.J., Chen, M.S., Calvert, J.M., and Rudolph, A.S. (1996) Fabrication and selective surface modification of 3-dimensionally textured biomedical polymers from etched silicon substrates. *J Biomed Mat Res* 33, 205-216.
- 62 Kōkonen, M. (1992) Effect of surface processing on the attachment, orientation and proliferation of human gingival fibroblasts on titanium *J Biomed Mat Res* 26, 1325-1341
- 63 Kooten, T G van, Whitesides, J F , and Recum, A F. von (1998) Influence of silicone (PDMS) surface texture on human skin fibroblast proliferation as determined by cell cycle analysis. *J Biomed Mat Res (Appl Biomater)* 43, 1-14
- 64 Levina, E M , Domnina, L V , Rovensky, Y.A , and Vasiliev, J.M. (1996) Cylindrical substratum induces different patterns of actin microfilament bundles in non-transformed and in ras-transformed epitheliocytes. *Exp Cel, Res* 229, 159-165
- 65 Matsuda, T., and Chung, D J. (1994) Microfabricated surface designs for cell culture and diagnosis. *ASAIO Journal* 40, m594-m597
- 66 Matsuda, T , and Sugawara, T. (1996) Control of cell adhesion, migration, and orientation on photochemically microprocessed surfaces. *J Biomed Mat Res* 32, 165-173.

- 67 Matsuzawa, M., Potember, R.S., Stenger, D.A., and Krauthamer, V. (1993) Containment and growth of neuroblastoma cells on chemically patterned substrates *J Neurosci Meth* 50, 253-260.
- 68 Meyle, J., Recum, A.F. Von and Gibbesch, B. (1991) Fibroblast shape conformation to surface micromorphology *J Appl Biomat* 2, 273-276.
- 69 Meyle, J., Gültig, K., Wolburg, H and Recum, A.F Von (1993) Fibroblast anchorage to microtextured surfaces. *J Biomed Mat Res* 27, 1553-1557
- 70 Meyle, J., Gültig, K. and Nisch, W. (1995) Variation in contact guidance by human cells on a microtextured surface. *J Biomed Mat Res* 29, 81-88.
- 71 Oakley, C., and Brunette, D.M. (1993) The sequence of alignment of microtubules, focal contacts and actin filaments in fibroblasts spreading on smooth and grooved titanium substrata. *J Cell Sci* 106, 343-54.
- 72 Oakley, C., and Brunette, D.M. (1995) Topographic compensation: guidance and directed locomotion of fibroblasts on grooved micromachined substrata in the absence of microtubules. *Cell Motil Cytoskeleton*, 31, 45-58.
- 73 Oakley, C , and Brunette, D M (1995) Response of single, pairs, and clusters of epithelial cells to substratum topography. *Biochem Cell Biol.*, 73, 473-489.
- 74 Oakley, C., Jaeger, N.A., and Brunette, D M. (1997) Sensitivity of fibroblasts and their cytoskeletons to substratum topographies: topographic guidance and topographic compensation by micromachined grooves of different dimensions. *Exp Cell Res* 234, 413-24.
- 75 Ohara, P.T. and Buck, R.C. (1979) Contact guidance *in vitro*. A light, transmission, and scanning electron microscopic study. *Exp Cell Res* 121, 235-249.
- 76 Picha, G. J., and Drake, R.F. (1996) Pillared-surface microtexture and soft-tissue implants: effect of implant site and fixation. *J Biomed Mat Res* 30, 305-312
- 77 Qu, J., Chehroudi, B., and Brunette, D M. (1996) The use of micromachined surfaces to investigate the cell behavioural factors essential to osseointegration. *Oral Dis* 2, 102-15
- 78 Schmidt, J.A. and Recum, A.F. Von (1991) Texturing of polymer surfaces at the cellular level. *Biomaterials* 12, 385-389.
- 79 Schutze, K., Maniotis, , A., and Schliwa, M. (1991) The position of the microtubule-organising center in directionally migrating fibroblasts depends on the nature of the substratum. *Proc Natl Acad Sci USA* 88, 8367-8371.
- 80 Singhvi, R., Stephanopoulos, G and Wang, D.I.C. (1992) Effect of substratum morphology on animal cell adhesion and behavior. *Mat Res Soc Symp Proc* 252, 237-245.
- 81 Taylor, S.R., and Gibbons, D.F. (1983) Effect of surface texture on the soft tissue response to polymer implants. *J Biomed Mat Res* 17, 205-227
- 82 Wang, H., Ip, W., Boissy, R., and Grood, E.S. (1995) Cell orientation response to cylindrically deformed substrates experimental validation of a cell model. *J Biomechanics* 28, 1543-1552
- 83 Webb, A., Clark, P., Skepper, J., Compston, A , and Wood, A. (1995) Guidance of oligodendrocytes and their progenitors by substratum topography. *J. Cell Sci* 108, 2747-2760.
- 84 Wójcicki-Stothard, B , Curtis, A.S.G., Monaghan, W , McGrath, M., Sommer, I and Wilkinson, C.D.W (1995) Role of the cytoskeleton in the reaction of fibroblasts to multiple grooved substrata. *Cell Motil Cytoskeleton* 31, 147-158
- 85 Wójcicki-Stothard, B , Madeja, Z , Korohoda, W., Curtis, A , and Wilkinson, C (1995) Activation of macrophage-like cells by multiple grooved substrata: topographical control of cell behaviour. *Cell Biol Int* 19, 485-490
- 86 Wójcicki-Stothard, B., Curtis, A , Monaghan, W , MacDonald, K , and Wilkinson, C (1996) Guidance and activation of murine macrophages by nanometric scale topography *Exp Cell res* 223, 426-435
- 87 Wójcicki-Stothard, B., Denyer, M , Mishra, M., and Brown, R A. (1997) Adhesion, orientation, and movement of cells cultured on ultrathin fibronectin fibers. *In vitro cell dev biol Animal* 33, 110-117
- 88 Wood, A. (1988) Contact guidance on micro-fabricated substrata: the response of teleost fin mesenchyme to repeating topographical patterns *J Cell Sci* 90, 667-681.

Growth behaviour of fibroblasts on microgrooved polystyrene

Walboomers, X.F., Croes, H.J.E., Ginsel, L.A., and Jansen, J.A.
Biomaterials **19**, 1861-1868 (1998)

INTRODUCTION

The biocompatibility of an implant material is determined by various factors, including surface topography. Microtexturing of a substrate surface has been shown to influence the behaviour of cells growing on such substrates^{1,2}. On a microgrooved substratum, i.e. a substratum provided with grooves and ridges sized in the order of micrometers, especially fibroblasts show a phenomenon known as 'contact guidance'. This means that cells tend to align themselves in the direction of the grooves. During the last years much research has been done to unravel the mechanisms underlying this phenomenon. On the basis of various experiments, three main explanations have been postulated.

A first explanation is that the closest contacts between a cell and its substratum, the focal adhesions³, cause contact guidance. Focal adhesions are considered to be stiff rectangular structures, up to 10 μm long⁴. When grooves are smaller than these measures, the focal adhesions are only able to attach themselves in an oriented way on the ridge. When the focal adhesions are oriented, so will be the actin filaments that originate from this point, and therefore the entire cell^{5,6}.

Secondly, surface texture can influence cell behaviour by an effect on extracellular matrix (ECM) protein adsorption. Cells produce ECM proteins, which are adsorbed by the surface. Subsequently, the cell adheres to these adsorbed ECM proteins. The composition and the conformation of this protein layer is determined by the surface properties of the substratum. One of the properties of importance is wettability. Due to an effect of microtexturing on the wettability properties of a substrate surface, cellular behaviour can be influenced⁷. If protein adsorption is different along the edges of ridges, focal adhesions might preferably be formed here, resulting in an oriented cell shape.

The third theory is focused on the response of cells on mechanical local signals⁸. The cytoskeleton is not a static, but a dynamic structure. External forces can be administered onto the cytoskeleton through the focal adhesions. Cells tend to find a state in which internal and external forces are in equilibrium, favorable for their differentiation^{9,10,11}. Cells cultured on microgrooved substrata could well be subjected to a certain pattern of forces, in which the equilibrium of forces induces an aligned cellular shape.

Until now, none of the three theories mentioned above has been proven correct. Besides, all information up to this point is obtained with materials not commonly used in cell culturing, like silica¹² or silicone rubber^{13,14,15}.

Therefore, we searched for a testing system in which microgrooved substrata could be made in polystyrene (PS), the most commonly used material for cell culturing. Silicon wafers provided with microgrooves allow the possibility of solvent casting polymers like polystyrene onto them¹⁶. In this way many PS substrata can be made easily and different kinds of histological techniques can be used to obtain information on the growth behaviour of cells on microtextured PS.

The goal of our study is to see how the cellular behaviour *in vitro* does relate to the microgeometrical properties of these surfaces. Using various analytical techniques, information is obtained about the relevance of the three theories mentioned above.

MATERIALS AND METHODS

Cell culture

Rat dermal fibroblasts (RDF) were obtained from the ventral skin of male Wistar rats, using standard procedure as described by Freshney ¹⁷. To ensure quick and constant availability cells are cryo-preserved. Before experimentation, cells are thawed and cultured in MEM- α containing Earle's salts, L-glutamine, 15% FCS, gentamicin (50 $\mu\text{g}/\text{ml}$). All experiments were performed with 5th or 6th culture generation cells. Onto the various substrata, 15 to 30 thousand cells were seeded per square centimeter. Cells were cultured for three days, and then used for the various experiments. At least two separate sets of experiments were performed. Each set included all materials in triplicate. For counting assays measurements were done in triplicate.

Production of surfaces and characterization

Microgrooved patterns were photo-etched in a silicon wafer by the MESA institute of the University of Twente, Enschede. This wafer is divided into 4 quadrants with a ridge- and groove width of 1, 2, 5 or 10 μm . The wafer has a uniform groove depth of 1.0 μm . The silicon wafer was used as a mold for the production of polystyrene (PS) substrates for cell culturing. PS was solvent cast in a similar manner as described by Chesmel and Black ¹⁶. In short, a casting solution was made by dissolving polystyrene bits from a Nunclon cell culture dish in chloroform (25 g/150 ml) and stirring gently overnight. After casting of this solution on the silicon mold, the chloroform was evaporated overnight. Replicas were removed from the mold and PS rings were glued to them, using a small amount of the casting solution. In this way, tissue culture vessels were created of 2.1 or 5.2 cm in diameter. Subsequently, these vessels were treated by radiofrequency glow-discharge (RFGD) treatment for 5 minutes at 100 mTorr ^{18,19,20}.

To exclude an interfering effect of remained chloroform molecules on the final experiments,



Figure 1: Rat dermal fibroblasts lying on a grooved (2 μm) polystyrene substratum. Methylene blue staining, original magnification 20x. Note the obvious alignment of cells with the grooves. Bar= 64 μm .

selected specimens were investigated by energy dispersive spectrometry (EDS) and cytotoxicity testing by a growth assay. Finally, before use, the substrates were examined by scanning electron microscopy.

Cellular orientation

To determine the orientational effect of the substrata, RDF were cultured for three days, fixed *in situ* in 100% methanol for five minutes, stained with methylene blue and dried to air. Cells were observed by transmitted light microscopy and micrographs were taken at a magnification of 20 times. The micrographs were digitalized and about 100 cells on each substratum were analyzed with Foster-Findlay PC-Image software. The average angle between cells and the grooves was measured (Figures 1 and 2). If the average angle between cells and the groove direction is 45 degrees, cells are supposed to lie in an *at random* orientation. If the average angle is lower, cells are supposed to be oriented.

Scanning electron microscopy

Qualitative information on the spreading and orientation of cells was obtained using scanning electron microscopy (SEM). After incubation, cells were fixed in 2% v/v glutaraldehyde in 0.1 M sodium-cacodylate buffered solution for 5 minutes. Cells were rinsed in cacodylate buffered solution, dehydrated in a series of ethanol, dried in tetramethylsilane to air and covered with gold. Finally they were examined in a JEOL 6310 scanning electron microscope.

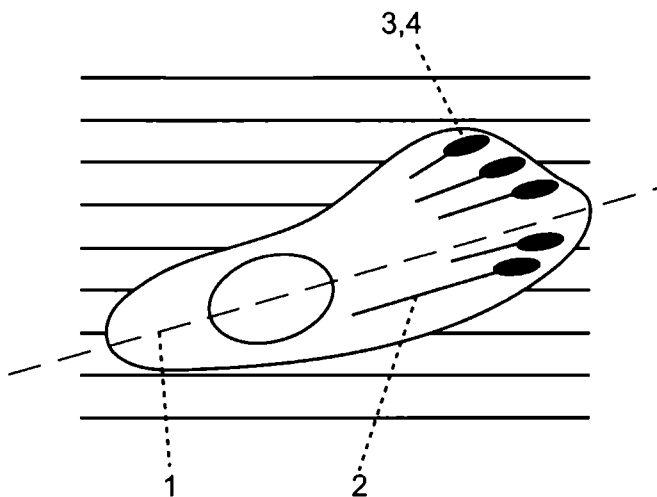


Figure 2: Schematic drawing of a RDF cell on a microgrooved substratum. From digital light microscopic and CLSM images the following parameters were derived: 1) angle between longest axis of the cell and groove direction, 2) angle between actin filaments and groove direction, 3) angle between focal adhesions and groove direction, and 4) position of the focal adhesions in relation to the substrate pattern

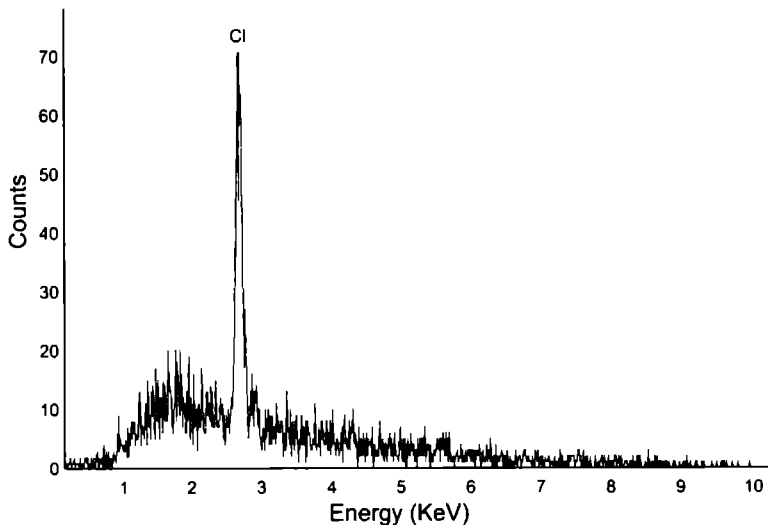


Figure 3 Energy dispersive spectrograph of solvent-cast polystyrene, showing the presence of chlorine atoms

Confocal laser scanning microscopy and image analysis

Components of the cytoskeleton can be imaged using fluorescent antibody-staining techniques. RFD cells, cultured on microgrooved substrata, were fixed for 20 minutes in 2% paraformaldehyde and permeabilized with 1% Triton X100. Then filamentous actin was stained with phalloidin-TRITC (Sigma). Focal adhesions contain vinculin^{21,22}. Therefore, vinculin was stained with mouse anti-vinculin (Sigma) followed by an incubation with goat anti-mouse-FITC (Sigma). Antibodies were diluted in phosphate buffer containing 1% BSA to block aspecific epitopes. Finally, the specimens were examined with a Biorad MRC 1000 confocal laser scanning microscope (CLSM) system.

The CLSM micrographs were analyzed with Foster-Findlay PC-Image software. The orientation of (vinculin-stained) focal adhesions was examined as well as the orientation of actin filaments (Figure 2). Similar to the cellular orientation assay, an angle of 45 degrees was considered to be critical for orientation of focal adhesions or actin filaments. For the evaluation, about 100 focal adhesions or actin filaments were measured on each substratum. In addition to this, the positions of the focal adhesions were determined and divided into three categories, adhesions lying in the groove, on the ridge, or adhesions touching the edge of a ridge.

Transmission electron microscopy

For transmission electron microscopic (TEM) analysis, substrata covered with cells were fixed in 2% glutaraldehyde in 0.1 M sodium cacodylate buffer. After postfixation in OsO_4 and dehydration in ethanol, they were cut into small pieces and embedded in epoxy resin. In the preparation process, standard procedures were followed except for the use of propyleneoxide. This was replaced with

ethanol, since propyleneoxide dissolves the polystyrene After the polymerization of the specimens, sections of about 5 μm thickness were cut and stained with toluidine-blue and examined After determination of the right cutting direction, i.e. perpendicular to the grooves, the embedded tissue block was trimmed to the desired size and cut into ultrathin sections for TEM analysis These were stained in uranylacetate/lead citrate Finally, sections were examined with a JEOL 1210 transmission electron microscope

RESULTS

Surface characterization

To exclude an interfering effect of remained chloroform molecules on the final experiments, selected specimens were investigated by energy dispersive spectrometry (EDS) EDS showed that some chloroform was left in the surface of the casted substrata (Figure 3) Cytotoxicity experiments showed that cell growth did not vary between commercially available dishes and casted culture dishes with RFGD treatment Cell growth was only significantly reduced when bacteriological or self-made PS dishes without RFGD treatment were used (Figure 4)

SEM revealed that, with few exceptions, the pattern of grooves and ridges was perfectly reproduced in the substrata (Figure 5) We observed that the ridges showed an additional nano-roughness This is due to the etching process as used to prepare the silicon wafers In the production of replicas, this roughness appears then on the ridges

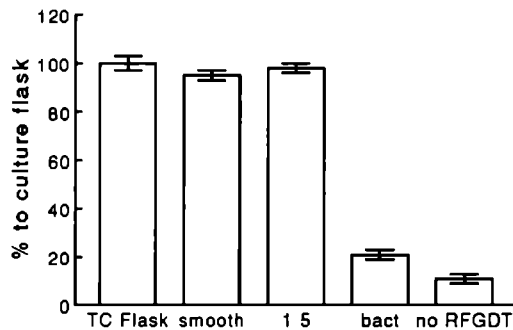


Figure 4 Cell growth assay of rat dermal fibroblasts on solvent-cast smooth (smooth) or textured with 1,5 μm grooves (1,5) polystyrene Positive control is a commercially available tissue culture flask (TC Flask), negative controls are bacteriological (bact) vessels and vessels that were not pretreated with a radiofrequency glowdischarge treatment (no RFGDT) Intervals indicate standard deviation

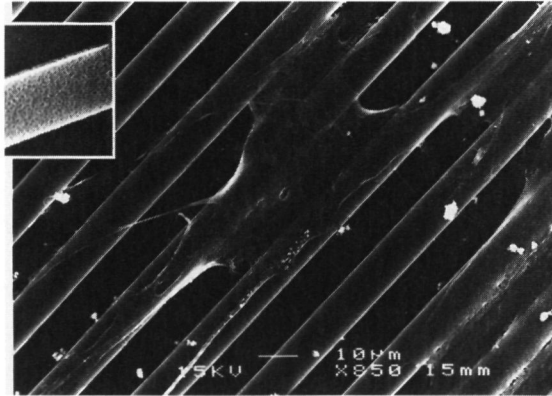


Figure 5: Scanning electron micrograph, showing a rat dermal fibroblast on a 10 μm wide grooved polystyrene substratum, at magnification 850x. Note the descending of cells into the groove. The inset displays the nano-roughness visible on the ridges of the groove pattern at a higher magnification.

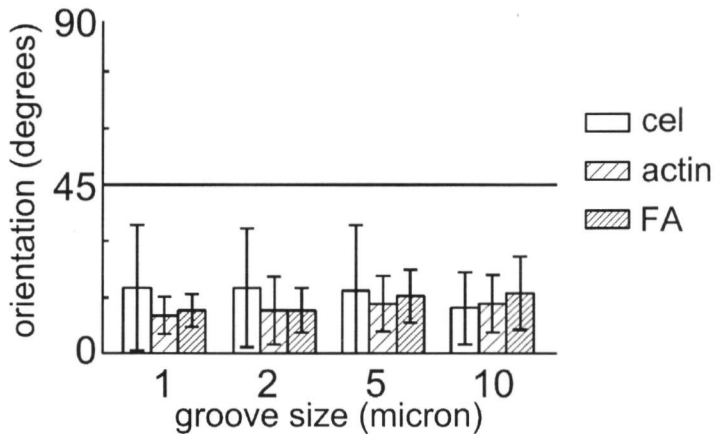


Figure 6: The average orientation of entire cells, actin filaments and focal adhesions on microgrooved polystyrene. Intervals indicate standard deviation.

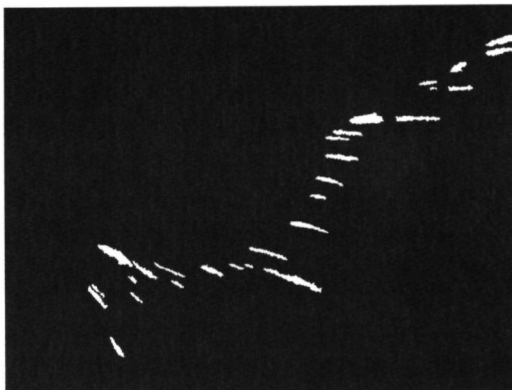


Figure 7: Digitalized confocal laser scanning image of vinculin, a protein abundant in focal adhesions. In this image, grooves were directed horizontally. From these images focal adhesion position and orientation were calculated. Original magnification 120x.

Light microscopy and image analysis

Light microscopical analysis revealed an orientational behaviour of RDF cells on all microgrooved surfaces (Figure 1). Image analysis of the light microscopic images revealed that the cellular alignment did not significantly (ANOVA) differ between the various groove widths (Figure 6).

Scanning electron microscopy

Scanning electron microscopy showed that the RDF cells had a very flattened appearance on PS substrata (Figure 5). Nevertheless, the cells did align obviously to the groove direction on all surfaces. Still, there was a clear difference between the various surface dimensions. Cells cultured on 1 or 2 μm wide grooves seem to lie on top of the ridges. In contrast, on the wider 5 and 10 μm grooves, the cell appears to be able to descend into the grooves. Further, cells showed micropodia and the nucleus, including the nucleoli, was clearly visible.

Confocal laser scanning microscopy and image analysis

In confocal laser scanning microscopy the actin cytoskeleton, vinculin, and the substratum microgrooves were visualized and digitalized. The focal adhesions were visible as somewhat elongated structures (Figure 7). Apparently, they were lying in the same direction as the actin filament where they attached to. Evaluation of the focal adhesion position revealed that on the 5 and 10 μm surfaces only 21% of the focal adhesions were located on the edge of a ridge. For the 2 μm surfaces this was 41% (Table 1). On the other hand, for these surfaces about 50% of the focal adhesions were just positioned on the ridge without touching its edge. Considering these findings, we suggest that there is no indication for a preferential position of the focal adhesions on the edges of ridges.

Further, we measured the orientation of focal adhesions and actin filaments (Figure 6). Both cell

structures appeared to show an orientational behaviour, as characterized by an average angle lower than 45 degrees. No significant differences (ANOVA) could be found between the different groove patterns, neither for the orientation of focal adhesions nor the actin filaments.

Transmission electron microscopy

Transmission electron microscopy was performed to provide detailed cross-sections of cells on the substrata. Prominent structures like the nucleus, mitochondria, ribosomes and rough endoplasmic reticulum appeared to be well preserved. As shown in Figure 8a-b, on the 1 and 2 μm groove patterns, cells very occasionally were seen to touch the bottom of the grooves. In contrast, on wider patterns the cells and even the entire nucleus were able to descend into the groove. On all substrata, focal adhesions were observed as thickened dark plaques in the plasma membrane. The adhesions were lying in the middle, and on the edge of ridges (Figure 8c). On the wider groove patterns focal adhesions were also seen at the bottom of the grooves. Figure 8d shows that focal adhesions are not stiff. An adhesion is observed that is bent around the edge of a ridge.

Table 1 Categorized positions of the place of focal adhesions on the microgrooved substrata. NA= not available

groove size (μm)	in groove (%)	on middle of ridge (%)	on edge of ridge (%)	ridge total (%)	total (%)
10	30	49	21	70	100
5	23	55	21	76	100
2	5	53	41	95	100
1	NA	NA	NA	NA	NA

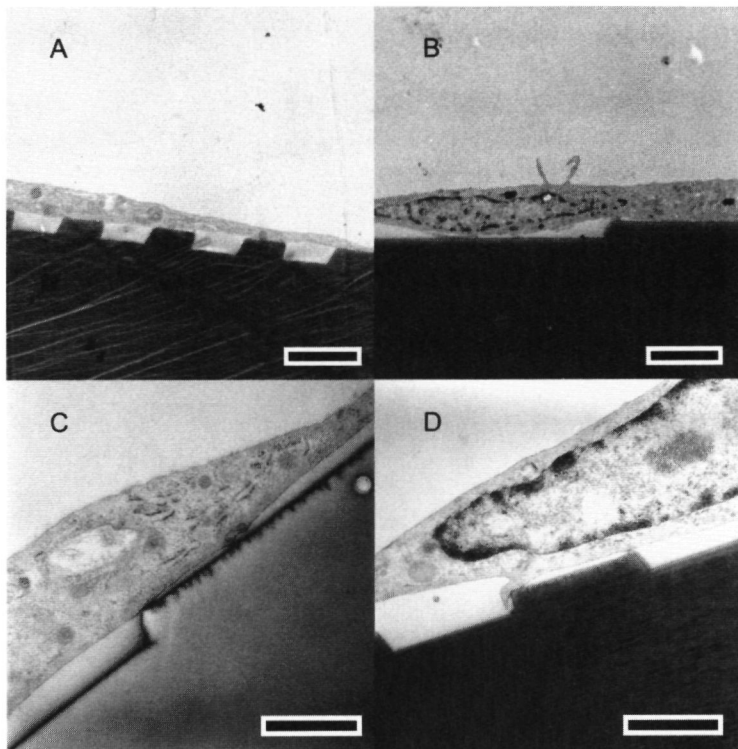


Figure 8: A) Transmission electron micrograph of rat dermal fibroblast on a 2 μm wide, 1 μm deep groove pattern. Note that the cell does not descend into the groove. Bar= 2 μm . B) as A), but 10 μm wide pattern. Note that the cell descends into the groove. Bar= 2 μm . C) At higher magnifications, focal adhesions can be observed. Here two adhesions on a 10 μm wide ridge are seen, one in the middle and one in the proximity of the edge of the ridge. Bar= 0.7 μm . D) A focal adhesion that is bent around the edge of a 2 μm wide ridge. Bar= 1 μm .

DISCUSSION

Polystyrene is the most common material used for cell culture and is easy to section for histology and TEM. Solvent casting of polystyrene seems to be an accurate and easy way to produce large numbers of microgrooved substrata. Our SEM and TEM analysis showed that the groove patterns were accurately reproduced from the various templates. Although EDS showed that some minor amounts of chlorine atoms were still present, cytotoxicity assays showed that this did not affect cellular growth. Further, we have to notice that it is impossible to quantify this maintained chloroform, since no standard, i.e. a polystyrene with a known chloroform content, can be produced. In scanning electron microscopy (SEM) a difference in nano-roughness was observed between grooves and ridges (Figure 5). This is inevitable with the etching procedure as used to produce the silicon wafers. Although we know that the differences in roughness of grooves and ridges can be reduced by etching the entire

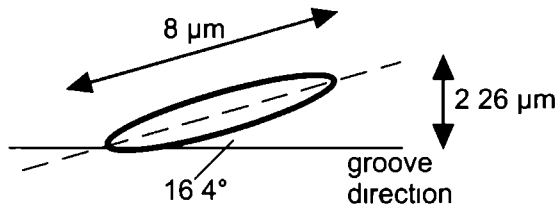


Figure 9 Schematic drawing of a focal adhesion. Adhesions are 8 μm large, and their average angle with the groove direction is 16.4°.

silicon wafer a second time, after the grooves are etched, we decided not to do this. Such a second etching procedure will decrease the sharpness of the edges of the ridges. Besides, etching a second time will not result in exact the same roughness for grooves and ridges.

Light microscopy and subsequent image analysis showed that the average orientation of cells varied between 12.1 and 17.9 degrees on grooved substrata. Apparently, the surface events cause contact guidance. However, the spacing of the used events did not lead to significant differences between the various textures. This means that the cells are lying in a fairly orientated way on all our grooved substrata.

Further SEM analysis of RDF on polystyrene showed that the cells had a flattened and widespread morphology. The cells seemed to be draped over the surface ridges, and alignment was evident. In the wider grooves, the cells were able to descend into the groove cavity, whereas in the smaller grooves cells were less wavelike. The observed morphological and alignment behaviour of the RDF cells differs with previous studies of den Braber in our group, in which similar texture dimensions were used. Then, we found that cells were somewhat rounder and not aligned to the surface texture on 10 μm wide substrata¹⁴. This difference in findings may be caused by three factors. First, the grooves in our experiments were deeper than used in these earlier experiments (1 μm vs 0.45 μm). Various studies^{12,23} already stressed the influence of groove depth on the alignment of cells. Secondly, in this study we used polystyrene, while den Braber casted replicas with silicone rubber. Recently, Singvi and coworkers¹ reviewed studies on the contact guidance phenomenon. They observed that until now numerous materials have been used to investigate cell orientation. However, no coherent studies exist comparing exclusively the effect of material properties while the same surface dimensions are created. Thirdly, the reproduction technique for polystyrene is much more accurate than for silicone rubber. This holds especially for the edge of the ridge which are less rounded in polystyrene.

In agreement with the above mentioned light microscopical results, also CLSM did not reveal differences in the orientation of cytoskeletal structures like vinculin and actin for the various substrata. This observation corresponds with an earlier report of den Braber¹⁵, that already described a strong correlation between cellular and cytoskeletal protein orientation.

Besides orientational effects, using CLSM and digital image analysis (DIA), the position of the focal adhesions was determined. This evaluation revealed no preferential position of the focal adhesion in relation to the edge of the ridge. This is supported by the following reckoning. Focal adhesions are elongated structures with an average length of 8 μm . Their measured average angle towards the groove direction is 16.4 degrees. The adhesion is calculated (see Figure 9) to cover 2.26 microns perpendicular

to the groove direction ($\sin(16.4) \cdot 8 = 2.26$). For the 10 μm surfaces it can be supposed that when all adhesions were spread totally at random over the surface, the probability of an adhesion touching an edge of a ridge would be 0.226 or 22.6% (2.26 microns divided by a 10 micron distance between the grooves). This agrees with the value as found in the experiment, which is 21%. For substrata with smaller grooves and ridges automatically more adhesions will touch the edge of ridges. In those cases, the predicted number according to our method will be even much more than the measured numbers. Finally, we have to notice that we did not determine the position of the focal adhesions on the 1 μm substrata. Focal adhesions on these substrata of course always touch the edge of the ridge, because of the limited space available on the ridge.

TEM even showed that FA plaques are able to bend around rather sharp corners. These findings dispute two of the theories, as mentioned in the introduction ^{5,7}, to explain contact guidance. The rejection of these two hypotheses, imply that contact guidance is the result of a mechanoreceptive response. Ingber ^{9,10,11} suggested that cell shape is based on the transduction of external forces onto the cells. He made so-called 'tensegrity models' of sticks interconnected with elastic strings. Speaking in terms of cells, this model could be translated into actins interconnected with contractile elements. If forces are administered on the model, rearrangement of the elements in its structure will result in a change in shape of the model. Comparably, when forces are administered on the actin skeleton, this will result in rearrangement of these filaments, in our case resulting in an aligned cell. The external forces are the result of the structure of the environment and are transduced onto the actin filaments via the focal adhesions ⁸. However, this system regards the actin filament to be a static structure. We rather suggest that the dynamics of the cytoskeleton, like actin polymerization, could be the explanation of contact guidance. Actin filaments are broken down and elongated constantly in live cells. The front edges of cells, the lamellopodia, contain actin microspikes. With these spikes, cells probe the substrate surface for suitable attachment places, after which focal adhesions and mature actin fibers are formed ^{24,25}. The probing of these microspikes could be influenced by surface discontinuities. When a spike faces a ridge it is faced with an unfavorable force and will not give rise to actin polymerization. Consequently, actin filaments will form and elongate oriented along the groove direction. This process will proceed until the cell on the microgrooved substratum reaches an equilibrium state, which corresponds with an orientational behaviour.

In summary, we can conclude that 1-10 μm wide and 1 μm deep microgrooves in polystyrene cause fibroblasts to orient themselves to the groovedirection. This orientation does not seem to be the result of alterations in focal adhesion orientation or positioning. Probably the breakdown and formation of fibrous cellular components, especially in the filopodium, is influenced by the microgrooves. Consequently, we hypothesize that microgrooves create a pattern of mechanical stress, which influence cell spreading and cause the cell to be aligned with surface microgrooves.

REFERENCES

- 1 Singhvi, R , Stephanopoulos, G and Wang, D I C , Review effects of substratum morphology on cell physiology *Biotechnol Bioeng* , 1994, **43**, 764-771

- 2 Von Recum, A.F., Shannon, C.E., Cannon, E.C., Long, K J , Van Kooten, T G. and Meyle, J., Surface roughness,
porosity, and texture as modifiers of cellular adhesion *Tissue Engineering*, 1996, **2**, 241-253.
- 3 Chen, W.-T. and Singer, S.J., Immunoelectron studies of the sites of cell-substratum and cell-cell contacts in
cultured fibroblasts. *J Cell Biol* , 1982, **95**, 205-222.
- 4 Burridge, K., Fath, K., Kelly, T., Nuckolls, G. and Turner, C., Focal adhesions: transmembrane junctions between
the extracellular matrix and the cytoskeleton. *Ann Rev Cell Biol.*, 1988, **4**, 487-525.
- 5 Ohara, P.T. and Buck, R.C., Contact guidance in vitro *Expl Cell Res* , 1979, **121**, 235-249.
- 6 Dunn, G.A. and Brown, A.F., Alignment of fibroblasts on grooved surfaces described by a simple geometric
transformation. *J Cell Sci* , 1986, **83**, 313-340
- 7 Baier, R E and Meyer, A.E., Implant surface preparation. *Int J Maxillofac Impl* , 1988, **3**, 9-20.
- 8 Banes, A.J., Tsuzaki, M., Yamamoto, J *et al* , Mechanoreception at the cellular level: the detection, interpretation,
and diversity of responses to mechanical signals. *Biochem Cell Biol* , 1995, **73**, 349-365.
- 9 Ingber, D.E., Integrins as mechanochemical transducers. *Curr Opin in Cell Biol* , 1991, **3**, 841-848.
- 10 Ingber, D.E., Cellular tensegrity; defining new rules of biological design that govern the cytoskeleton. *J Cell Sci* ,
1993, **104**, 613-627.
- 11 Ingber, D.E. Cellular tensegrity and mechanochemical transduction. In: Cell Mechanics and Cellular Engineering,
Eds Mow, V.C., Guilak, F., Tran-Son-Tay, R., Hochmuth, R.M , Springer-Verlag, New York, 1994, 329-342.
- 12 Clark, P., Connolly, P., Curtis, A.S.G., Dow, J.A.T and Wilkinson, C D.W., Cell guidance by ultrafine topography
in vitro. *J Cell Sci.*, 1991, **99**, 73-77.
- 13 Braber, E.T den, Ruijter, J.E. de, Smits, H.T.J., Ginsel, L.A., Recum, A.F. von and Jansen, J.A., Quantitative
analysis of cell proliferation and orientation on substrata with uniform parallel surface micro grooves. *Biomat* ,
1996, **17**, 1093-1099.
- 14 Braber, E.T. den, Ruijter, J.E. de, Ginsel, L.A., Recum, A F von and Jansen, J.A., Quantitative analysis of
fibroblast morphology on microgrooved surfaces with various groove and ridge dimensions. *Biomat* , 1996, **17**,
2037-2044.
- 15 Braber, E T. den, Ruijter, J.E. de, Ginsel, L.A , Recum, A.F. von and Jansen, J A , Orientation of ECM protein
deposition, fibroblast cytoskeleton, and attachment complex components on silicone microgrooved surfaces. *J*
Biomed Mat. Res , 1998, **40**, 291-300.
- 16 Chesmel, K and Black, J., Cellular responses to chemical and morphologic aspects of biomaterial surfaces. I. A
novel *in vitro* model system. *J Biomed Mat Res* , 1995, **29**, 1089-1099.
- 17 Freshney, R.I., Culture of animal cells: a manual of basic technique New York, Alan R Liss Inc., 1987
- 18 Baier, R.E. and DePalma, V.A., Electrodeless glow discharge cleaning and activation of high-energy substrates
to insure their freedom from organic contamination and their receptivity for adhesives and coatings. Calspan
Report, 1970, **176**.
- 19 Amstein, C.F. and Hartman, P A , Adaptation of plastic surfaces for tissue culture by glowdischarge. *J Clin*
Microbiol , 1975, **2**, 46-54.
- 20 Chunn, J A., Horbett, T A and Ratner, B D., Laboratory preparation of plasticware to support cell culture. *J Tiss*
Culture Meth , 1994, **16**, 155-159.
- 21 Geiger, B., Tokuyasu, K.T., Dutton, A.H. and Singer, S.J., Vinculin, an intracellular protein localized at
specialized sites where microfilament bundles terminate at cell membranes. *Proc Natl Acad Sci USA*, 1980, **77**,
4127-4131.
- 22 Luna, E.J. and Hitt, A.L., Cytoskeleton-plasma membrane interactions. *Science*, 1992, **258**, 955-964
- 23 Clark, P, Connolly, P , Curtis, A.S.G., Dow, J A T and Wilkinson, C.D W , Topographical control of cell
behaviour: II. Multiple grooved substrata. *Development*, 1990, **108**, 635-644
- 24 Mitchinson, T.J. and Cramer, L.P., Actin-based cell motility and cell locomotion. *Cell*, 1996, **84**, 371-379.
- 25 Small, J.V., Anderson, K and Rottner, K., Actin and the coordination of protrusion, attachment and retraction in
cell crawling *Biosc Reports*, 1996, **16**, 351-368.

Attachment of fibroblasts on smooth and microgrooved polystyrene

Walboomers, X.F., Monaghan, W., Curtis, A.S.G., and Jansen, J.A.
J Biomed Mater Res **46**, 212-220 (1999)

INTRODUCTION

Providing a substrate-surface with micrometer-sizes grooves, has been shown to influence the behaviour of our cells growing on such substrates *in vitro*^{1,2} Cells, like fibroblasts, recognize these surface features, and react accordingly, probably by reshaping the actin filaments in their surface-probing structures like filopodia³ The result is a cell which is lying in the same direction as the surface grooves This phenomenon is known as 'contact guidance'⁴ Microgrooves are also known to influence a range of other biological processes, like cellular attachment, and protein production⁵ Consequently, it has been proposed that such surfaces could be used to influence the performance of medical implants^{5,8} Microtextures could be helpful in directing and organizing capsule formation around implants

During the last 5 years, several studies have been performed in both our laboratories, to learn more about 'cell orientation' phenomena for application to implants^{3,7,14} From one of their studies⁹, the "Nijmegen" group concluded that apparently the ridge width of the microgrooved patterns had more effect on the alignment of rat dermal fibroblasts (RDF) than the groove width The results further suggested that the groove depth was unimportant In this study however, only grooves with a depth of 0.45 and 1.00 μm were used In contrast, Clark and coworkers investigated in the "Glasgow" laboratory a very large range of depths up to 20 μm ^{11,12} From these studies they concluded that the groove depth was much more important in alignment of cells than the spacing of the grooves Curtis and Clark¹³ reviewed the effects of topographic properties on cellular behaviour, again stressing the importance of groove depth Even when patterns of nanometric scale were used, an increase in groove depth led to better alignment¹⁴ Because of the contradictions in the findings, the present cooperative paper between both involved laboratories provides further data about the possible relevance of groove depth Besides, we have to bear in mind that probably surfaces with deeper grooves are also able to support larger numbers of cells, simply due to the fact that the total available surface in a culture vessel is larger

In our previous studies we also reported about the application of transmission electron microscopy (TEM) to examine the cellular contact of RDF cells with microgrooved substrate surfaces^{3,10} This technique has several disadvantages, which can interfere with the final conclusions For example, TEM does not provide a complete overview of the cell Only a small part of the plasma membrane can be sampled Also no living cells can be examined, and the preparation of TEM specimens is very laborious As a result, artefacts can be introduced¹⁵ Therefore for a correct estimation of the cellular proximity to a substrate surface, other more reliable techniques have to be used, such as interference reflection microscopy (IRM)¹⁶ This method allows the *in situ* observation of complete living cells without prior handling or fixation

Consequently, the objective of this *in vitro* study is to quantify the influence of groove depth on alignment and maximal cell support in RDF cell cultures Further, the attachment of the plasma membrane as seen in IRM, was determined In these experiments, we used microgrooved polystyrene substrates, which were produced by a solvent-casting technique This method enables the preparation of large numbers, high quality, culture surfaces^{3,17}

MATERIALS AND METHODS

Culturing substrata

Using photo-lithographic techniques, various microgrooved patterns were made at the Department of Electronics and Electrical Engineering of the University of Glasgow, UK. Fused silica (TSL Quartz, Newcastle) was cleaned by immersion in a solution of 7:1 sulphuric acid/hydrogen peroxide (98% H_2SO_4 , 30% H_2O_2) at 75°C for 5-10 minutes, rinsed in water and blow dried. Samples were spin coated with AZ Primer (Shipley) and S1818 photoresist (Shipley) followed by a softbake at 90°C for 30 minutes. This gave a final resist thickness of 1.8 microns. The samples were patterned by exposing to UV light through a chrome mask (Hoya, Japan). The exposed resist was developed, rinsed and blow dried. Subsequently, the patterned quartz was dry etched in a Plasma Technology (Bristol) Reactive Ion Etch Unit. After the etch process the remaining resist was removed by rinsing in acetone followed by a clean in the sulphuric acid/hydrogen peroxide solution, rinsed and blow dried. Finally, to maintain uniform chemistry, all samples were blanket etched with CHF_3 for 1 minute. Using similar techniques, microgrooves were made in three inch silicon wafers, at the MESA institute, University of Twente, Enschede, the Netherlands.

Both the silica and silicon surfaces were used as molds for the production of microgrooved substrates for cell culturing. For the production of smooth, control surfaces, a glass plate was used. Polystyrene (PS) was solvent cast in a similar manner as described by Chesmel and Black¹⁷. A casting solution was made by dissolving bits from tissue culture PS (Greiner, Germany) in chloroform (LabScan, UK) (25 g/150 ml) and stirring gently for 24 hrs. After casting of this solution on the molds, the chloroform was evaporated overnight in a laminar flow hood. Replicas then were removed from the molds, and PS rings were glued to them, using a small amount of the casting solution. In this way, tissue culture vessels were created of 2.1 cm in diameter. Before use, all substrates were given a radio frequency glow discharge (RFGD) treatment^{18,20}, for 5 minutes at 100 mTorr. The dimensions of all substrates used are summarized in Table 1. For a complete characterization of the obtained PS surfaces we refer to one of our earlier publications³.

Table 1 Summary of the dimensions of the used substrata. Substrates provided with microgrooves have a larger total surface, compared to smooth ones. For the substrates that were included in the confluency assay, the percentage of extra surface and number of used substrates are presented in the last column.

Substrate	groove width (μm)	ridge width (μm)	groove depth (μm)	extra surface (number)
0.5PS1	1	1	0.5	50% (11)
0.5PS2	2	2	0.5	25% (15)
0.5PS5	5	5	0.5	10% (18)
0.5PS10	10	10	0.5	5% (12)
1PS1	1	1	1	100% (15)
1PS2	2	2	1	50% (12)
1PS5	5	5	1	20% (15)
1PS10	10	10	1	10% (12)
1.5PS1	1	1	1.5	150% (9)
1.5PS2	2	2	1.5	75% (12)
1.5PS5	5	5	1.5	30% (6)
1.5PS10	10	10	1.5	15% (12)
1.8PS2	2	2	1.8	
1.8PS5	5	5	1.8	
1.8PS10	10	10	1.8	
1.8PS20	20	20	1.8	
5.4PS2	2	2	5.4	
5.4PS5	5	5	5.4	
5.4PS10	10	10	5.4	
5.4PS20	20	20	5.4	
SMOOTH	0	0	0	0% (18)

Cell culture

Rat dermal fibroblasts (RDF) were obtained from the ventral skin of male Wistar rats, using the standard procedure described by Freshney²¹. To ensure quick and constant availability, cells were cryo-preserved. Before experiments, cells were thawed and cultured in MEM- α containing Earle's salts and L-glutamine (Gibco, UK), supplemented with 15% heat treated FCS (Gibco), and gentamicin (50 $\mu\text{g/ml}$; Gibco). All experiments were performed with 5th or 6th culture generation cells, 15 thousand cells were seeded per square centimeter of substrate.

Cellular orientation assay

To determine the orientational effect of the various substrata, RDF were cultured for three days, fixed *in situ* for 5 minutes in methanol, stained with methylene blue, washed, and dried to air. The 1.5 μm deep specimens were not included in this experiment, because of the similar 1.8 μm deep specimens. All specimens were examined with a Leica DM RBE light microscope at a magnification of 40x. The microscopic images were digitalized with a Sony DXC151P CCD camera attached to the light microscope. Subsequently, the orientation of at least 60 cells on each substratum were analyzed with PC-Image software (Foster-Findlay Associates, UK). For each cell, the mean angle between the longest axis of the cell and the groove-direction was measured, and the mean angles were calculated. This mean angle is then considered to be representative for the entire population of cells on a particular substrate. An angle of 45 degrees was considered to be critical for orientation of the cells. If the mean angle between cells and the groove direction was 45 degrees, cells were supposed to lie in an *at random* orientation. The lower the mean angle, the better the cells were said to be oriented³.

Confluency assay

To measure how many cells are present on the various substrates, when covered by a confluent monolayer of RDF cells, we performed a confluency assay. On the basis of a previous proliferation assay, for the assessment of confluency, cells were cultured on all the different 0.5, 1.0, and 1.5 μm deep substrata for 14 days. After the culturing period, cells were harvested by trypsinization for subsequent counting with a Coulter Counter. The experiment was performed twice. In each experiment the substrates were present at least in triplicate (see also Table 1).

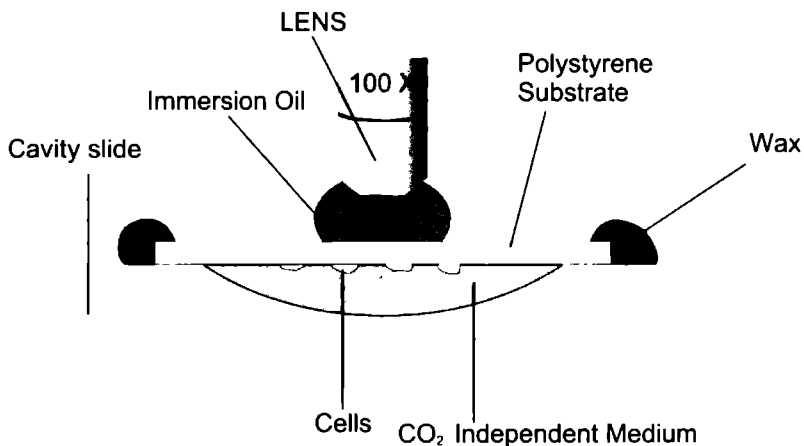


Figure 1: Schematic representation of the way cells were observed. Polystyrene substrata, covered with cells, were mounted onto a cavity microscope slide sealed with paraffin wax. Then they were observed 'upside down'.

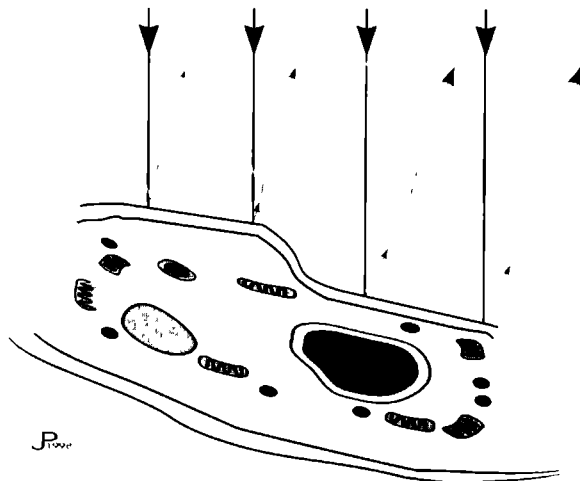


Figure 2: Schematic representation of a cell being observed with interference reflection microscopy. Both at the polystyrene-medium interface, and at the medium-cell interface bundles of light will be reflected. The reflected bundles of light will interfere with each other and so form the interference reflection pattern.

Interference Reflection Microscopy (IRM)

Interference reflection microscopy was carried out as described before by Curtis¹⁶. On at least three specimens of all substrates, RDFs were cultured for one or two days. Cellular densities at this point were still low to exclude effects of contact inhibition. Then, the substrata covered with cells were mounted onto a cavity slide filled with CO₂ -independent medium²² (Gibco) and sealed with paraffin wax (Figure 1). These specimens were illuminated with an intense monochromatic beam of collimated light, obtained by using a mercury arc lamp with a 546 nm filter. Its intensity was reduced with neutral density filters to ca. 1% to avoid damage to the cells. The images were made at a light level not easily visible to the human eye.

Light will be reflected at two interfaces: first at the substrate-medium interface and second at the medium-cell interface. These reflections will interfere with each other, due to their phase differences, which will result in an interference image (Figure 2). This interference reflection image was observed with a light microscope (Vickers, UK) with a 100x oil-immersion objective. Images were digitized with a CCD camera (low light level, Reece Scientific Ltd, Berkshire, UK) attached to an image enhancer (Adv-2, Reece Scientific Ltd, Berkshire, UK). The micrographs were stored on a computer using Matrox Intellicam Interactive software (version 2.0, Matrox Electronic Systems Ltd), for later evaluation. Background subtraction was performed to improve the images. This was done after image analysis, to prevent any influence on the measurements.

IRM image analysis

The IRM micrographs are patterns made out of dark and light interfering reflections. The intensity of reflected light, after interference, has been described in literature^{16,23} and is given by the equation:

$$p = \frac{n_1^2(n - n_0)^2 \cos^2\left(\frac{\pi}{\lambda} 2n_1 d \cos\theta\right) + (n_1^2 - n_0 n)^2 \sin^2\left(\frac{\pi}{\lambda} 2n_1 d \cos\theta\right)}{n_1^2(n + n_0)^2 \cos^2\left(\frac{\pi}{\lambda} 2n_1 d \cos\theta\right) + (n_1^2 + n_0 n)^2 \sin^2\left(\frac{\pi}{\lambda} 2n_1 d \cos\theta\right)} \quad (1)$$

In this equation λ is the wavelength of the used light, d is the distance between cell and substrate, and θ is the angle of incidence light (normally 0°). There are three refractive indices in the formula, namely n_1 of medium in the gap between cell and substrate, n of the cells, and n_0 of the polystyrene. In the experiment we used monochromatic light of 546 nm. The n_1 and n are known to be 1.340 and 1.370 respectively¹⁶. The n_0 was measured with a refractometer, and was 1.715. Since all values but p and d are known, a relation between p and d could be plotted (Figure 3). In this figure also the background reflectivity is represented, calculated from:

$$P_{background} = \left(\frac{n_1 - n_0}{n_1 + n_0}\right)^2 \quad (2)$$

Attachment of fibroblasts on smooth and microgrooved polystyrene

For the analysis of the IRM micrographs, grey levels of certain parts of these pictures were measured, using Scion Image software (version beta 2, based on NIH image software for MacIntosh; ScionCorp, Frederick, Maryland, USA). In such a grey level measurement 0 represents completely white, while a grey level of 255 represents totally black.

With the image analysis software, the grey level of the darkest part in the reflection pattern was measured. The same was done for the lightest part that could be found in the micrograph. These measured grey levels can be calculated in a change in optical density (OD) using the calibration curve (Figure 4), specific for the used microscope. These OD changes could then be calculated into changes in reflectivity (p) using the following formula:

$$OD = -2 \log p \quad (3)$$

So now our measured grey levels are recalculated to a p value. Using the curve from formula 1 (Figure 3) these p values can easily be coupled to distances.

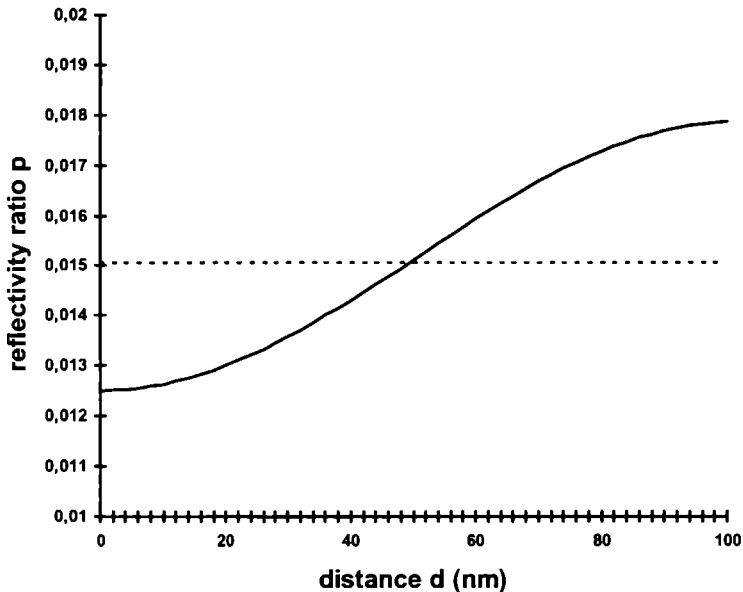


Figure 3: Curve of reflectivity ratio (p) against gap-distance (d) The dotted line indicates the background reflectivity

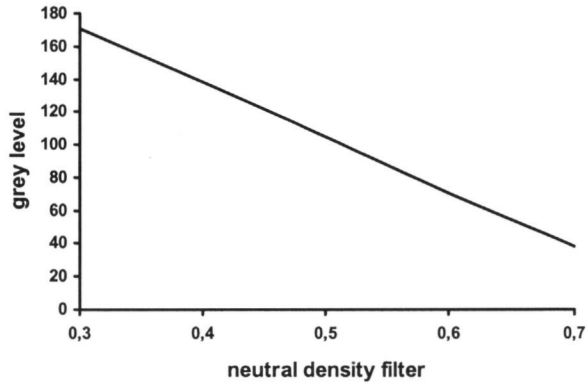


Figure 4: Calibration curve, for the used optical system. The curve is made by adding various neutral density filters to the lightway, and measuring the effect on the grey level of the background.

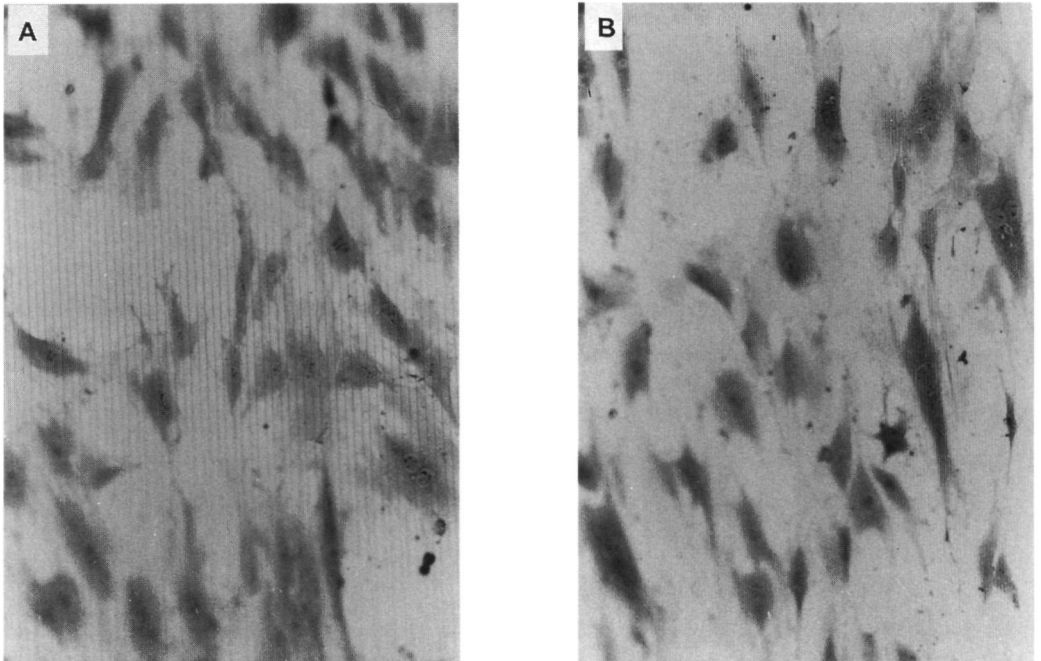


Figure 5: Light micrographs of RDF cells on a 0.5PS10 (A), and a 1.5PS1 (B) substrate. Groove direction is vertical, methylene blue staining, original magnification 20 x. Note the alignment of the cells towards the groove direction.

RESULTS

Cellular orientation assay

Light microscopical analysis showed clearly contact guidance of RDF on most of the microgrooved substrates. Light micrographs of the cells are shown in Figure 5. The orientation of single cells was measured and then the mean orientation was determined. The calculated mean angles between cells and the direction of the grooves, as well as the distribution of the data are shown in Figure 6. If the cells have all aligned with the surface grooves, the mean is very low, with a relatively small distribution. If the cells have not aligned, the mean is about 45 degrees, with a large dispersal. The statistical analysis of the orientation assay was performed with a unpaired t-test (StatMost 2.01, DataMost corporation, Salt Lake City, USA). Clearly, the substrates can be divided into three groups. On the 0.5PS10 and 0.5PS5 substrates, cells show no or hardly any orientation. On all other 0.5 μm deep, and on the 1 μm deep substrates the RDF show orientation, but the distribution of the orientations is very wide. On the deepest groove patterns, i.e. 1.8 and 5.4 μm deep, the RDF are very well oriented. The distribution of the data is very small, which indicates that nearly all cells have adapted to this orientation.

Confluency assay

To measure how many cells at most were present on the various substrates, RDF were cultured upon confluency. Counting with a Coulter Counter showed that on all microgrooved surfaces the number of cells was significantly increased (t-test, $p < 0.05$), compared with the smooth reference surface (Figure 7a). On the other hand, Figure 7a also proved that the surface enlargement does not directly correlate with an increase in cell number.

In Figure 7b the same data are represented, pooled for all groove depths, but now corrected for surface enlargement. For instance, a 1PS5 substrate has a 1 μm groove wall spaced at each 5 μm . This provides for 20% of extra surface, when compared to a smooth culturing substrate. Consequently, the number of cells measured on such a surface was divided by 1.2, to correct for surface enlargement of the 1PS5 substrate. The percentages of extra surface for each used substrate are shown in Table 1. From Figure 7b it becomes apparent that an increase in groove depth was not used by the cells for extra proliferation. Otherwise, all bars would have been of the same height. In contrast, the 1.5 μm deep textures showed even a significantly lower number, relative to their total surface. If the same procedure is followed for all groove widths (Figure 7c) than the same remark can be made about narrow grooves.

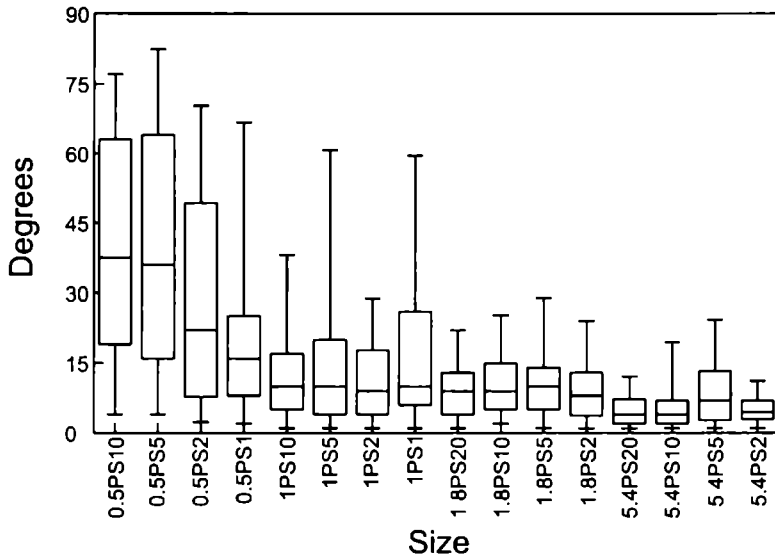


Figure 6: Box-whisker plot of the orientation of the cells. Line indicates the median of the orientations measured, the box indicates 50% of the data points, and whiskers 75% of the data points

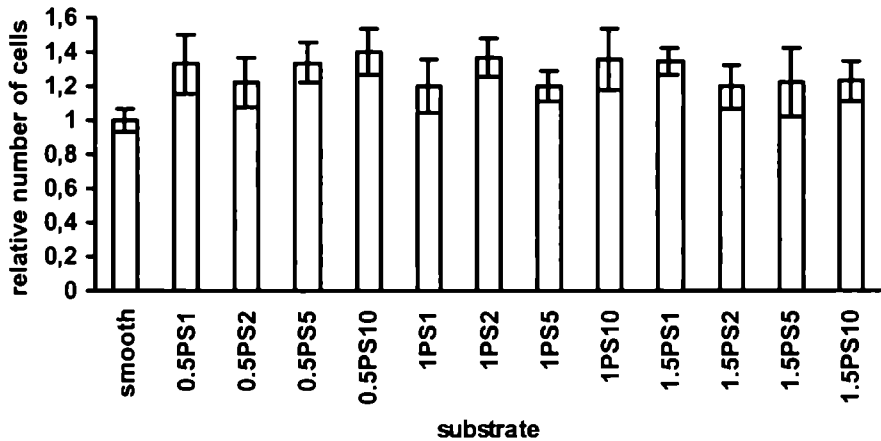


Figure 7a: Results of the confluency assay. The relative number of cells is shown, compared to that of smooth tissue culture vessels. Error bars represent one standard deviation.

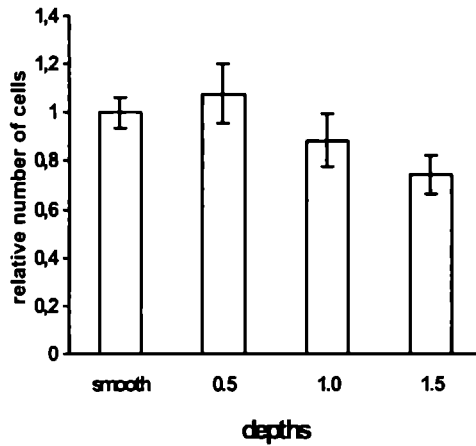


Figure 7b: Results of the confluency assay, when all depths are pooled. Error bars represent one standard deviation.

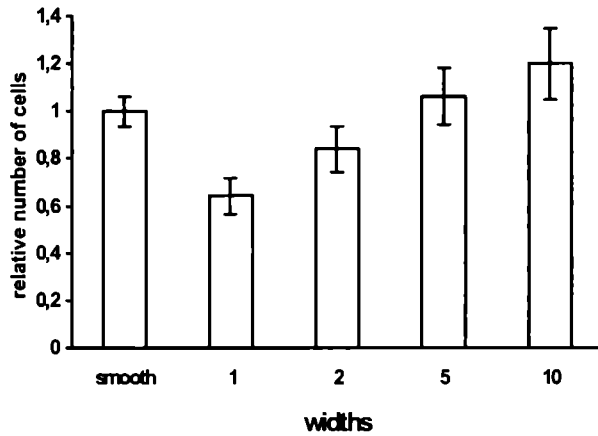


Figure 7c: Results of the confluency assay, when all widths are pooled. Error bars represent one standard deviation.

Interference reflection microscopy

With the help of IRM, the contact side of cells can be visualised, which is seen as areas with various darker and lighter reflections (Figure 8a). The dark areas resemble a close contact between cell membrane and substrate, whereas the lighter areas indicate that the membrane was further away from the substrate. In the micrographs as obtained in our study, we measured grey levels of darkest parts in the image, and of the lightest parts that could be found. The results are presented in Table 2. Subsequently, we calculated that the darkest parts, which represent the focal adhesion points, were 10 nm from the substrate surface. The lightest parts indicated that the cell membrane there was about 41 nm from the substrate.

Table 2: The grey levels (0 is dark, 255 is light) as measured in dark, middle, and light areas in the IRM micrograph shown in Figure 8a. From these values, the distances between the membrane and the substrate are calculated.

	average grey level	distance (nm)
dark	94.99	10
light	132.19	41

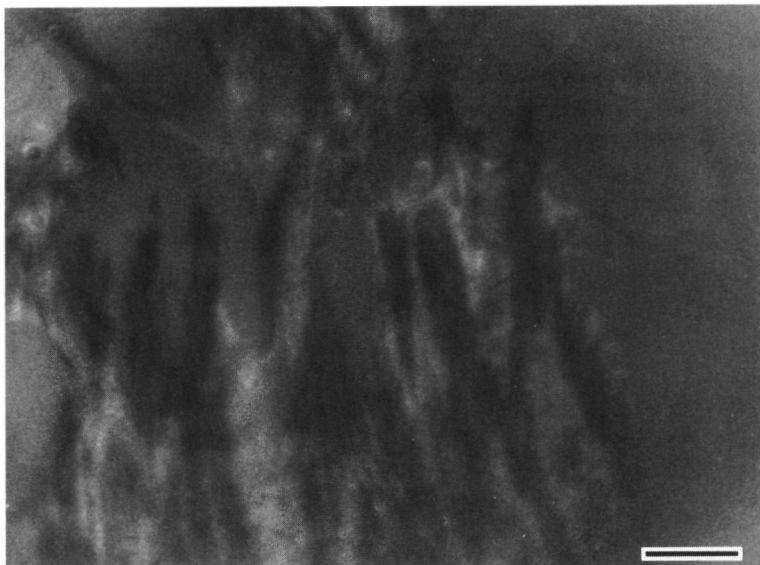


Figure 8a: IRM image of a RDF cell on a smooth polystyrene substrate. Bar= 5 μ m.

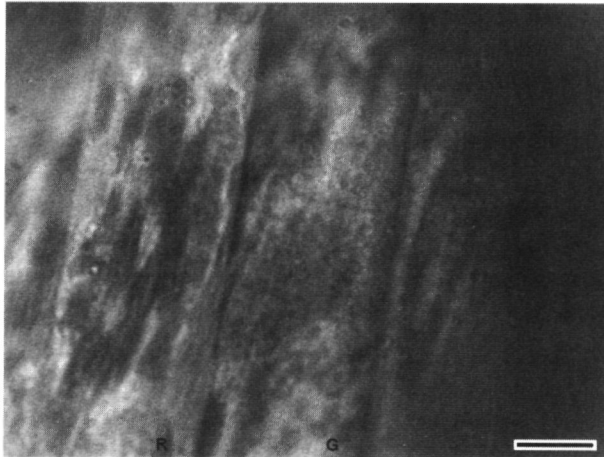


Figure 8b: IRM image of a RDF cell on a microgrooved polystyrene substrate (0.5PS10). Grooves are 10 μm wide, and 0.5 μm deep. Notice that reflection patterns are observed on both the groove (G) and the ridge (R). Bar= 5 μm .

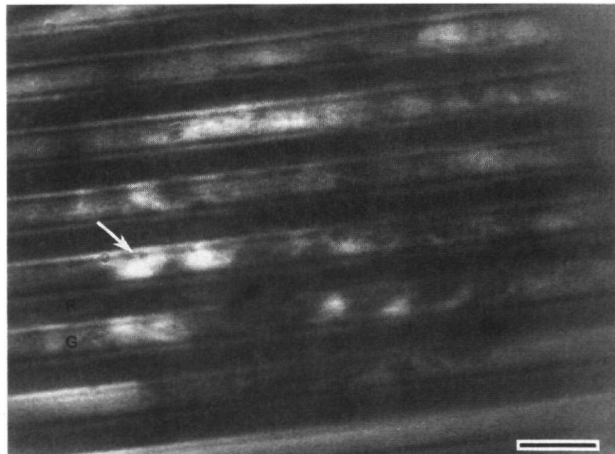


Figure 8c: IRM image of a RDF cell on a microgrooved polystyrene substrate (1.5PS2). Grooves are 2 μm wide, and 1.5 μm deep. When focused on the grooves (G) no reflection patterns are observed, except for distant reflections (arrow) that can be seen as white spots. Bar= 5 μm .

In RDF cultures on shallow microgrooves, like the 0.5PS2 or 0.5PS10 (Figure 8b) substrate, the reflection-pattern was quite similar to that of cells on smooth substrata. Reflections of the entire cellular membrane could be observed, which means that the cell membrane perfectly follows the contours of the substrate. In contrast, on deep grooves like the 1.5PS2, reflections were almost only found on the tops of ridges. This is not an effect of being out-of-focus. When we focused on the grooves, only occasional distant reflections are seen (Figure 8c). These distant reflections were seen as white spots. This indicated that, though the cell might locally descend somewhat into the groove, at no point did the underside of the cell come close to the substrate.

DISCUSSION

In our study we investigated the attachment of rat dermal fibroblasts (RDF) on polystyrene substrata, by various analytical techniques. The substrates used, were either smooth or microgrooved. The groove width varied between 1-20 μm , and the groove depth between 0.5-5.4 μm .

The polystyrene grooved material was produced by solvent casting, which proved to be fast and reliable method to produce a large number of identical substrates. The reflective index of polystyrene made in this way, was 1.715. This was somewhat higher than the 1.5129 mentioned in literature for polystyrene²⁴. This difference is probably due to the fact that solvent casting resulted in terms of density and purity in a different quality polystyrene than 'commercial' polystyrene. Either casting condensed the matter more than it normally is, or a much higher refractive index impurity was included in the process.

Light microscopy, and additional image analysis confirmed that RDF are oriented on microgrooved surfaces. This observation was made for almost the whole range of available microgrooves. When comparing cellular alignment, it became apparent that the rate of orientation increased drastically when the grooves are made deeper.

After two weeks of culture, cells had stopped proliferating on basis of contact inhibition and formed confluent monolayers. The analysis of these layers of RDF showed that microgrooves are able to support greater numbers of cells. This might be caused by effects of the grooves on cell division, diffusion of nutrients and factors, or other processes. More likely, this increase is due to the surface-enlargement. In a tissue culture vessel provided with microgrooves, the total available surface is higher compared with a smooth one. On the other hand, we have to emphasize that we could not conclude from our measurements that narrow and deep grooved surfaces support the largest numbers of cells. This is surprising because these surfaces have the most of 'extra' surface, and cells on these surfaces exhibit the best alignment.

The IRM measurements showed that the RDF formed focal adhesions to the polystyrene. These adhesions mainly occurred at the edges of the fibroblast. In this area, the cells were colored very dark, which was calculated to correspond with a distance of only 10 nm from the polystyrene substrate. Similar distances are well known in literature for glass and commercial polystyrene^{12,25}. This indicated that the produced polystyrene is a suitable cell-culturing material, regarding the forming of close focal attachments of RDF to the substrate.

IRM also showed that RDF followed the contours of shallow microgrooves perfectly, with

attachments all over the substrate. In the grooves and on the ridges throughout the whole cell reflection patterns were observed. In order to get these patterns, the cell membrane must have been closer to the substrate than a few tens of nanometers.

In contrast, on deeper microtextures, the RDF seemed to bridge the grooves, like for example the used 1 5PS2 substrate. When these substrates were observed in IRM, reflection patterns were not, or hardly, found in the grooves. This means that the under side of the cells did not reach to the substrate at these places. This difference in cellular attachment between cells on differently sized microgrooves might account for the results found in the confluency assay. The highest number of cells were not found on the deep grooves, which exhibit the biggest surface-enlargement. Though cells are oriented on these surfaces, they bridge the grooves and therefore are unable to use the 'extra' surface for attachment.

For the observed bridging of the grooves by the RDF cells we propose two possible mechanisms. First, the membrane, including the adjacent actin cell cortex, might be too stiff to bend totally into the deep grooves, or this would be energetically very unfavourable. Second, it could also be possible that in these deeper grooves the RFGD treatment does not accurately penetrate. This will result in an additional pattern of differences in wettability properties between grooves and ridges, which may also cause cellular alignment^{26,27}. This last phenomenon is an issue that deserves attention and further experimentation.

We theorize that the depth of the applied grooves is a determining factor in establishing the reaction of the cells towards microtexture. In our study it was shown, that cells on substrates to 1 μm deep are well able to reach the bottom of the grooves. On these surfaces, the dynamics of actin polymerization, could be the explanation of contact guidance. At the front edges of cells, the lamellopodia contain actin microspikes. With these spikes, cells probe the substrate surface for suitable attachment places. When such a place is found, focal adhesions and mature actin fibers are formed. The probing of these microspikes could be influenced by surface discontinuities. When a spike faces a ridge, it is faced with an unfavorable force and will not give rise to actin polymerization. Consequently, actin filaments will form and elongate oriented along the groove direction. This process will proceed until the cell on the microgrooved substrate reaches an equilibrium state, which corresponds with an orientational behaviour^{3,28,29}. In such a situation, the distribution of the orientations of the cells are relatively wide, and is depending on the number of surface discontinuities. In the current assay, the spacing of the groove pattern. The more tightly spaced this pattern is, the better the orientation. For instance, in contrast with the 0 5PS1 substrate, on our 0 5PS10 substrates no orientation is observed.

Besides, on surfaces with deeper grooves, there is an additional effect. Here, the cells also lose the contact with the bottom of the grooves. This results in a state, where cellular extensions only probe the ridges, and therefore only extend along these surface ridges. Consequently, the variation in the orientations of the cells on these substrates is very small, and does not or hardly depend on the spacing of the surface grooves. The cells always elongate in the groove direction, without significant difference in behaviour between a 2 or 20 μm wide groove.

On the basis of our observations, we suggest that polystyrene made by solvent casting is a suitable material for fibroblast attachment. When microgrooves are applied to a biomaterial surface, they are able to change the orientation of cells. Evidently, the depth of the grooves is a determining factor in the cellular response. Also the numerical cellular adhesion is influenced. This could be a

finding of interest for implantology, since implants in soft tissues of the body are usually covered with a capsule, containing fibroblasts. Further *in vitro* studies are required to investigate the influence of RFGD treatment in deeper microgrooves. In addition, further *in vivo* studies are necessary to clarify the benefits of microtextures for implantology.

LITERATURE

- 1 R. Singhvi, G. Stephanopoulos, and D.I.C Wang, "Review. effects of substratum morphology on cell physiology," *Biotechnol Bioeng* , **43**, 764-771 (1994).
- 2 A.F. Von Recum, C.E. Shannon, E.C. Cannon, K.J. Long, T.G. Van Kooten, and J Meyle, "Surface roughness, porosity, and texture as modifiers of cellular adhesion," *Tissue Engineering*, **2**, 241-253 (1996)
- 3 X F Walboomers, H.J.E Croes, L.A. Ginsel, and J.A Jansen, "Growth behaviour of fibroblasts on microgrooved polystyrene," *Biomaterials* **19**, 1861-1868 (1998).
- 4 P. Weiss, "Experiments on cell and axon orientation in vitro the role of colloidal exudates in tissue organization," *J Exp Zool* , **100**, 353-386 (1945).
- 5 D M Brunette, "Effects of surface topography on cell behaviour in vitro and in vivo," in: *Nanofabrication and biosystems*, H.C. Hoch (ed.), Cambridge University Press, New York, 1996, 335-366.
- 6 A.F. Von Recum, and T.G van Kooten, "The influence of micro-topography on cellular response and the implications for silicone implants.," *Journal of Biomaterials Science - Polymer Edition*, **7**, 181-198 (1995).
- 7 X.F. Walboomers, H.J.E Croes, L.A. Ginsel, and J A. Jansen, "Microgrooved subcutaneous implants in the goat," *Journal of Biomedical Materials Research*, **42**, 634-641 (1998)
- 8 E.T. den Braber, J.E. de Ruijter, and J.A. Jansen, "The effect of a subcutaneous silicone rubber implant with shallow surface micro grooves on the surrounding tissue in rabbits," *J Biomed Mater Res* , **37**, 539-547 (1997).
- 9 E T. den Braber, J.E. de Ruijter, L.A. Ginsel, A.F. Von Recum, and J.A. Jansen, "Quantitative analysis of fibroblast morphology on microgrooved surfaces with various groove and ridge dimensions," *Biomaterials*, **17**, 2037-2044 (1996).
- 10 E.T. den Braber, J.E. de Ruijter, H J.E Croes, L A. Ginsel, and J.A Jansen, "Transmission electron microscopical study of fibroblast attachment to microtextured silicone rubber surfaces," *Cells and Materials*, **7**, 31-39 (1997)
- 11 P. Clark, P. Connoly, A.S.G. Curtis, J.A.T Dow, and C D W Wilkinson, "Topographical control of cell behaviour I. Simple step clues," *Development*, **99**, 439-448 (1987).
- 12 P. Clark, P. Connoly, A.S.G. Curtis, J A.T Dow, and C.D.W. Wilkinson, "Topographical control of cell behaviour. II. Multiple grooved substrata," *Development*, **108**, 635-644 (1990).
- 13 A.S.G. Curtis and P. Clark, "The effects of topographic and mechanical properties of materials on cell behaviour," *Critical reviews in Biocompatibility*, **5**, 343-362 (1990)
- 14 P. Clark, P. Connoly, A.S.G. Curtis, J A T Dow, and C.D.W. Wilkinson, "Cell guidance by ultrafine topography in vitro," *J Cell Sci* **99**, 73-77 (1991).
- 15 P.B. Bell, "The preparation of whole cells for electron microscopy," in: *Science of biological specimen preparation*, , AMF O'Hare, Chicago, 1996, 45-59.
- 16 A.S.G. Curtis, "Adhesion of cells to glass," *J Cell Biol.*, **20**, 199-215 (1964).
- 17 K Chesmel, and J Black, "Cellular responses to chemical and morphologic aspects of biomaterial surfaces. I. A novel *in vitro* model system" *J Biomed Mat Res* , **29**, 1089-1099 (1995)
- 18 R.E. Baier, and V.A. DePalma, "Electrodeless glow discharge cleaning and activation of high-energy substrates to insure their freedom from organic contamination and their receptivity for adhesives and coatings," *Calspan Report*, **176** (1970).
- 19 C F Amstein, and P A. Hartman, "Adaptation of plastic surfaces for tissue culture by glowdischarge," *J Clin Microbiol* , **2**, 46-54 (1975).

- 20 J.A. Chinn, T.A. Horbett, and B.D. Ratner, "Laboratory preparation of plasticware to support cell culture," *J Tiss Culture Meth.*, **16**, 155-159 (1994).
- 21 R.I. Freshney, *Culture of animal cells: a manual of basic technique*. New York, Alan R. Liss Inc., 1987.
- 22 P.J. Batista, and S.A. Weiss, "Development and application of a carbon dioxide-independent medium," *Focus*, **13**, 110-114 (1991).
- 23 A. Vasicek, *Optics of thin films*. North-Holland publishing company, Amsterdam, 1960.
- 24 J.E. Mark (ed.), *Physical properties of polymers handbook*, CD-ROM version, AIP Press, Woodbury, NY, 1996.
- 25 B. Alberts, D. Bray, J. Lewis, M. Raff, K. Roberts, and J.D. Watson, *Molecular biology of the cell*. Third edition, Garland Publishing, New York, 1995.
- 26 S. Britland, P. Clark, P. Connolly, and G. Moores, "Micropatterned substratum adhesiveness. a model for morphogenetic cues controlling cell behaviour," *Exp Cell Res.*, **198**, 124-129 (1992)
- 27 P. Clark, P. Connolly, and G.R. Moores, "Cell guidance by micropatterned adhesiveness *in vitro*," *J Cell Sci.*, **103**, 287-292 (1992)
- 28 T.J. Mitchinson, and L.P. Cramer, "Actin-based cell motility and cell locomotion," *Cell*, **84**, 371-379 (1996).
- 29 J.V. Small, K. Anderson, and K. Rottner, "Actin and the coordination of protrusion, attachment and retraction in cell crawling," *Biosc Reports* **16**, 351-368 (1996).

Contact guidance of rat fibroblasts on various implant materials

Walboomers, X.F., Croes, H.J.E., Ginsel, L.A., and Jansen, J.A.
Journal of Biomedical Materials Research, **47**, 204-212 (1999)

INTRODUCTION

Microtexturing of a substrate-surface has been shown to influence the behaviour of cells growing on such substrates *in vitro* ^{1,3} Studies on the response of fibroblasts, epithelial, and bone cells to microgrooved substrata showed that, while the response is cell type dependent, overall the cell elongates in the direction of the groove and travels guided by the grooves This phenomenon is known as 'contact guidance' ⁴ The determinants of the alignment response are the depth and width of the grooves The alignment response is reflected in changes to the cytoskeleton and the deposited extracellular matrix (ECM) Even after short incubation periods, the cells show the polymerization of F-actin parallel to the direction of the groove edges Although significant progress has been made, the exact cellular and molecular mechanisms that lead from the detection of the microgroove to the formation of aligned cytoskeleton and ECM are not yet completely known

Examining previous *in vitro* studies on microgrooved culturing substrata, it becomes apparent that a number of materials of different substrate chemistry have been used, i.e. silicone rubber ^{5,6}, polystyrene ^{7,8}, silicon ⁹, silica microscope slides ¹⁰, perspex ¹¹, titanium ^{12,14}, epoxy ¹⁵, and araldite ¹⁶ Besides surface chemistry, also the used surface designs were far from uniform In view of this, it is not very surprising that all results do not corroborate with each other It can be supposed that the observed differences in cellular behaviour might just be caused by the differences in substrate properties Still, a lot of researchers claim that the response towards textures is predominantly dependent on surface topography, and that variation of the material has little effect ¹

On basis of the above mentioned, we prefer to hypothesize that contact guidance of fibroblasts, using substrates with the same groove pattern, can be altered by varying the material Currently, no study compared exclusively the differences in contact guidance in relation to differences in material composition Consequently, the objective of this study is to determine the effects of different surface patterns and substrate chemistry on fibroblast growth behaviour Therefore, we cultured primary dermal fibroblasts on relevant metallic (titanium) and polymeric (polystyrene, poly-L-lactic acid, silicone) implant materials, which were provided with uniform parallel grooves and ridges varying in distance

MATERIALS AND METHODS

Culturing substrata

Using photo-lithographic techniques, microgrooved patterns were made in three inch silicon wafers (Twente Microproducts, Enschede, the Netherlands) The wafers were divided into 4 quadrants with a ridge- and groove width of 1, 2, 5 or 10 μm and a groove depth of 0.5 μm Three similar wafers were used These wafers were used as molds for the production of substrates for cell culturing For the production of smooth, control surfaces, non-textured glass plates were used The experimental materials were

- 1) Polystyrene (PS) PS was solvent cast in a similar manner as described before by Chesmel and Black ⁸ A casting solution was made by dissolving bits from tissue culture PS (Greiner, Germany) in chloroform (LabScan, UK) (25 g/150 ml) and stirring gently for 24 hrs After casting of 3 ml of this solution on the molds, the chloroform was evaporated overnight in a

laminar flow hood Replicas were removed from the molds, and PS rings were glued to them, using a small amount of the casting solution In this way, tissue culture dishes were created of 2.1 cm in diameter

- 2) Titanium coated polystyrene (PSTi) Polystyrene dishes were made as described above Additionally, a thin film of titanium was deposited on the inner surface of the prepared polystyrene dishes, using high vacuum coating apparatus (CV-18, Consolidated Vacuum Corporation, Rochester, New York) equipped with a film thickness monitor A commercially pure titanium wire (Drijfhout, Amsterdam, the Netherlands) was wrapped around a tungsten wire and evaporated by critical heating to incandescence at a pressure of approximately 10^{-4} Torr The deposited titanium layers had a thickness of 50 nm
- 3) Silicone (SIL) Silicone substrata were made as described before by den Braber *et al*¹² In short, molds were covered with polydimethylsiloxane (NuSil MED-4211, NuSil Technology, Carpinteria, California) After polymerization, replicas were removed from the molds, and cut to desired size, i.e. rounds with a diameter of 15 mm They were washed in 10% Liquinox (Alconox, New York, N Y), cleaned ultrasonically in 1% Liquinox solution, rinsed thoroughly, and given an overnight Soxhlet rinse in distilled, deionized water
- 4) Poly-L-lactic acid (PLL) Poly-L-lactic acid (Purac Biochem, Gorinchem, the Netherlands) was dissolved in chloroform (10 g/300 ml) Solvent casting was performed by putting 12 ml of the PLL solution on a wafer After evaporation of the chloroform, substrata were placed overnight in a heating stove of 45°C Replicas were removed from the molds, and PS rings were glued to them, using a small amount of the PLL casting solution In this way, tissue culture vessels were created of 2.1 cm in diameter

Just before use, all experimental substrates for cell culturing were given a radiofrequency glow discharge (RFGD) treatment^{17,19}, for 5 minutes at 100 mTorr, to improve the surface wettability of the substrates

Measurement of elastic modulus and wettability

To assess the elastic properties of the PS, SIL, and PLL materials, bars were cut measuring 5x15 mm, and a thickness of 0.2 mm (for the PS and PLL) or 1.1 mm (for the SIL) These bars were used for a tensile test From the stress-strain curve, the elastic modulus was derived The measurements were performed using an Instron mechanical testing machine with a cross head speed of 0.5 mm/sec At least three specimens of each material were used

The water wettability of smooth substrate materials before and after glow discharge was determined using the sessile drop method²⁰ A drop of milli-Q (10 µl) was placed on the test substrates The drops were photographed immediately after positioning on the substrate surface The contact angle (θ) was calculated from the height (h) and breadth (b) of the drop according to

$$\theta = 2 \arctan \frac{2h}{b} \quad (1)$$

In this way, the wettability of each substrate was measured in sixfold

Cell culture

Rat dermal fibroblasts (RDF) were obtained from the ventral skin of male Wistar rats, using standard procedure as described by Freshney ²¹ To ensure quick and constant availability cells were cryo-preserved Before experimentation, cells were thawed and cultured in MEM- α containing Earle's salts, L-glutamine, 15% FCS, gentamicin (50 μ g/ml) All experiments were performed with 5th culture generation cells Onto the various surfaces, 15 thousand cells are seeded per square centimeter of substratum

Proliferation assay

Cells were cultured on the various experimental materials for 1, 3, and 7 days Only smooth substrates were used Both RFGD treated and non-RFGD treated substrates were included The non-treated surfaces were sterilized by washing in 70% EtOH and subsequent drying to air in a sterile environment After the culturing periods, cells were harvested by trypsinization, and subsequently quantified with a Coulter Counter (Coulter Z1, Coulter Electronics Ltd, UK) Two runs of the experiment were carried out In each run, all substrata were present in threefold, and also all counts were performed in triplicate

Scanning electron microscopy

Qualitative information on the reproduction quality of the substrates, and on the morphology of the cells was obtained using scanning electron microscopy (SEM) After 3 days of incubation, the cells on PS, PST₁, and PLL were fixed in 2% v/v glutaraldehyde in 0.1 M sodium-cacodylate buffered solution for 5 minutes Cells were rinsed in cacodylate buffered solution, dehydrated in a series of ethanol, and dried in tetramethylsilane (TMS, Merck) to air For SIL surfaces, the same procedure was followed, except for TMS-drying SIL specimens were dried to air directly from EtOH 100% Finally, specimens were sputtercoated with a thin layer of gold, and examined in a JEOL 6310 scanning electron microscope

Cellular orientation assay

From previous research in our group it is known that the orientation of cells is highly correlated to the orientation of intracellular actin filaments ^{7,22} This orientational effect can be very precisely measured using actin staining, confocal laser scanning microscopy (CLSM), and subsequent digital image analysis Therefore, to determine the contact guidance effect of the substrata, the orientation of cells was measured in this way

RDF were cultured on microgrooved substrata for three days, fixed *in situ* for 20 minutes in 2% paraformaldehyde and permeabilized with 1% Triton X100 Then filamentous actin was stained with phalloidin-TRITC (Sigma) Subsequently, the specimens were examined with a Biorad MRC 1000 CLSM system Digital micrographs were taken at a magnification of 20 times and were analyzed with Scion Image software (v beta 2, based on NIH image, ScionCorp, Frederick, Maryland, USA) For each cell in the image, the angle between the actin skeleton and the groove-direction was measured Then, average angles and standard deviations were calculated These were considered to be representative for the orientation of the entire population of cells on the particular substrate If the cells have all aligned with the surface grooves, the average angle is very low, with a relatively small standard deviation If the cells have not aligned, the average is about 45 degrees, with a large standard deviation

Angles were therefore compared using an unpaired t-test. This test is suitable for comparing two distributions with significantly different variances. For the evaluation, over 50 measurements were made on each substratum.

Transmission electron microscopy

The PS⁷ and SIL²³ specimens have been described in our group in detail before, and were therefore not further elaborated for TEM examination. For transmission electron microscopic (TEM) analysis, PSTi and PLL substrata covered with cells were fixed in 2% glutaraldehyde in 0.1 M sodium cacodylate buffer. After postfixation in OsO₄ and dehydration in ethanol, they were cut into small pieces and embedded in epoxy resin. In the preparation process, standard procedures were followed except for the use of propyleneoxide. This was replaced with ethanol, since propyleneoxide would dissolve PS and PLL. After polymerization of the specimens, sections of about 5 μm thickness were cut and stained with toluidine-blue and examined. After determination of the right cutting direction, i.e. perpendicular to the microgrooves, embedded tissue blocks were trimmed to the desired size and cut into ultrathin sections for TEM analysis. These were stained in uranylacetate/lead citrate. Finally, sections were examined with a JEOL 1210 transmission electron microscope.

RESULTS

Measurement of elastic modulus and wettability

The results of the E-modulus measurements are summarized in Table 1. Statistical analysis (ANOVA) revealed that all values are different. The E-modulus of PLL appeared to be twice as low as that of PS, while the elastic modulus of the silicone is a factor 1000 lower.

The results of the wettability measurements are shown in Table 2. Statistical analysis, using a one-way analysis of variance (ANOVA) and a multi-comparison test (Student Newman Keuls, $p < 0.05$) was performed. The measurements showed that Ti-coating improves the wettability of PS. The RFGD treatment improves the wettability of all substrates. On the other hand, the effect of the RFGD treatment is much higher on the PS and PSTi substrates, than on the PLL and SIL materials. The wettabilities of the various substrate materials were significantly different, after the RFGD treatment. The wettability of the RFGD-treated surfaces can be described as good for PS and PSTi, intermediate for SIL, and remains moderate for the PLL material.

Table 1: Elastic moduli of the materials

Material	Elastic modulus (Mpa)	Standard deviation
PS	894	69
PLL	539	155
SIL	0 39	0 15

Table 2: Contact angles (degrees) of water droplets on the culturing materials, before and after a RFGD treatment

Material	Contact angle (-RFGD)	Standard deviation	Contact angle (+RFGD)	Standard deviation
PS	85	2	13	2
PST ₁	66	4	7	1
PLL	79	4	52	3
SIL	88	5	33	3

Proliferation assay

The results of the proliferation experiment are shown in Figure 1. Statistical analysis was performed using an analysis of variance (ANOVA) followed by a multi-comparison test (Student Newman Keuls, $p < 0.05$).

After three days, cells were observed to be proliferating exponentially on all RFGD-treated substrates. On the PLL substrates more cells were present than on SIL, but no further differences could be found. On all substrates without RFGD treatment, cell proliferation was significantly lower. On SIL and PST₁ substrates, cell numbers had not increased compared with day 0 (seeding). On PS and PLL substrates cell numbers had even decreased.

After five days, cells are still proliferating exponentially on the RFGD treated substrates. Some differences can be observed between the materials. PLL substrates show significantly more cells than PS and PST₁ substrates, but not more than on SIL. The substrates without RFGD treatment show less proliferation compared with their treated counterparts. On the other hand, it can be clearly observed that on the non-treated substrates cells also have started to proliferate. Especially on the PST₁ and PLL substrates, cell numbers have increased compared with day 3.

Finally, after seven days of culturing, cells appear to be growing exponentially on all RFGD treated substrates. Cell numbers on PLL and on SIL are somewhat higher than on PS, but no other differences can be found. The substrates without RFGD treatment still show less cells compared with their treated counterparts. Nevertheless, cells appeared to be growing rapidly. There are no differences between untreated PST₁, PLL, or SIL substrates. However, cell proliferation on the untreated PS is still significantly lower.

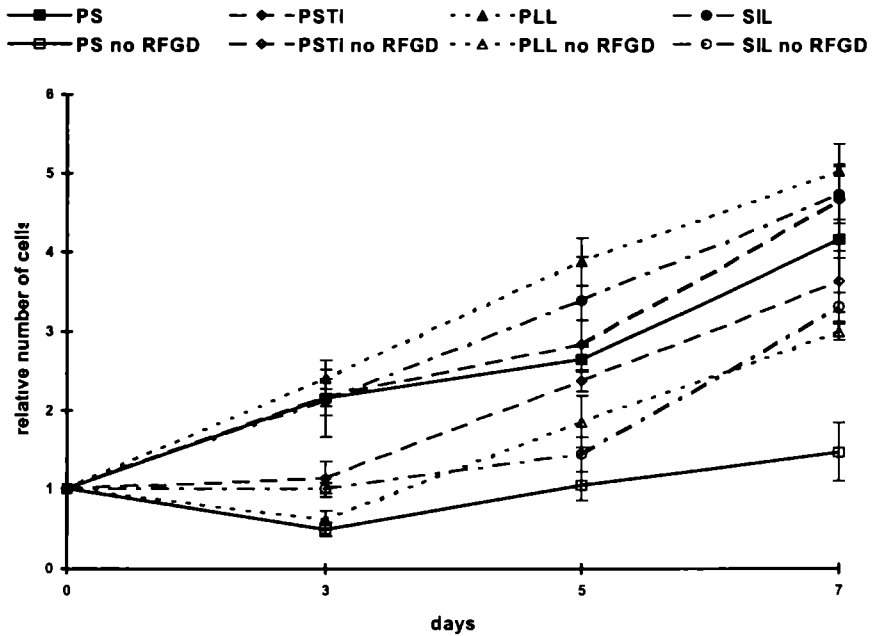


Figure 1 Proliferation assay of RDF cells on polystyrene titanium coated polystyrene, poly-l-lactic acid, and silicone smooth culturing substrata. No significant differences were found between the various substrates.

Scanning electron microscopy

General observation of the RDF cells by SEM showed that the cells had attached to, and spread out on the various substrata. Micropodia, nucleus, and nucleoli were clearly visible in most cells. This indicated that all substrates were suitable for cell culture, and that fixation, dehydration, and drying of the cells had been sufficient.

On PS substrata, SEM observation showed that the RDF cells had a very flattened appearance (Figure 2a,b). Cells did align obviously to the groove direction on surfaces. Qualitatively, there was a difference between the various surface dimensions. Cells cultured on 1 or 2 μm wide grooves seem to be better oriented, and were lying on top of the ridges. In contrast, on the 5 and 10 μm grooves, cells had descended more frequently into the grooves. On PST1 substrata cells appeared to have similar morphological properties as on PS material (Figure 3a,b). On the other hand, on PST1 cells appeared to be less aligned with the surface grooves. On PLL substrata (Figure 4a,b), cells were observed to be a little more rounded than on PS and PST1 materials. Especially, on substrates with 1 μm wide grooves, cells rounded up and seemed spindle-like.

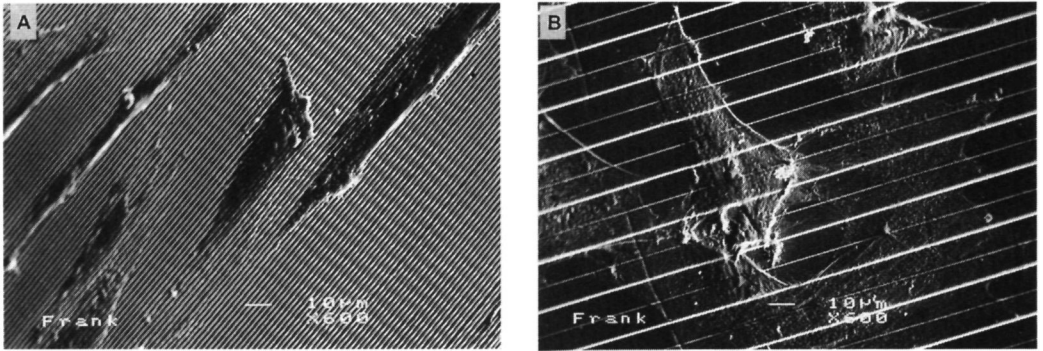


Figure 2: Scanning electron micrographs of cells on PS substrates: a) PS1 b) PS10. Note the alignment on the narrower grooves. PS1 is a substrate with 1 μm wide grooves, etcetera.

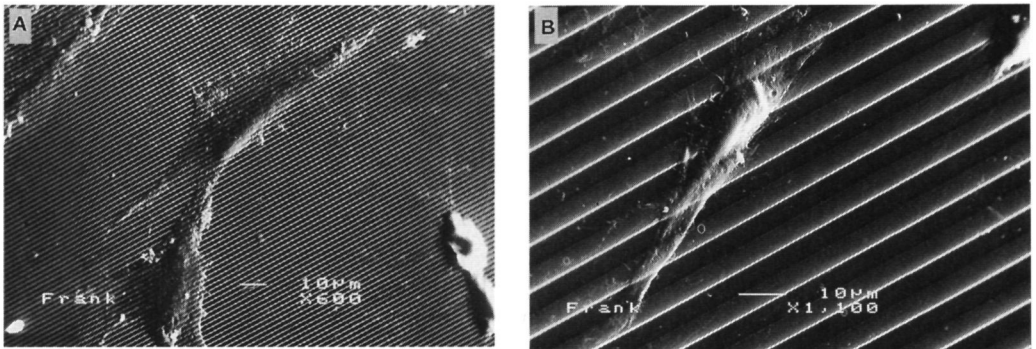


Figure 3: Scanning electron micrographs of cells on PSTi substrates: a) PSTi1 b) PSTi10.

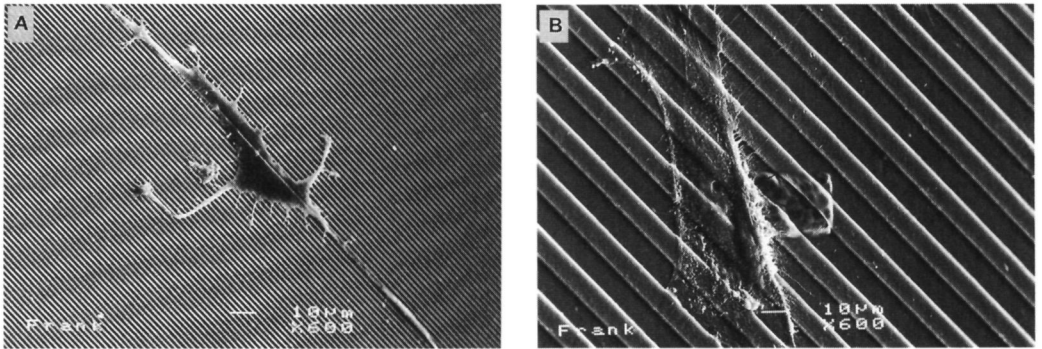


Figure 4: Scanning electron micrographs of cells on PLL substrates: a) PLL1, note the extreme spindle-like shape of the cells, and b) PLL10.

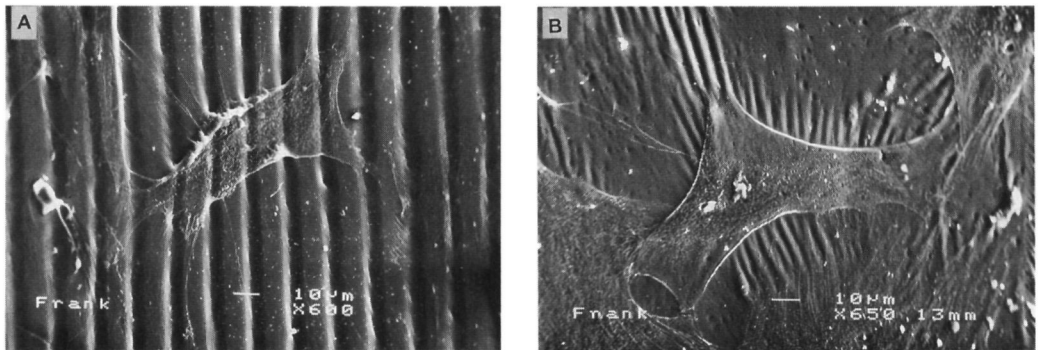


Figure 5: Scanning electron micrographs of cells on SIL substrates: a) SIL10 b) smooth SIL material. Note the deformation of the grooves in 5a, and the wrinkling of the substratum in 5b.

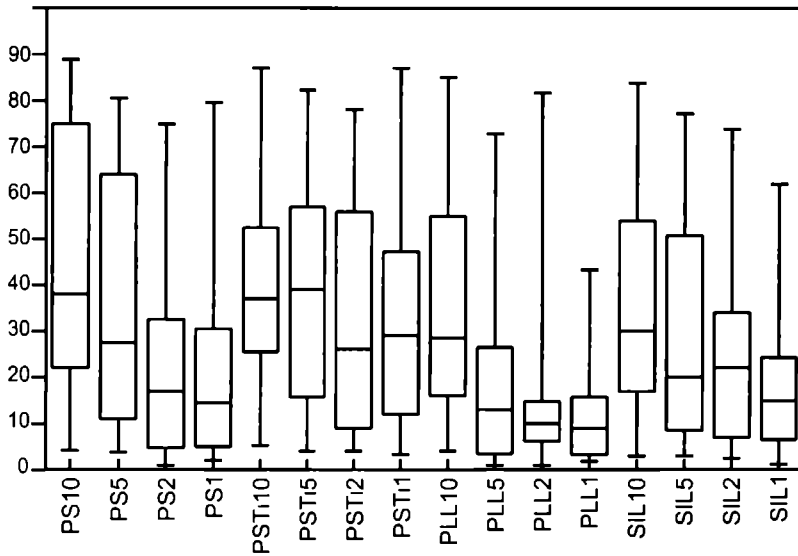


Figure 6: Box whisker plot of the orientation of the RDF cells on the various surface grooves. Line indicates the median of the orientations measured, the box indicates 50% of the data points, and whiskers 75% of the data points

The SIL substrata (Figure 5 a,b) apparently are not as accurately reproduced from the molds, compared with PS. The edges of the ridges seemed to not be as sharp. The morphology of the cells resembled that of PS substrates. However, it can also be clearly seen that the cells have contracted and deformed the substrate surface grooves. The smooth substrates seemed wrinkled (Figure 5a), and on microgrooved substrates, even the ridges were pulled together by the cells (Figure 5b).

Cellular orientation assay

Observation with a light microscope showed that on most microgrooved surfaces cells had aligned towards the microgrooves. Confocal laser scanning microscopy and subsequent digital image analysis confirmed this cellular alignment. The results of these measurements are shown in the box-whisker plot in Figure 6. All significant differences between the alignment of cells are summarized in Table 3. We have to notice that no Bonferroni correction was applied, and therefore not every single significance mentioned in the table is to be regarded individually. Generally speaking we can see that the 0.5 μm deep and 10 μm wide grooves hardly induced alignment on the PS substrates. When the groove width was decreased up to 1 μm , the alignment improved drastically. The RDF also align on PSTi substrates. However, an improvement of alignment with decreasing groove width was not observed here. The PLL substrates seemed to be much more potent in inducing alignment. The best cellular alignment was found on the 1 μm wide PLL substrates. Finally, the orientation of RDF on SIL was comparable to that on the PS structures.

Table 3: Differences between the cellular orientation on the various substrates, as calculated by an unpaired t-test (+ indicates a significant difference, - indicates no significant difference).

	PS10	PS5	PS2	PS1	PSTi10	PSTi5	PSTi2	PSTi1	PLL10	PLL5	PLL2	PLL1	SIL10	SIL5	SIL2	SIL1
PS10																
PS5	-															
PS2	+	+														
PS1	+	+	-													
PSTi10	-	-	-	+												
PSTi5	-	-	+	+	-											
PSTi2	+	-	-	-	-	-										
PSTi1	-	-	-	-	-	-	-									
PLL10	+	-	-	-	-	-	-	-								
PLL5	+	+	-	-	+	+	+	-	-							
PLL2	+	+	-	-	+	+	+	+	-	-						
PLL1	+	+	-	-	+	+	+	+	+	-	-					
SIL10	-	-	+	+	-	-	-	-	-	+	-	+				
SIL5	+	-	-	-	+	-	-	-	-	-	-	+	-			
SIL2	+	+	-	-	+	+	-	-	-	-	-	+	+	-		
SIL1	+	+	-	-	+	+	-	+	+	-	-	-	+	+	-	

Transmission electron microscopy

Transmission electron microscopy was performed to provide detailed cross-sections of cells on the PSTi and PLL substrata. In all sections, prominent cell structures like nucleus, mitochondria, ribosomes and rough endoplasmic reticulum appeared to be well preserved.

Titanium coating, seen as an electron-dense layer, covered the substratum surface very uniformly. On the narrow grooves cells bridged the grooves, contacting only the ridges. In contrast, on wider groove patterns, cells had descended into the grooves, and contacted the groove bottom (Figure 7a,b). Further, a striking observation was that the ridges on the substrate appeared to be somewhat rounded.

On PLL substrates generally a similar cell morphology was observed. In contrast with the PSTi substrates, on this material the cells were never able to establish contacts with the bottom of the grooves. This was observed both for the wide as the narrow groove patterns (Figures 7c,d). In contrast to the PSTi substrates, with the PLL the surface pattern appeared to be very sharp.

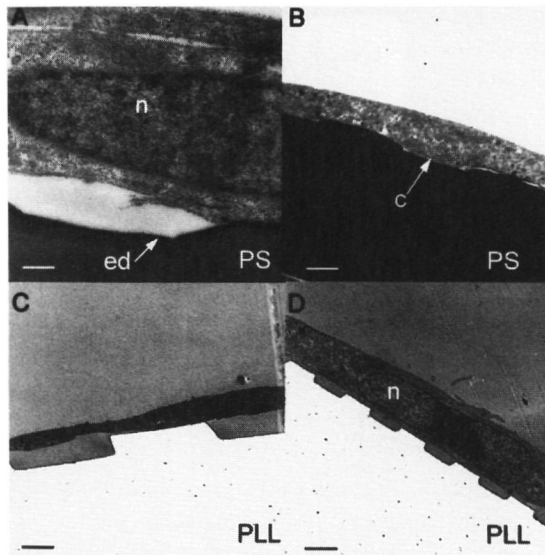


Figure 7: Transmission electron micrographs of cells on microgrooved substrates. PS = polystyrene, PLL = poly-l-lactic acid, n = nucleus. A) PSTi2: Note the electron dense (ed) layer, and the bridging of the grooves by the cells. Bar = 0.25 μm . B) PSTi10: Note that cells descend into the grooves, and contact (c) the groove bottom. Bar = 4 μm . C) PLL5: Note that the cells bridge the grooves. Bar = 1.2 μm . D) PLL2: Bar = 2 μm .

DISCUSSION

In this study, we determined the behaviour of fibroblasts on microgrooved culturing substrata with a standardized texture, but with different chemical composition. The proliferation assay showed that cells proliferated exponentially on all used culturing materials that were RFGD treated. This indicates that each material was suitable for the attachment and proliferation of fibroblasts. On the non-RFGD treated substrates, cell numbers initially stayed the same or even decreased, indicating poor cellular attachment or cell death. This result strongly correlates with the findings of the wettability measurements, i.e. the materials with the highest contact angles were found to be the least favorable for cell attachment. Nevertheless, after five days the cells that attached seem to proliferate in a similar way as the treated substrates. Apparently, as observed before^{24,25}, absence of RFGD treatment resulted in a delay of proliferation.

Of the substrates that were given a glow discharge treatment, PLL showed the highest proliferation. Here, cell proliferation was not correlated perfectly with the measurements of wettability. Of course, wettability is not the only factor involved in cell behaviour. Certain chemical groups, present on the surface of the material can alter cell response²⁶. Besides, we have to remark that PLA is a biodegradable material. Degradation of the PLA could alter surface roughness and composition, and therefore influence the final behaviour of cells on the material. Current pilot experiments, using atomic

force microscopy (AFM), already showed this degradation of the surface of PLA materials

The polystyrene used in this study, has to be considered as a reference material. First, because polystyrene is the most commonly used material for cell culturing techniques. Second, because we already used this material in earlier studies on the effect of surface texture on fibroblast behaviour. The current observations agree also with these previous studies, i.e. that almost no alignment is observed on wide grooves, and strong cellular orientation on narrow grooves.^{7, 22, 27}

Titanium was used as a substrate material, because it is still the most widely used implant material. The titanium was applied as a thin coating on the textured polystyrene. We know that the chemical composition of such a titanium coating is not completely similar to bulk titanium material. On the other hand, we have to emphasize that in an earlier study in our group, textured bulk titanium substrates were used.¹² The current SEM and TEM findings corroborate perfectly with this earlier study. Only the cell alignment results are somewhat different. In the earlier study, improved alignment was observed with decreasing groove width, while in the current study no such relationship was seen. Two explanations can be given for this observation. First, in the bulk titanium study, the prepared surface grooves had a depth of 1-2 μm . In our study, the groove depth was only 0.5 μm . We know that groove depths affect cellular orientation.²⁷ A further explanation for the lesser alignment is provided by the TEM analysis of the PST₁ substrates. The applied layer of titanium seemed continuous, and the deposition does have exactly the same thickness throughout the whole coated area. However, it was observed in TEM that the groove pattern had lost its sharp edges. Probably, this is caused by the developed heat during the evaporation of the titanium onto the thermoplastic polymer material.

From this last observation an important conclusion can be drawn. Some studies propose that contact guidance is a result of preferential protein adsorption on sharp surface discontinuities, like the edges of ridges on microgrooved substrates.^{3, 28} In the PST₁ substratum, no sharp discontinuities are present, but still these textures are potent of inducing contact guidance. This implies that such preferential adsorption theories are probably not valid. Consequently, we suggest again that contact guidance is caused by mechanical forces on the cells' filopodia, which cause the cells to reshape actin filaments here, and adjust to the substrate topography.⁷

The casting of PLL has proven to be of the same accuracy as PS. It is obvious from the SEM and CLSM analysis that the RDF had strongly aligned to the surface grooves, and showed a much more rounded morphology than on the other materials. Especially on the 1 μm wide grooves, cells seem to be extremely spindle-like. Also, in contrast with the other materials, TEM revealed that on PLL the cells are nowhere able to establish contacts with the bottom of the grooves, neither on wide, nor on narrow groove patterns. We assume, that this is due to the hydrophobic nature of the PLL, even after RFGD treatment. Probably, PLL adsorbs specific serum proteins differently than the other materials, or adapt the conformational state of these proteins. Despite the shallowness of our grooves, we can also not exclude for all our samples that the RFGD treatment does not reach the bottom of the microgrooves. If the penetration of the treatment is insufficient for the grooves, the resulting would be an additional pattern of different wettabilities between grooves and ridges. Such an additional patterning effect will be enhanced when the to be treated material is already very hydrophobic, and not really "sensitive" for RFGD. This could explain why no cell contacts with the bottom of the grooves were formed, and the cells were caused to bridge the grooves.^{29, 30}

SEM observations of the SIL substrates showed that the reproduction of the surface patterns was not as accurate, compared to PS. This was already observed earlier by Den Braber *et al.*²³ in a TEM study with microtextured silicone rubber. We suppose that this is due to the viscoelastic properties of silicone. Silicone has a relative high viscosity. If this viscosity is too high, the silicone might not be able to flow into the sharp corners of the grooves. The more viscous a reproductive material is, the poorer the quality of reproduction of the mold. Besides surface patterns, we have to notice that also the mechanical properties of silicone differ significantly from the other used materials. This is also obvious in the scanning electron micrographs. Apparently, the morphology of the cells is influenced by the shape of the substratum, but substratum is also deformed by the forces applied by the cells. Similar observations have been done in earlier studies²³. We have to emphasize that the distorted shape of the grooves in combination with the inferior reproduction of the surface patterns makes it very complex to compare results from studies on contact guidance performed on silicone with studies using textures in other materials.

In summary we can conclude that the accuracy of microtexture production depends greatly on the used material. Also coating techniques, as described in many studies, can affect the applied patterns and subsequent contact guidance. Nevertheless, even if no sharp discontinuities are present, microtextures can still induce contact guidance. Consequently, explaining contact guidance by the use of preferential adsorption theories seems unlikely. Finally, there is a definitive influence on cell morphology and behaviour, caused by differences in the used substrate. Material properties like wettability or elasticity are just as well of influence on cellular behaviour, as the topographical properties like texture size and shape.

LITERATURE

- 1 A F Von Recum, C E Shannon, E C Cannon, K.J. Long, T G Van Kooten, and J. Meyle, "Surface roughness, porosity, and texture as modifiers of cellular adhesion," *Tissue Engineering*, **2**, 241-253 (1996).
- 2 D M. Brunette, "Effects of surface topography on cell behaviour *in vitro* and *in vivo*," in: *Nanofabrication and biosystems*, H C Hoch (ed), Cambridge University Press, New York, 1996, 335-366
- 3 A S G. Curtis, and C Wilkinson, "Topographical control of cells," *Biomaterials*, **18**, 1573-83 (1997).
- 4 P. Weiss, "Experiments on cell and axon orientation *in vitro* the role of colloidal exudates in tissue organization," *J Exp Zool*, **100**, 353-386 (1945)
- 5 A F Von Recum, and T G van Kooten, "The influence of micro-topography on cellular response and the implications for silicone implants ," *Journal of Biomaterials Science - Polymer Edition*, **7**, 181-198 (1995)
- 6 G J Picha, and R F Drake, "Pillared-surface microtexture and soft-tissue implants. effect of implant site and fixation," *J Biomed Mat Res*, **30**, 305-312 (1996).
- 7 X F Walboomers, H.J E. Croes, L.A. Ginsel, and J A. Jansen, "Growth behaviour of fibroblasts on microgrooved polystyrene," *Biomaterials*, **19**, 1861-1868 (1998)
- 8 K Chesmel, and J. Black, "Cellular responses to chemical and morphologic aspects of biomaterial surfaces. I. A novel *in vitro* model system" *J Biomed Mat Res*, **29**, 1089-1099 (1995).
- 9 J. Meyle, K Gültig, and W Nisch, "Variation in contact guidance by human cells on a microstructured surface," *J Biomed Mater Res*, **29**, 81-88 (1995).
- 10 S. Britland, H. Morgan, B Wojak-Stodart, M. Riehle, A Curtis, and C. Wilkinson, "Synergistic and hierarchical adhesive and topographic guidance of BHK cells," *Exp Cell Res*. **228**, 313-325 (1996).

Chapter 4

- 11 P. Clark, P. Connolly, A.S.G. Curtis, J.A.T. Dow, and C.D.W. Wilkinson, "Topographical control of cell behaviour. I Simple step clues," *Development*, **99**, 439-448 (1987).
- 12 E.T. den Braber, H V Jansen, M J de Boer, H J E Croes, M. Elwensproek, L.A Ginsel, and J.A Jansen, "Scanning electron microscopic, transmission electron microscopic, and confocal laser scanning microscopic observation of fibroblasts cultures on microgrooved surfaces of bulk titanium substrata," *J Biomed Mater Res* , **40**, 425-433 (1998).
- 13 D.M. Brunette, G.S. Kenner, and T.R.L. Gould, "Grooved titanium surfaces orient growth and migration of cells from human gingival explants," *J Dent Res* , **62**, 1045-1048 (1983).
- 14 B. Cheroudi, T.R.L. Gould, and D M. Brunette, "Effects of a grooved titanium-coated implant surface on epithelial cell behaviour in vitro and in vivo," *J. Biomed Mater Res* , **23**, 1067-1085 (1989)
- 15 P T. Ohara, and R.C Buck, "Contact guidance in vitro A light, transmission, and scanning electron microscopic study," *Exp Cell Res* , **121**, 235-249 (1979)
- 16 J. Meyle, K Gültig, H Wolburg, and A F. von Recum, "Fibroblast anchorage to microtextured surfaces," *J Biomed Mater. Res* , **27**, 1553-1557 (1993).
- 17 R.E Baier, and V.A. DePalma, "Electrodeless glow discharge cleaning and activation of high-energy substrates to insure their freedom from organic contamination and their receptivity for adhesives and coatings," *Calspan Report*, **176** (1970).
- 18 C.F Amstein, and P A Hartman, "Adaptation of plastic surfaces for tissue culture by glowdischarge," *J Clin Microbiol.*, **2**, 46-54 (1975).
- 19 J A. Chinn, T A. Horbett, and B D Ratner, "Laboratory preparation of plasticware to support cell culture," *J Tiss Culture Meth* , **16**, 155-159 (1994).
- 20 H P. de Jong, A.W.J. van Pelt, and J. Arends, "Contact angle measurements on human enamel - an in vitro study of influence of pellicle and storage period," *J. Dent. Res.*, **61**, 11-13 (1982).
- 21 Freshney, R.I., *Culture of animal cells a manual of basic technique* New York, Alan R. Liss Inc , 1987
- 22 E.T den Braber, J.E. de Ruijter, L.A Ginsel, A F von Recum, and J A. Jansen, "Orientation of ECM protein deposition, fibroblast cytoskeleton, and attachment complex components on silicone microgrooved surfaces," *J Biomed Mater Res*, **40**, 291-300 (1998)
- 23 E.T den Braber, J.E. de Ruijter, H.J.E. Croes, L.A. Ginsel, and J.A Jansen "Transmission electron microscopical study of fibroblast attachment to microtextured silicone rubber surfaces," *Cell and Materials*, **7**, 31-39 (1998).
- 24 J A Jansen, J P C.M van der Waerden, and K. de Groot "Effect of surface treatments on attachment and growth of epithelial cells," *Biomaterials*, **10**, 604-608 (1989).
- 25 J A Jansen, J P C M van der Waerden, and K de Groot "Fibroblast and epithelial cell interactions with surface-treated implant materials," *Biomaterials*, **12**, 25-31 (1991)
- 26 T G Ruardy, J M Schakenraad, H C van der Mei, and H J Busscher "Preparation and characterization of chemical gradient surfaces and their application for the study of cellular interaction phenomena," *Surf Science Reports*, **29**, 1-30 (1997)
- 27 X.F. Walboomers, W Monaghan, A S.G. Curtis, and J A Jansen "Attachment of fibroblasts on smooth and microgrooved polystyrene," *J Biomed Mater Res*, **46**, 212-220 (1999)
- 28 R E Baier, and A E Meyer "Implant surface preparation," *Int J Maxillofac Impl* , **3**, 9-20 (1988)
- 29 S Britland, P. Clark, P Connolly, and G Moores, "Micropatterned substratum adhesiveness: a model for morphogenetic cues controlling cell behaviour," *Exp Cell Res* , **198**, 124-129 (1992)
- 30 P Clark, P Connolly, and G R Moores, "Cell guidance by micropatterned adhesiveness *in vitro*," *J Cell Sci* , **103**, 287-292 (1992)

Early spreading events of fibroblasts on microgrooved substrates

Walboomers, X F , and Jansen, J A
Journal of Biomedical Materials Research, in press (1999)

INTRODUCTION

Various studies already proved that substrate surfaces provided with micrometer-sizes grooves force the cells cultured on them to align to these features^{1,4}. This phenomenon is known as 'contact guidance'⁵. On basis of a previous study, we suggested that this contact guidance phenomenon is probably based on mechanical clues^{6,7}. The breakdown and formation of fibrous cellular components, is influenced by microgrooves. They create a pattern of mechanical stress, which influences cell spreading and causes cell alignment. Besides, we also noticed that the extracellular matrix (ECM) possesses certain specific mechanical properties. Many *in vitro* studies already indicated that cell-generated forces of tension can actually re-organize the organization of the ECM into structures that direct the behaviour of single cells^{8,12}. As cells cannot penetrate in narrow (<2 µm) or deep (>0.5 µm) grooves, and only attach to the ridge surface^{13,14}, the exerted forces can achieve a reorganization of deposited ECM proteins. Definitely, this will have an effect on cellular spreading and elongation. In this way, alignment, and directed cell migration will be established. Of course, the validity of this theory has to be proven in further studies.

If indeed mechanical clues are the basis of contact guidance, we would expect the phenomenon to occur from the earliest phases of cell spreading, directly after cell attachment. In view of this, cellular behaviour (i.e. cytoskeletal formation) has to be examined, shortly after attachment.

Therefore, the current investigation is aimed at further investigating the influence of microgrooves on initial cell morphology and cytoskeletal development. To further unravel the role of the cytoskeleton, cells were also incubated in the presence of the actin polymerization inhibitor cytochalasin-B^{15,16}.

MATERIALS AND METHODS

Substrate production

Using photo-lithographic techniques, microgrooved patterns were made in a three inch silicon wafer (Twente Microproducts, Enschede, the Netherlands). The wafer was divided into 4 quadrants with a ridge- and groove width of 1, 2, 5 or 10 µm and a groove depth of 0.5 µm. This wafer was used as a mold for the production of substrates for cell culturing. For the production of smooth, control surfaces, non-textured glass plates were used. Polystyrene (PS) was solvent cast in a similar manner as described by Chesmel and Black^{17,18}. A casting solution was made by dissolving bits from tissue culture PS (Greiner, Germany) in chloroform (LabScan, UK) (25 g/150 ml) and stirring gently for 24 hrs. After casting of 3 ml of this solution on the molds, the chloroform was evaporated overnight in a laminar flow hood. Replicas were removed from the molds, and PS rings were glued to them, using a small amount of the casting solution. In this way, tissue culture dishes were created of 2.1 cm in diameter. Just before use, all substrates used for cell culturing were given a radiofrequency glow discharge (RFGD) treatment^{19,21}, for 5 minutes at 100 mTorr, to improve the surface wettability of the substrates.

Cell culture

Rat dermal fibroblasts (RDF) were obtained from the ventral skin of male Wistar rats, using standard procedure as described by Freshney ²². To ensure quick and constant availability cells were cryo-preserved. Before experimentation, cells were thawed and cultured in MEM- α (Gibco) containing Earle's salts, L-glutamine, 15% FCS, gentamicin (50 $\mu\text{g/ml}$). All experiments were performed with 5th culture generation cells. Prior to the assays, cells were detached with a solution of 0.25% Trypsin / 1 mM EDTA (pH 7.2), for 2 minutes. Subsequently, cells were washed and resuspended in culturing medium. For each experiment, about 15 thousand cells were seeded per square centimeter on the various experimental substrates. Cells were incubated for 15, 30, 45, 60, 120, or 240 minutes. All experiments were also performed with addition of cytochalasin-B to the culturing medium, at a concentration of 2.5 $\mu\text{mol/L}$.

Light microscopy

Quantitative information on cell spreading was obtained using light microscopy (LM). After the various incubation periods, the cells were fixed in methanol p.a., stained in methylene blue dye, washed in milliQ water, and dried in iso-propanol. Subsequently, they were observed with use of a Leica DM RBE light microscope. Digital micrographs were made using a Donpisha 3CCD camera attached to a computer that was equipped with Leica Qwin Pro software (v. 2.2, Leica, Germany). These images were analyzed using Scion Image software (v. beta-2, based on NIH image software for MacIntosh; ScionCorp, Frederick, Maryland, USA). Measurements were made in 12 randomly chosen areas of observation of 0.2 mm^2 . First we measured the numerical cell adhesion, by counting the total number of cells in the area of observation. The attachment percentages were calculated by considering 100% cell attachment to occur on the smooth control surfaces. Second, cell orientation was measured, as the angle between the long axis of the cell and direction of surface grooves. Third, cell surface area space occupied by each cell was determined. Statistical analysis was performed using an analysis of variance (ANOVA), followed by a Student Newman Keuls test ($p < 0.05$). Analysis of the orientation assay was performed with a unpaired t-test. All statistics were performed with StatMost (v. 2.01, DataMost corporation, Salt Lake City, USA). Data are the result of two separate experiments. In each experiment all substrates were present at least in twofold.

Scanning electron microscopy

Qualitative information on the morphology of the cells was obtained using scanning electron microscopy (SEM). After the various incubation periods, the cells were fixed in 2% v/v glutaraldehyde in 0.1 M sodium-cacodylate buffered solution, for 5 minutes. Cells were rinsed in cacodylate buffered solution, dehydrated in a series of ethanol, and dried in tetramethylsilane (TMS, Merck) to air. Finally specimens were sputtercoated with a thin layer of gold, and examined in a JEOL 6310 scanning electron microscope. One experiment was performed, with all substrates present in threefold.

Confocal laser scanning microscopy

Components of the cytoskeleton were imaged using fluorescent antibody-staining techniques. For this purpose, cells were fixed for 20 minutes in 2% paraformaldehyde and permeabilized with 1% Triton X100. Then, filamentous actin was stained with phalloidin-TRITC (Sigma), diluted in phosphate buffer containing 1% BSA to block aspecific epitopes. Finally, the specimens were examined with a Biorad MRC 1000 confocal laser scanning microscope (CLSM) system. Digital micrographs were made, and analyzed using Scion Image software.

Actin organization was evaluated using a method described by Sinha *et al.*²³. For this purpose, the cells were divided into three types. Type I cells display a faint staining with no discernable actin filament formation; Type II cells show cortical filaments below the cell membrane with some radially oriented filaments; and Type III cells have distinct, well formed actin filaments that are oriented parallel to one another and to the long axis of the cell. For each specimen an average of 20 cells was observed. Statistical analysis was performed using an analysis of variance (ANOVA), followed by a Student Newman Keuls test ($p < 0.05$). Data are the result of two separate experiments. In each experiment all substrates were present in twofold.

RESULTS

Light microscopy

Figure 1 shows the numerical cell adhesion, relative to smooth control surfaces. Statistical analysis revealed that at 30 and 45 minutes of incubation, cell numbers on all grooved surfaces were significantly lower compared with smooth control surfaces. After this time point, cell numbers increased to comparable levels. Finally, after 4 hours of culturing the cell number found on 1 μm wide grooves was significantly higher than on smooth surfaces.

Quantitative evaluation of the number of attached cells in cultures that were incubated with cytochalasin-B showed that up to 2 hours almost no cells had attached. Only after 2 and 4 hours of incubation, fibroblasts were present. Nevertheless, cell numbers were extremely low compared to the normal cultures ($< 25\%$). Therefore, for the rest of the quantitative experiments with cytochalasin supplemented culture medium no time points before 2 hours were examined.

Figure 2 shows the distribution of cellular orientation. The calculated median angles between cells and direction of the grooves, as well as the data distribution are shown in a box-whisker plot. The boxes indicate 25th to 75th percentile, and the whiskers indicate the 5th and 95th percentile of the data. Cellular alignment with the surface grooves, is characterized by a very low median, and a relatively small distribution. If no alignment exists, the median is about 45 degrees, with a large dispersion. The data showed that no orientation occurred at any time point on the smooth surfaces. Furthermore, we found that the occurrence of cell orientation for different groove sizes started at different time points. On 1 μm wide grooves, strong cell orientation was found after 1 hour; on 2 and 5 μm wide grooves after 2 hours; and on 10 μm wide grooves after 4 hours of incubation (Figure 3). The measurements regarding cellular orientation in the presence of cytochalasin-B are presented in Figure 4. On the 1 μm wide grooves, orientation was seen after 2 hours. After 4 hours, cells were also found to be oriented on 2 μm wide grooves. In addition, the rate of orientation on 1 μm textures was further increased. On the

5 and 10 μm wide grooves and smooth control surfaces no orientation was observed.

Figure 5 shows the surface area covered by the cells, during cell spreading. After 15 and 30 minutes the area was relatively small. Cells did not spread (area $< 10 \mu\text{m}^2$). From 45 minutes on the area started to increase, indicating that spreading had started. The standard deviation at these time points is very high. Evidentially not all cells start spreading at the same time. Although at 2 and 4 hours cell spreading on the 1 and 2 μm surfaces appeared to be less, no significant differences in cell area could be determined between smooth and the various textures at any incubation time.

Cells that were cultured in the presence of cytochalasin-B after 2 and 4 hours showed less spreading. These cells covered surface areas that were comparable to normal cultures, at 1 and 2 hours respectively.

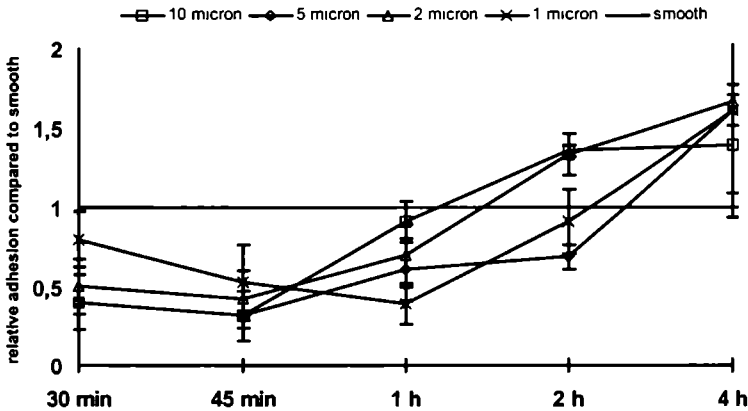


Figure 1: Numerical cell numerical adhesion in time, relative to smooth control surfaces (=1). There are no differences between the textures At 30 and 45 minutes cell numbers are lower than 1, whereas they are significantly higher than 1 on 1 μm after 4 hours.

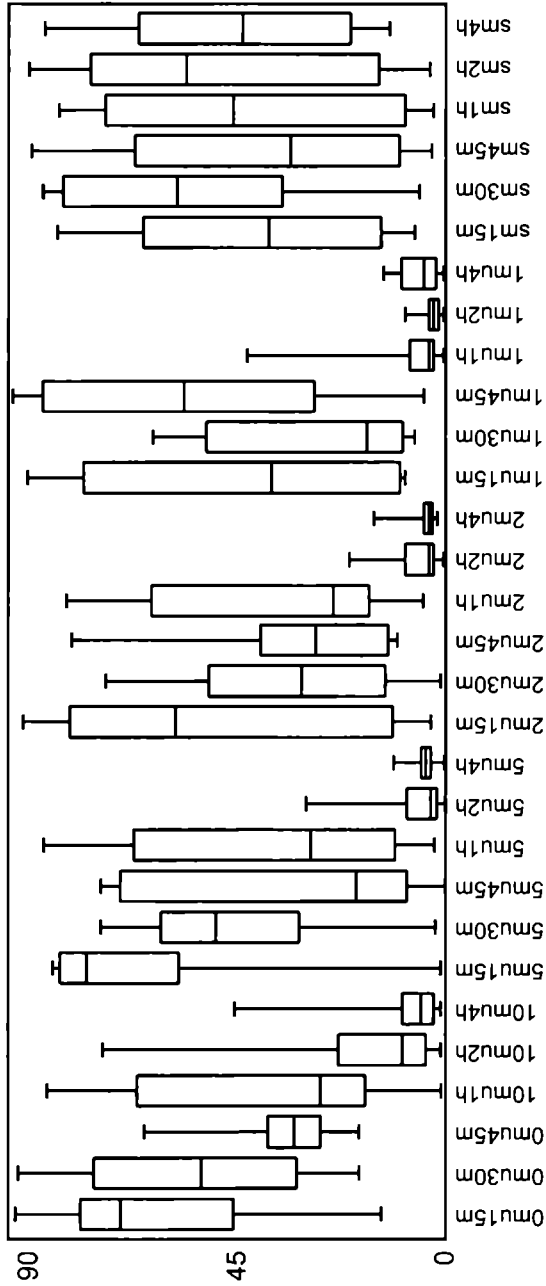


Figure 2: Box-whisker plot showing the distribution of cellular orientation. Note that no orientation is observed on smooth surfaces, and that the onset of orientation is dependent on the applied groove size. 10µ15m means 10 µm wide grooves and 15 minutes of culturing, etcetera

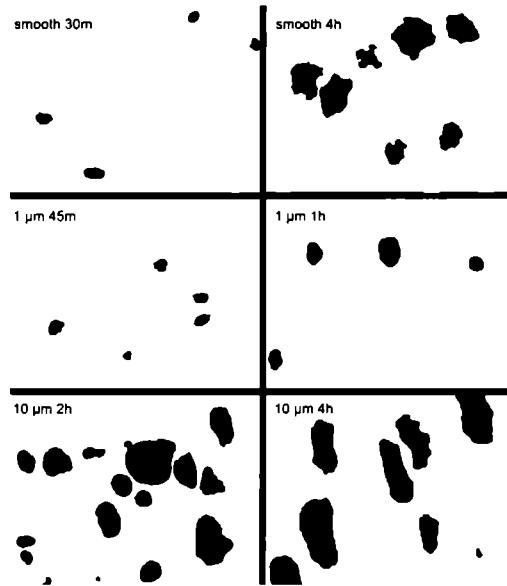


Figure 3: Digitalized light micrographs of cells on various substrates. On smooth surfaces no alignment is observed. On 1 μm wide grooves, cellular orientation is established after 1 hour, on 10 μm wide grooves cellular orientation is only found after 4 hours of incubation. Original magnification 20x.

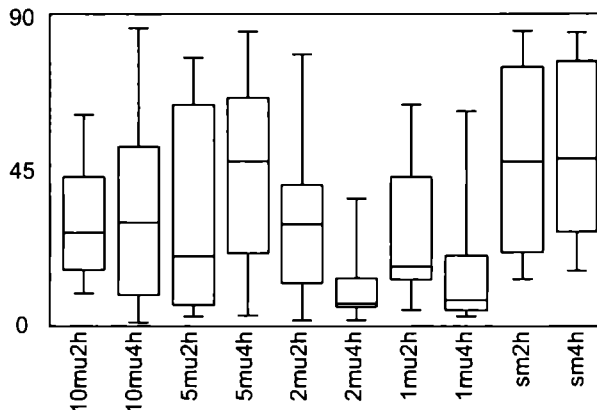


Figure 4: Cellular orientation, in cultures supplemented with 2,5 $\mu\text{mol/L}$ cytochalasin-B. No orientation is observed, except for 1 μm textures at 2 hours, and 1 and 2 μm at 4 hours.

Scanning electron microscopy

Figures 6a-b show scanning electron micrographs of representative cells on microgrooved substrates. It was observed that after 15 minutes cells exhibited a very rounded morphology. After 30 minutes, cells showed extensive membrane extensions in all directions. After 45 minutes, the cell surface seemed smooth again, and cells were spreading. Finally, after 4 hours of incubation cells were totally flattened.

Figures 7a-b show SEM micrographs of a similar experiment, in the presence of cytochalasin-B. After 15 minutes no cells could be found on the substrates. After 30 and 45 minutes, only some rounded cell fragments were found. Notably, after 2 and 4 hours, the fibroblasts seemed to have spread like the cells that were cultured without the presence of cytochalasin, but with a marked delay.

Confocal laser scanning microscopy

Figure 8a-c are representative micrographs of the actin staining of cells cultured on the various surfaces. We observed that up to 2 hours of incubation actin staining remained rather diffuse. This indicated the absence of well-formed cellular actin filaments. On the other hand, apparent differences were seen after 4 hours, between smooth and all textured substrates. Cellular actin was better developed in cells that were cultured on microgrooved surfaces. Actin fibers were aligned to the surfaces grooves. Cells in the cultures supplemented with cytochalasin-B showed no distinct cellular actin skeleton, even after 4 hours of incubation.

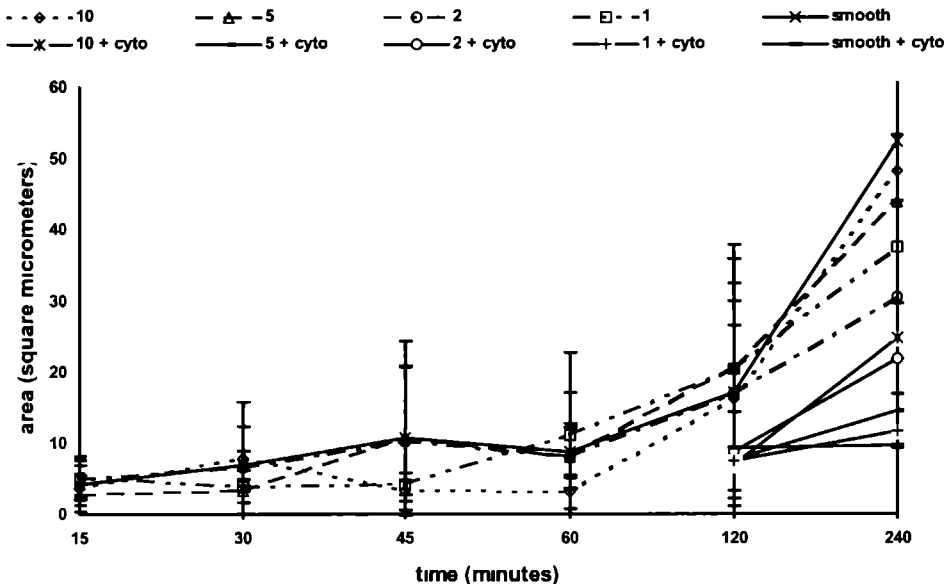


Figure 5 Surface area covered by the cells. Note that from 45 minutes, the size of the areas start to increase. No differences in cell area could be determined between smooth surfaces, and the various textures. Cells incubated in the presence of cytochalasin-B show a delay in spreading.

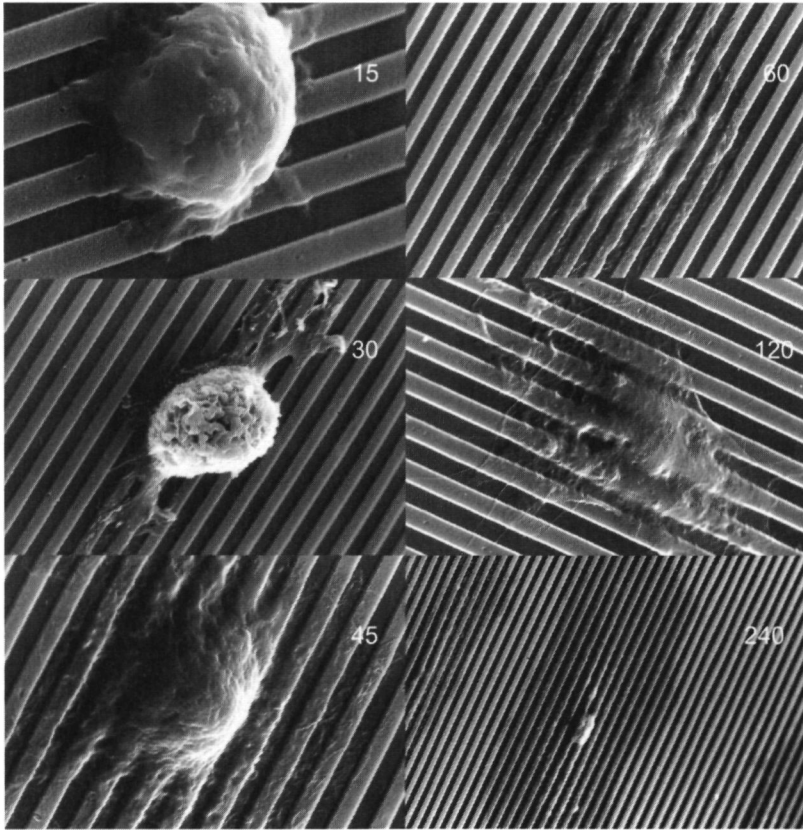


Figure 6a: Scanning electron micrographs of cells on substrates with 2 μm wide grooves. Extensive membrane extensions in all directions are formed after 30 minutes. Original magnifications 5500x, 2500x, 3500x, 2300x, 3000x, and 900x.

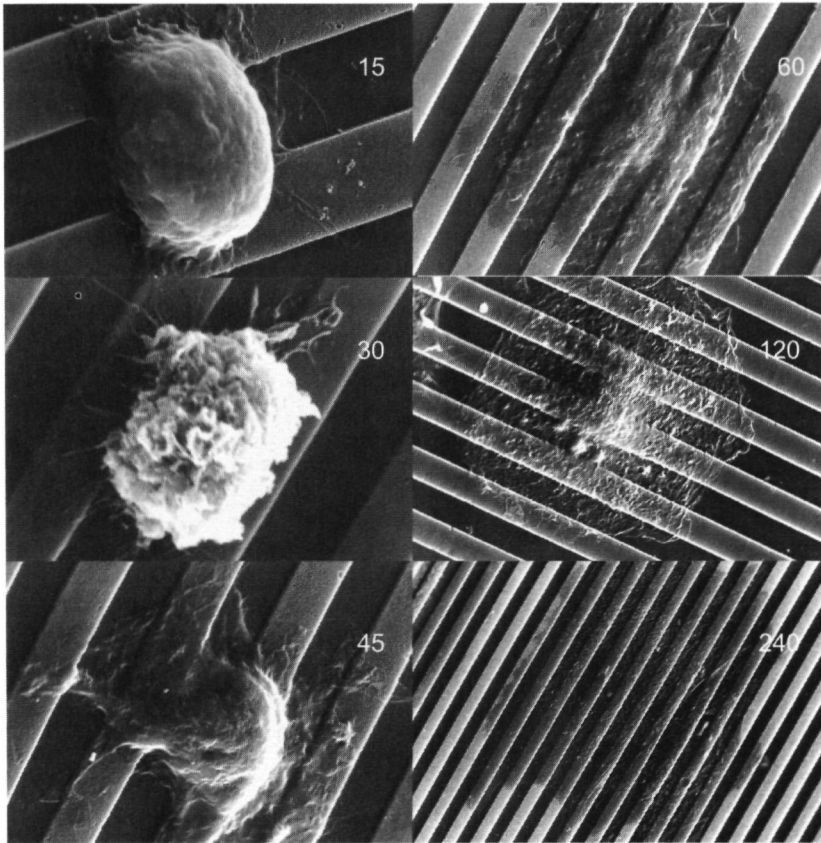


Figure 6b: Scanning electron micrographs of cells on substrates with 5 μm wide grooves. Original magnifications 5500x, 5500x, 3500x, 2300x, 1700, and 850x.

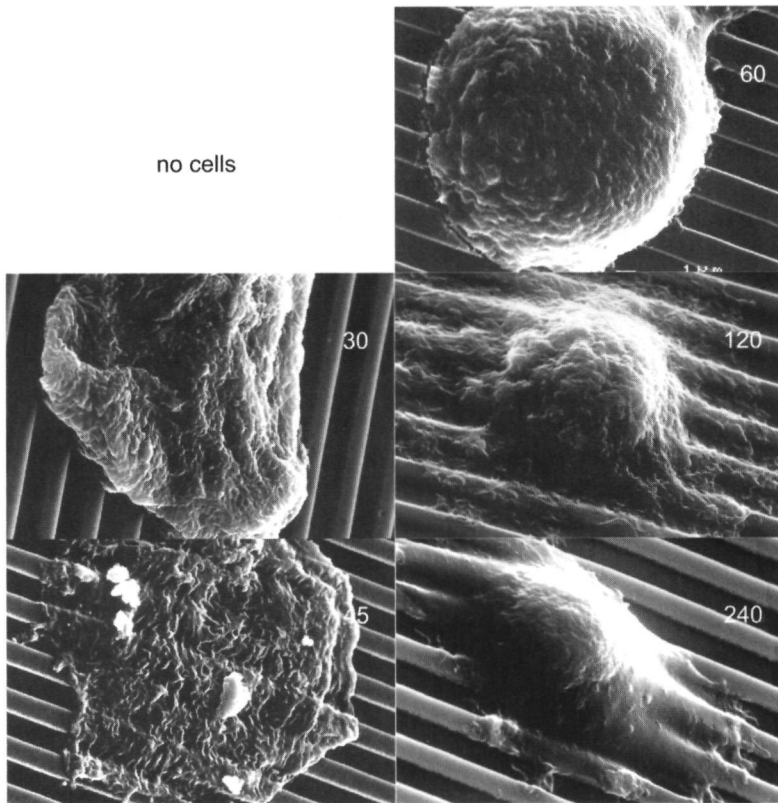


Figure 7a: Scanning electron micrographs of cells on substrates with $2\ \mu\text{m}$ wide grooves, in the presence of cytochalasin-B. After 2 and 4 hours the fibroblasts have spread like cells that were cultured without the presence of cytochalasins. Original magnifications 3300x, 3000x, 4300x, 3500x, and 3500x.

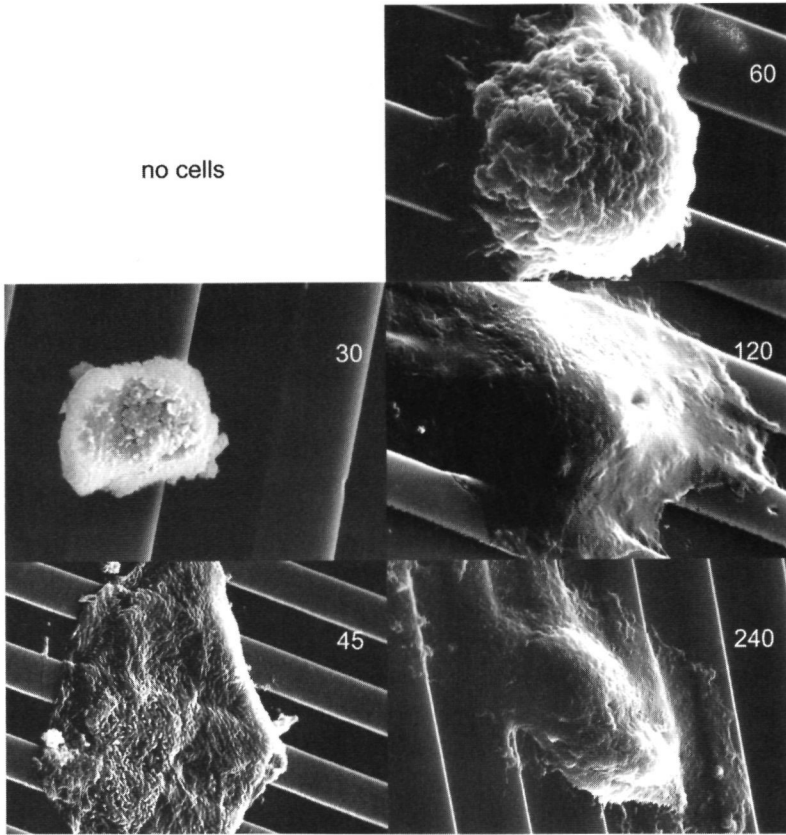


Figure 7b: Scanning electron micrographs of cells on substrates with 5 μm wide grooves, in the presence of cytochalasin-B. Original magnifications 5500x, 2200x, 5000x, 3000x, and 2300x.

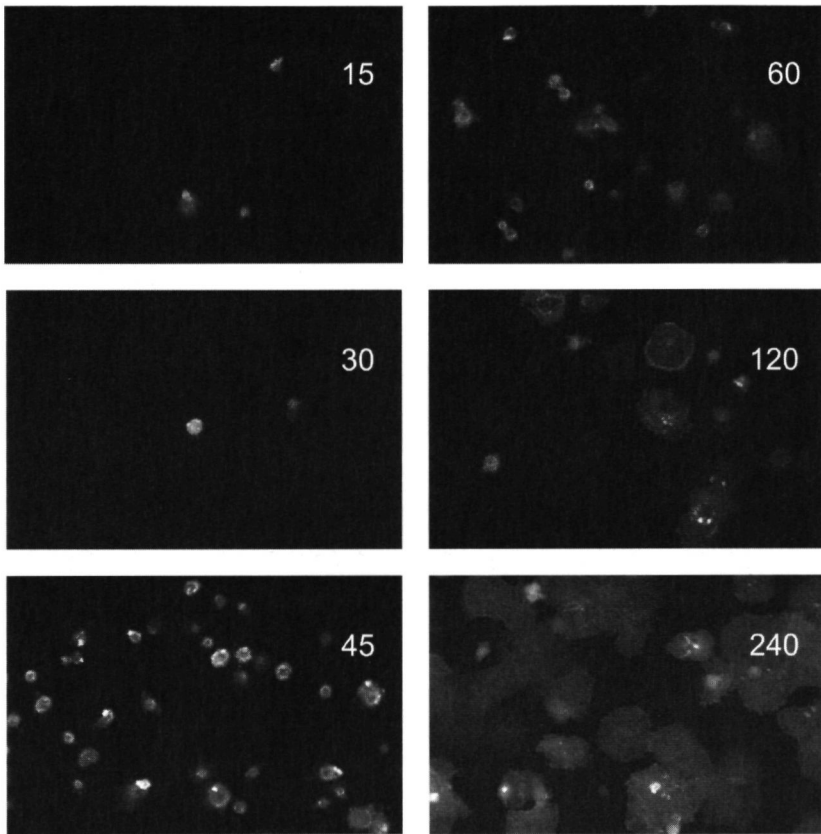


Figure 8a: Confocal laser scanning micrograph of actin-stained cells on a smooth substrate. In the early phases of cell spreading actin staining remains diffuse. Original magnification 20x.

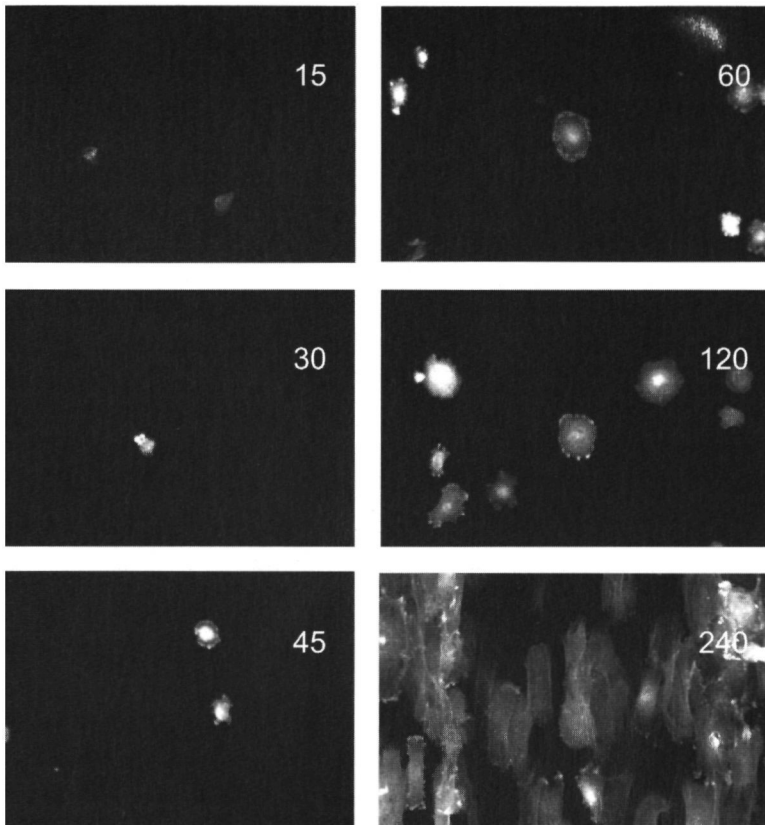


Figure 8b: Confocal laser scanning micrograph of actin-stained cells on a substrate, equipped with 2 μm wide grooves. Note that differences occur after 4 hour with smooth substrates, where cellular actin is less developed. Original magnification 20x.

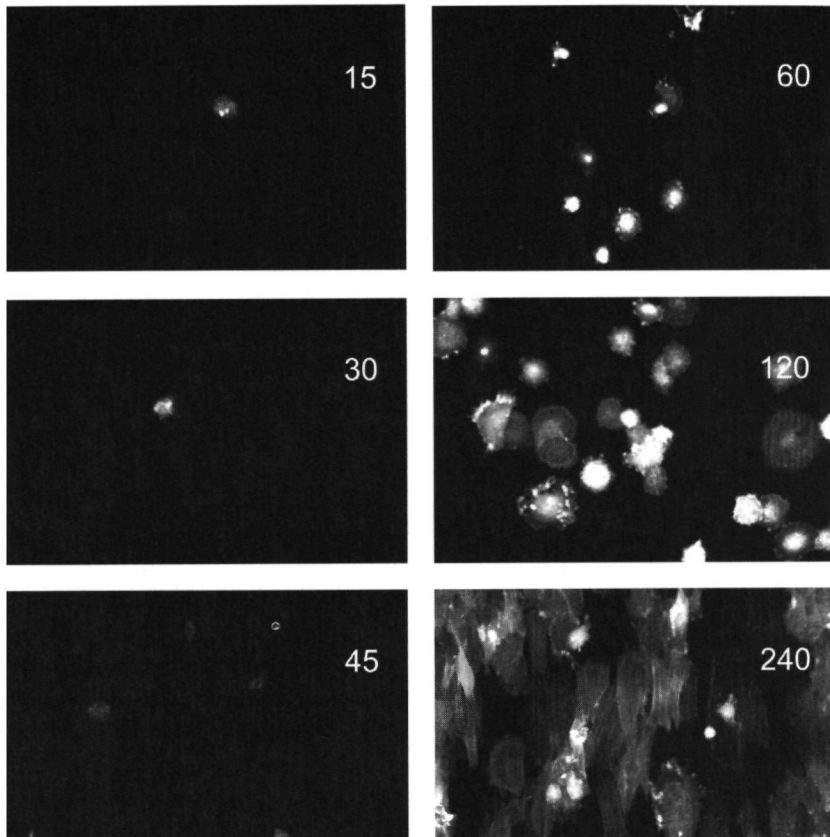


Figure 8c: Confocal laser scanning micrograph of actin-stained cells on a substrate, equipped with 5 μm wide grooves. Original magnification 20x.

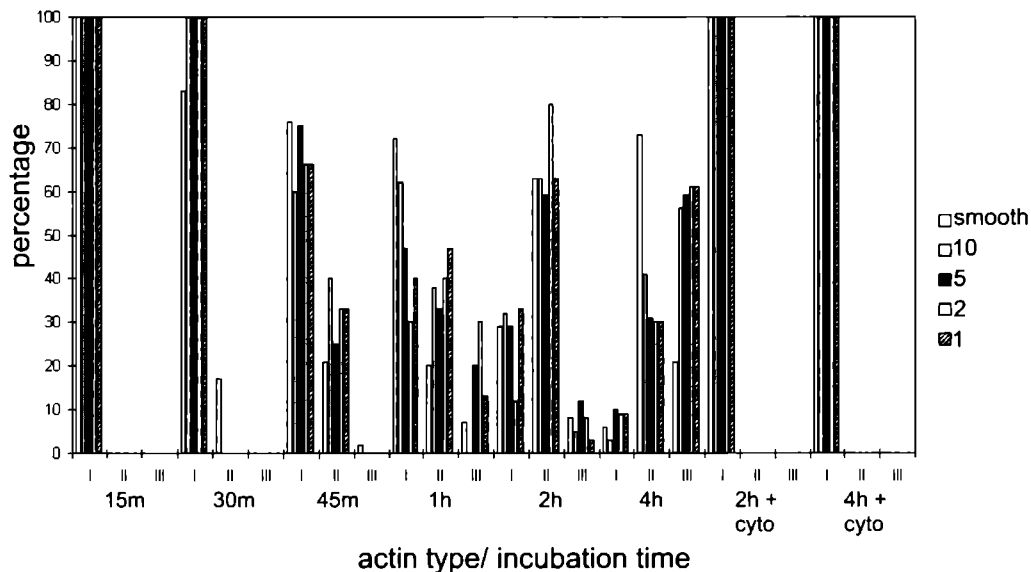


Figure 9: Actin typing of the cells from the CLSM micrographs. After 15 minutes of culturing, all cells exhibit type I. Later also type II and III are observed. No differences between the various textured substrates were found. Smooth surfaces cells are the first to exhibit types II and III (after 45 minutes), but after 4 hours still exhibit little type III actin. Cells incubated in the presence of cytochalasin-B only exhibit type I.

Actin typing (Figure 9) revealed that after 15 minutes of culturing, all cells exhibited type I actin organization. After longer culturing periods, also type II and III were observed. No differences were present among the various textured substrates, but significant differences were found between textured and smooth control surfaces. On smooth surfaces, cells were the first to exhibit type II (after 30 minutes) and type III (after 45 minutes). Strikingly, cells on smooth surfaces after 4 hours still exhibited mostly type II and very little type III. On the other hand, after 4 hours of incubation, on the textured surfaces type III expression was more pronounced. Finally, all cells cultured in the presence of cytochalasin-B exhibited type I staining only.

DISCUSSION AND CONCLUSIONS

Our study confirmed again that surface microgrooves influence *in vitro* fibroblast behaviour. The numerical cell attachment evaluation revealed that no differences existed between the various textures. In contrast, significant differences were observed with smooth control surfaces. At the early time points a decrease is seen, but at later phases cell attachment drastically increased to levels like, or even

exceeding that of smooth surfaces. A reasonable explanation for this observation is that the formation of organized cell-substrate contact junctions is hampered on textured surfaces. As a consequence no stable cell adhesion can be ensured resulting in initially reduced attachment percentages.

The importance and effect of the formation of cell adhesions is confirmed by the morphology and orientation assays. SEM images showed that after 30 minutes the cells formed abundant membrane extensions. Probably, the cell is then in the process of exploring and probing the surface. Of course, these extensions are made in all directions, since in its natural environment a cell is totally surrounded with neighbouring cells and ECM material. When the presence of suitable attachment sites is confirmed, contacts are established with the ECM proteins as deposited on the substrate surface. Thereafter, the cells exert forces on these adhesive junctions and start to spread. In case of a microgrooved substrate surface, cellular spreading is associated with a rapid orientation parallel to the surface grooves. In view of this, we have to notice that the driving force which finally results in cellular alignment is clearly determined by the groove dimensions. As we observed, surfaces provided with the narrowest grooves induced faster orientation.

To determine the effect of the actin cytoskeleton in the cell alignment process, we typed the actin organization as occurred within the cells during time. CLSM showed that up to 2 hours no distinct (type III) cellular actin filaments were present. Even after 4 hours, the amount of type III filaments was still limited (about 60%). This is remarkable, since in the light microscopical assays, cells were already found to be aligned at these time points. The importance of this finding is further emphasized in the comparative experiments where cytochalasin-B was added to the cultures. Cytochalasin-B is an active inhibitor of actin polymerization. It is especially effective in the actin microspikes in the lamellopodia.¹⁵ Surprisingly, cells still aligned to the 1 and 2 μm grooves after 4 hours of incubation. Apparently, as confirmed by the attachment, SEM and CLSM results, the chemical is only able to postpone cell attachment and subsequent spreading. Except this delay, no other obvious effect on cell shape could be determined. These findings corroborate with studies of Oakley *et al*¹⁶, who also reported that the addition of cytochalasin results in a delay of cell spreading.

Finally, besides the morphological appearance, we found that cellular alignment had no effect on the totally occupied cell area. This indicates that oriented cells have gained in length associated with a proportional decrease in width. This finding is in contrast with earlier studies by Chehroudi *et al*²⁴ and den Braber *et al*¹³, in which cellular alignment could only be related to a decrease in cell width complemented by a small increase in cell height. We suppose that this difference is due to the used cell type, and substrate material. Chehroudi used epithelial cells, which are much smaller in size. Den Braber used silicone rubber substrates on which cell spreading is lower than on more hydrophilic polystyrene substrates.²⁵

In conclusion, the results suggests that 1) a well formed cellular actin cytoskeleton is no prerequisite for the occurrence of contact guidance, and 2) orientation of cytoskeletal actin filaments in the cell body is more the result than the origin of cell alignment. This hypothesis is supported by our observation that even if type III actin filaments in the cell body are absent, cellular alignment still occurs. Consequently, we assume that a clear distinct has to be made between the cellular actin skeleton, and actin microspikes that are present in the cells lamellopodia. The alignment of cells on microgrooves is not dependent on the properties or the dynamics of a formed actin cellular

cytoskeleton. The delay of spreading by administration of cytochalasin-B confirms that the breakdown and formation of fibrous components in the filopodium appear to be a much bigger determinant in the establishment of contact guidance.

Usually, cell movement starts with a cell making thin extensions in all directions. These lamellopodia contain short filamentous pieces of actin, so-called microspikes. Here, actin monomers attach so that the growing end of the spikes abuts the front edge of the lamellopodium. If a microspike meets a precursor contact, i.e. a non-specific approach of the cell membrane to the substrate surface, this contact is stabilized^{26,27}. We suggest that at this stage contact guidance is already induced. The forces of attraction and rejection between surface-adsorbed ECM molecules and probing membrane extensions are the determining factor²⁸⁻³⁰. Subsequently, vinculin and other proteins accumulate. Eventually, the adhesions will mature into a complete focal adhesion (a cluster of integrins). This focal adhesion induces the further formation of the actin stress fiber into the cytoplasm.

Our theory also corroborates the results found in our previous *in vitro* studies^{14,25}. For instance, we observed that the depth of the applied grooves is an important factor in determining the rate of cellular alignment¹⁴. The direction of the forces exerted onto the ECM is related to the direction of the grooves. Besides, the deeper the grooves get, the more the cells will be unable to attach to the bottom of the groove. As a consequence, with increasing groove depth cell spreading will predominantly occur along the ridges on the surface. This phenomenon is also independent of the design of the surface texture. It will occur on all surfaces where discontinuities can be detected by cells. This confirms why there is no need for the presence of sharp surface texture, as we observed before²⁵. Finally, the theory explains why the substrate material itself has also influence on contact guidance. In general, the physico-chemical properties of a substrate material determine the quantity, strength, and conformation of ECM absorption. As a consequence, via this pathway the amount of force that cells can exert onto these proteins, and thus their spreading behaviour is influenced²⁵.

LITERATURE

- 1 Singhvi R, Stephanopoulos G, Wang DIC. Review effects of substratum morphology on cell physiology. *Biotechnol Bioeng* 1994; 43, 764-771
- 2 Von Recum AF, Shannon CE, Cannon EC, Long KJ, Van Kooten TG, Meyle J. Surface roughness, porosity, and texture as modifiers of cellular adhesion *Tissue Engineering* 1996, 2, 241-253.
- 3 Curtis ASG, Wilkinson C Topographical control of cells. *Biomaterials* 1997; 18; 1573-1583
- 4 Brunette DM. Effects of surface topography on cell behaviour *in vitro* and *in vivo*. in: *Nanofabrication and biosystems*, H C. Hoch (ed), Cambridge University Press, New York, 1996, 335-366.
- 5 Weiss P. Experiments on cell and axon orientation *in vitro*. the role of colloidal exudates in tissue organization. *J Exp Zool* 1945, 100; 353-386.
- 6 Walboomers XF, Croes HJE, Ginsel LA, Jansen JA. Growth behaviour of fibroblasts on microgrooved polystyrene. *Biomaterials* 1998; 19, 1861-1868.
- 7 Jansen JA. Textured and porous materials. In. *Biomaterials science: an introduction to materials in medicine* second edition, B.D. Ratner (ed), Academic press, San Diego, California, 1999, submitted.
- 8 Vernon RB, Sage EH. Between molecules and morphology *Extracellular matrix and creation of vascular form*. *Am J Pathol* 1995; 147, 873-883.

- 9 Erickson HP. Reversible unfolding of fibronectin type III and immunoglobulin domains provides the structural basis for stretch and elasticity of titin and fibronectin Proc Natl Acad Sci USA 1995; 91; 10114-10118.
- 10 Choquet D, Felsenfeld DP, Sheetz MP. Extracellular matrix rigidity causes strengthening of integrin-cytoskeleton linkages Cell 1997; 88; 39-48.
- 11 Janmey PA, Chaponnier C. Medical aspects of the actin cytoskeleton. Curr Opin Cell Biol 1995; 7; 111-117
- 12 Janmey PA. The cytoskeleton and cell signaling: component localization and mechanical coupling. Physiol Rev 1998; 78; 763-781.
- 13 Den Braber ET, de Ruijter JE, Smits HTJ, Ginsel LA, von Recum AF, Jansen JA. Quantitative analysis of fibroblast morphology on microgrooved surfaces with various groove and ridge dimensions Biomaterials 1996, 17; 2037-2044.
- 14 Walboomers XF, Monaghan W, Curtis ASG, Jansen JA Attachment of fibroblasts on smooth and microgrooved polystyrene. J Biomed Mater Res 1999; 46; 212-220.
- 15 Cooper JA Effects of cytochalasin and phalloidin on actin J Cell Biol 1987, 105; 1473-1478
- 16 Oakley C, Jaeger NA, Brunette DM. Sensitivity of fibroblasts and their cytoskeletons to substratum topographies: topographic guidance and topographic compensation by micromachined grooves of different dimensions. Exp Cell Res 1997; 234; 413-424.
- 17 Chesmel K, Black J. Cellular responses to chemical and morphologic aspects of biomaterial surfaces I. A novel *in vitro* model system J Biomed Mater Res 1995; 29; 1089-1099.
- 18 Chesmel K, Clark CC, Brighton CT, Black J. Cellular responses to chemical and morphologic aspects of biomaterial surfaces II The biosynthetic and migratory response of bone cell populations. J Biomed Mater Res 1995; 29, 1101-1110.
- 19 Baier RE, DePalma VA. Electroless glow discharge cleaning and activation of high-energy substrates to insure their freedom from organic contamination and their receptivity for adhesives and coatings Calspan Report 1970; 176.
- 20 Amstein CF, Hartman PA Adaptation of plastic surfaces for tissue culture by glowdischarge J Clin Microbiol 1975, 2, 46-54.
- 21 Chinn JA, Horbett TA, Ratner BD. Laboratory preparation of plasticware to support cell culture J Tiss Culture Meth 1994; 16; 155-159.
- 22 Freshney RJ. Culture of animal cells a manual of basic technique New York, Alan R Liss Inc , 1987.
- 23 Sinha RK, Morris F, Shah SA, Tuan RS Surface composition of orthopaedic implant metals regulates cell attachment, spreading, and cytoskeletal organization of primary human osteoblasts in vitro. Clin Orthop 1994, 305, 258-272.
- 24 Chehroudi B, Soorany E, Black N, Weston L, Brunette DM Computer-assisted three-dimensional reconstruction of epithelial cells attached to percutaneous implants. J Biomed Mater Res 1995, 29, 371-379
- 25 Walboomers XF, Croes HJE, Ginsel LA, Jansen JA Contact guidance of rat fibroblasts on various implant materials J Biomed Mater Res 1999; 47; 204-212.
- 26 Small JV, Anderson K, Rottner K Actin and the coordination of protrusion, attachment and retraction in cell crawling. Biosc Reports 1996, 16, 351-368.
- 27 Mitchinson TJ, Cramer LP Actin-based cell motility and cell locomotion. Cell 1996, 84, 371-379
- 28 Palecek SP, Horwitz AF, Lauffenburger DA Kinetic model for integrin-mediated adhesion release during cell migration. Ann Biomed Eng 1999; 27; 219-235
- 29 Palecek SP, Huttenlocher A, Horwitz AF, Lauffenburger DA Physical and biochemical regulation of integrin release during rear detachment of migrating cells J Cell Sci 1998, 111; 929-940
- 30 Palecek SP, Loftus JC, Ginsberg MH, Lauffenburger DA, Horwitz AF Integrin-ligand binding properties govern cell migration speed through cell-substratum adhesiveness Nature 1997, 385, 537-540

The effect of microgrooved poly-l-lactic acid on osteoblast-like cells *in vitro*

Matsuzaka, K., Walboomers, X.F., de Ruyter, J.E., and Jansen, J.A.
Biomaterials **20**, 1293-1301 (1999)

INTRODUCTION

Currently, there is an increasing need for biomaterials, which not only allow and support cellular attachment, spreading and growth, but which also improve cellular function. For example, in the treatment of periodontitis or periimplantitis, bony defects of the alveolar ridge have to be reconstructed. Besides grafting procedures, guided tissue regeneration (GTR) has been suggested as treatment technique^{1,2}. The principle of GTR is sealing off a bone defect around the tooth root or implant surface by means of a synthetic membrane to improve healing. The membrane acts as a mechanical barrier. It excludes undesirable cells from the wound area and creates a secluded space into which cells from the surrounding bone can migrate. The membranes are not involved in a real regeneration of the required tissue, e.g. by guidance or migratory stimulation of the involved cells. Already a lot of different materials have been used in GTR. Despite some favorable reports, GTR is still frequently associated with significant clinical problems^{3,4,5}, like preliminary exposure of the membrane to the oral cavity, and deformation or collapse of the membrane. Consequently, the outcome of this therapy is still unpredictable^{6,7,8}.

In view of the above mentioned problems with GTR materials, we have to notice that the biological properties of an implant material are determined by bulk as well as surface properties. Important bulk properties are chemical composition and mechanical characteristics. Surface properties considered of interest are: surface free energy and surface geometry. In addition, these various material parameters have different effects. While surface free energy specifically influences cell adhesion, chemistry and surface geometrical properties are of importance for cell spreading and growth. For extensive reviews about the relationship implant material and biological interactions reference can be made to the excellent reviews by Schakenraad⁹, von Recum¹⁰, Harris¹¹, and Shinghvi *et al*¹². Briefly, four different components are supposed to be involved in the orientation, growth and differentiation of cells to substrate surfaces, i.e. (1) serum components adsorbed to the substratum, (2) extracellular matrix components secreted by the cell, (3) cell adhesion molecules, like integrins, and (4) cytoskeleton. Through the use of *in vitro* experiments, considerable progress has been made in the understanding of cell-substratum interactions.

Recognizing the importance of material surface properties to manipulate cellular growth and orientation in relation to the problem associated with GTR, the purpose of the current *in vitro* study is to evaluate the potential of microtextured surfaces for periimplant and periodontal bone regeneration.

MATERIALS AND METHODS

The production of substrates

Using photo-lithographic techniques, microgrooved patterns were made in silicon wafers (Twente Microproducts, Enschede, the Netherlands). Three types of wafers with different groove depths i.e. 0.5, 1.0 and 1.5 μm were produced. Each wafer surface was divided into 4 quadrants with a ridge and groove width of 1, 2, 5 and 10 μm . The wafers were used as templates to make polymeric surface replicas. For this purpose, the templates were covered by polystyrene (PS) or polylactic acid (PLA) casting solution. The PS solution was made by dissolving PS bits from a culture dish in chloroform (25g / 150ml). The PLA solution was made by dissolving PLA (Purasorb, poly-l-lactide, Purac Biochem B. V., Gorinchem, The Netherlands) in chloroform (5g / 150ml). After evaporation of the chloroform, the PS and PLA surface replicas were removed from the templates. The dimensions of the obtained surfaces are summarized in table 1.

Table 1: Dimensions of the micro features on the substrates surfaces (Gd = groove depth, G-R w = groove and ridge width, PLA = poly-l-lactic acid, PS = polystyrene)

	Gd (μm)	G-R w (μm)
PLA or PS 0.5-1	0.5	1.0
PLA or PS 0.5-2	0.5	2.0
PLA or PS 0.5-5	0.5	5.0
PLA or PS 0.5-10	0.5	10.0
PLA or PS 1.0-1	1.0	1.0
PLA or PS 1.0-2	1.0	2.0
PLA or PS 1.0-5	1.0	5.0
PLA or PS 1.0-10	1.0	10.0
PLA or PS 1.5-1	1.5	1.0
PLA or PS 1.5-2	1.5	2.0
PLA or PS 1.5-5	1.5	5.0
PLA or PS 1.5-10	1.5	10.0
PLA or PS smooth	0.0	0.0

Before use, out of the center of each microtextured sheet a 20mm diameter round disc was cut, which contained all 4 different groove / ridge dimensions as present on each wafer (Figure 1). Besides, four

additional 15mm round discs were cut out of each microtextured sheet. All experimental substrates were washed manually in 80% ethanol. Then, they were air-dried and bonded to a polystyrene ring (inside diameter 20mm or 15mm) with a small amount of the casting solution. Finally, all substrates were treated by a radiofrequency glow-discharge (RFGD) treatment (PDC-3XG, Harrick; Argon, 0.1Torr, 5 min). For comparative reasons, smooth control substrates were manufactured in the same way using non-textured silicon wafer as moulding surface. The surface characterization of the produced materials was described before by our group^{13,14}.

Cell culture

For biological evaluation of the test materials a rat bone marrow cell culture technique was used as described by Maniatopoulos¹⁵. Briefly, bone marrow cells were obtained from femora of male Wistar rats, 40 to 43 days of age (100-130 g). Epiphyses were cut off, and both diaphyses were flushed out, using alpha-MEM (Gibco, Life Technologies BV, Breda The Netherlands) supplemented with 10% fetal calf serum (FCS, heat induced at 56 °C for 35 min., Gibco), 50 mg/ml freshly prepared ascorbic acid (Sigma, Chemical Co., St. Louis, MO., USA), 10mM Na beta-glycerophosphate (Sigma), 10⁻⁸ M dexamethason (Sigma) and antibiotic (gentamicin). Per femur 15 ml of this medium was used. Cells were suspended and cultured in three 80 cm² tissue culture flasks (Nunc Products by Gibco). Finally, cultures were incubated in a humidified atmosphere of 95% air, 5% CO₂ at 37 °C.

After 8 days of primary culture, cells were detached using trypsin/ EDTA (0.25% w/v trypsin/ 0.02% EDTA; pH 7.2). Subsequently, cells were resuspended in the supplemented culture medium as described above, and used for the experiments.

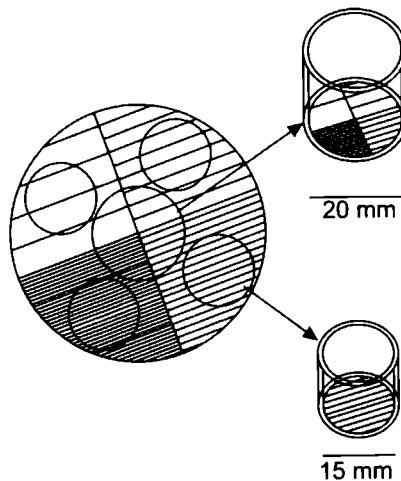


Figure 1: schematic drawing of the manufacturing of the substrates. From a textured mold, replicas were made in polystyrene or poly-L-lactic acid. Onto these replicas rings were glued. In this way tissue culture dishes were produced, one with a 20mm diameter containing 4 different textures, and four with a 15mm diameter each containing one texture.

Scanning electron microscopy

Cell suspension (approximately 15×10^3 cells / substrate) was seeded to smooth and each type of grooved 20mm disc. The cultures were incubated for 8 or 16 days to evaluate the influence of the substrate surface composition and geometry on RBM cell morphology and extracellular matrix (ECM) synthesis using a scanning electron microscope (SEM). At the end of both incubation times, the non-attached cells on the various substrates were removed by rinsing twice with 0.1M sodium-cacodylate buffer (pH 7.4, 37 °C). Subsequently, fixation was carried out for 5 minutes at room temperature in 2% glutaraldehyde in the same buffer. Cells were rinsed in cacodylate buffered solution, dehydrated in a series of ethanol, dried by tetramethylsilane (Merck, Germany) and sputter-coated with gold. Finally, they were observed in a JEOL 6310 scanning electron microscope at an accelerating voltage of 15kV. Three runs of experiments were carried out, which included all different samples in threefold.

To observe the contact side of the cells and ECM with the substrate, the multilayer of cells of the 16 days specimens was scratched and peeled off using a needle and forceps. This layer was turned upside down, sputter coated with gold and examined with SEM. Also the original specimens were examined again, to observe if any residual layer was left.

Tetracycline assay

In this experiment again approximately 15×10^3 RBM cells were seeded on smooth and all different grooved 20mm substrates. A fluorescent technique, as described by Todescan *et al* (1996), was used to quantify the calcified ECM produced by the RBM cells. Where bone mineral is being formed, tetracycline antibiotics bind to hydroxyapatite, through chelating with calcium. Therefore, starting from incubation day 3 tetracycline (9 µg/ml) replaced the early mentioned antibiotics (Gentamicin) in the culture medium. After 16 days of incubation, the medium was removed, the cultures were rinsed twice in 70% ethanol, and finally dehydrated in 100% ethanol at 4 °C for 6 hours. Subsequently, the cultures were allowed to dry in a dark room. After drying, a Biorad MRC 1000 confocal laser scanning microscope (CLSM) was used to visualize fluorescence. This CLSM was equipped with a krypton / argon mixed gas laser (Ion Laser Technology, Salt Lake City, UT, USA), which was mounted on a Nikon diaphot microscope with non-cover glass objective lens (Nikon, X 40). The specimens were illuminated at an excitation wavelength of 488 nm. For each groove depth and width, 10 randomly chosen areas were imaged. The 10 observed areas covered in total 7.15mm^2 of the substrate.

The resulting digital images were stored on hard disc. Digital image analysis of the images was performed using Scion image software (v beta-2, based on NIH Image, Scion corp, Frederick, Maryland, USA). Mineralization was quantified by calculating the area of the excited pixels, and expressed as a percentage of the total surface area. Three runs of experiments were carried out. In each run, all substrates were measured in tenfold.

Measurement of alkaline phosphatase activity

Approximately 10×10^3 RBM cells were seeded on smooth and all types of grooved 15mm substrates. The cultures were incubated for 8 and 16 days. After removal of the culture medium, the cell layers were rinsed in PBS. Then, demineralized H_2O (milliQ) was added to each substrate and specimens were put on ice. Finally, the cells were harvested with a rubber policeman and the cell suspension was

transferred in a 10 ml tube. The cells were sonicated for 10 minutes, and centrifuged at 2000 rpm for 10 minutes. Subsequently, 100 μ l aliquot of this cell lysate was added to 100 μ l working reagent in a 96 well culture plate and incubated for 1 hour at 37 $^{\circ}$ C. The working reagent consisted of 0.5M 2S-amino-2methyl-1-propenyl (Sigma, St. Louis, MO), 5mM p-nitrophenol phosphate (Sigma), and 5mM magnesium chloride (1:1:1). The reaction was stopped using 100 μ m of 0.3M sodium hydroxide, and the finally absorbance read at 405nm using a microplate reader (Biorad 450, USA).

To determine the Alkaline Phosphatase (ALP) specific activity, protein production from the same lysate was determined using the Pierce BCA protein assay (Pierce, Rockford, IL). A 150 μ l aliquot of the cell lysate was added to 150 μ l of BCA working reagent in 96 well culture plate and incubated for 2 hours at 37 $^{\circ}$ C. Absorbance was measured at 562 nm using the microplate reader. The ALP specific activity was determined using the following formula:

$$ALP \text{ specific activity } (\mu\text{mol}/\mu\text{g}/\text{sec}) = \frac{ALP \text{ conc. } (\mu\text{mol}/\text{ml})}{\text{protein conc. } (\mu\text{g}/\text{ml})} \times \frac{1}{ALP \text{ incubation time (sec)}}$$

Two runs of experiments were carried out. In each run, two specimens of each sample type were used.

RESULTS

Scanning electron microscopical observation

Scanning electron microscopy showed that all substrates were covered with osteoblast-like cells after 8 days of incubation. The cells had a very flattened appearance on both PS and PLA substrates. Cells cultured on the grooved substrates were aligned parallel to the surface grooves. In contrast, cells on the smooth surfaces grew in an at random orientation. Cell protrusions on all 1 and 2 μ m grooved substrates attached predominantly to the surface ridge. In contrast, on the 5 and 10 μ m substrates cell protrusions attached also to the bottom of the grooves (Figure 2-a, b). Further, cells cultured on the 1 and 2 μ m grooved surfaces appeared to span the surface grooves independent on the groove depth. The cells on the 5 and 10 μ m surfaces protruded into the grooves. Frequently, the cells on these surfaces did contact with the bottom of the grooves.

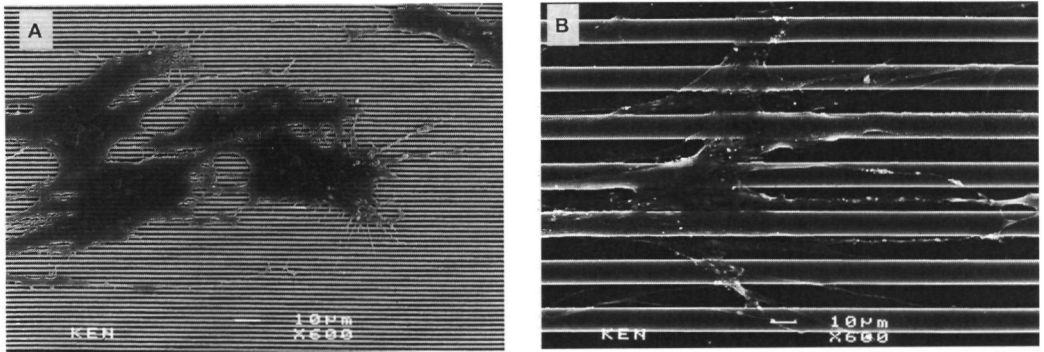


Figure 2: Scanning electron micrographs of RBM cells on grooved surfaces after 8 days of incubation. a) a PLA 1.5-1 substrate; Note that cell extensions attach to the groove ridge and b) a PS 1.5-10 substrate; Note that cell extensions attach to both ridge and bottom.

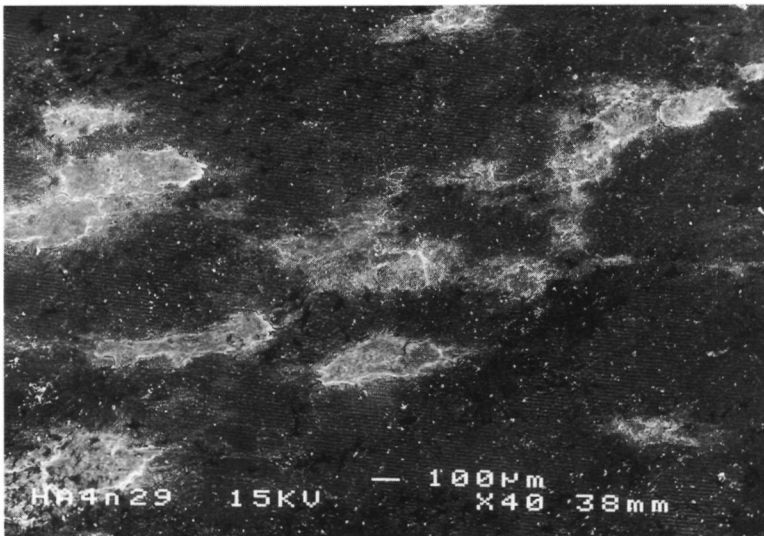


Figure 3: Scanning electron micrographs showing the formation of ECM on PS1.0-2 surface after 16 days of incubation. Note that layers of mineralized ECM can be observed onto the cells.

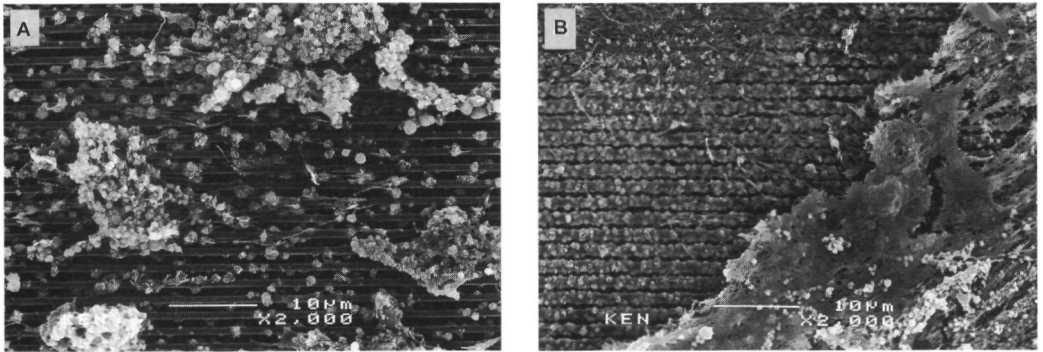


Figure 4: Scanning electron micrographs of microtextured substrates, after scratching. The multilayer of cells is removed, but still substrates are covered with a residual layer of ECM. a) a PS1.0-1 substrate. Note that calcified globuli are covering the entire substrate, and b) a PLA1.5-1 substrate. Here, calcified globuli are preferentially attached to the surface ridge.

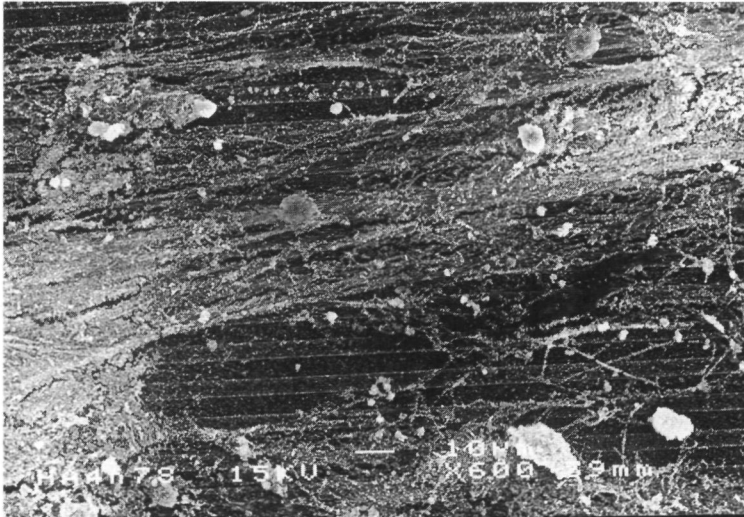


Figure 5: Scanning electron micrograph of RBM cells on PLA0.5-5 surface after 16 days of incubation. Note that in general the deposited collagen bundles were aligned parallel to the surface pattern.

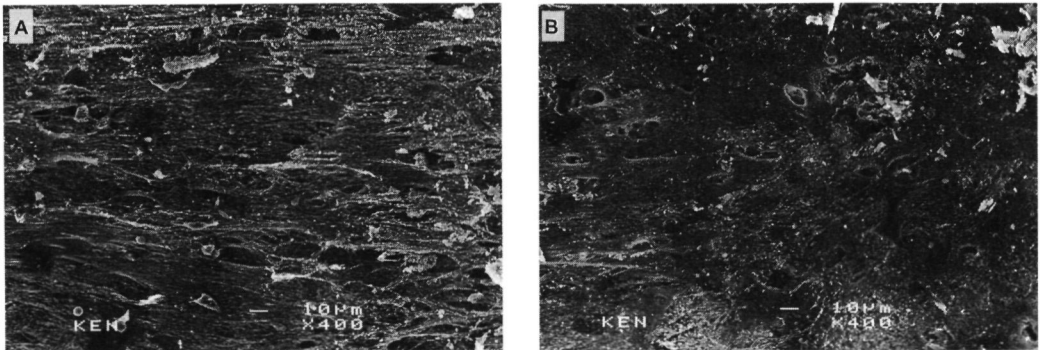


Figure 6: Scanning electron micrographs of the scratched-off cellular/ ECM layers. The side that originally contacted the substrate is shown. A) a PLA 1.0-2 substrate, and b) a PS 0.5-2 substrate.

After 16 days of incubation, a layer of mineralized globuli was seen on all substrates. On the grooved surfaces, the globular accretions were aligned parallel to the surface grooves (Figure 3). Further, on the 0.5 and 1.0 μm depth PS substrates calcified globuli were also formed on the bottom of the grooves. A different situation was observed on the 1.5 μm deep PS and all types of PLA substrates (Figure 4-a, b). On these surfaces mineralized globuli were mainly attached to the ridges. Besides this mineralized layer, a rich fibrous collagen matrix was observed. The deposited collagen bundles were oriented parallel to the surface grooves irrespective of the groove dimensions (Figure 5).

Figure 6 shows SEM images of mineralized ECM in contact with the substrate side. It was observed that the ECM on 1.0 and 1.5 μm deep PLA substrates was oriented more to the groove direction, than on 0.5 μm deep PLA, and all types of PS substrates.

Tetracycline assay

The tetracycline labeling experiment confirmed the aligned direction of the produced mineralized layers on the grooved surfaces. Figure 7 shows the image analysis results. Statistical evaluation was performed by ANOVA testing, to reveal if significant differences existed between similar groups. If so, post-ANOVA Tukey testing was performed. It was found that on grooved substrates more fluorescent labeling was found, than the smooth control substrates. This was true for both the PS and PLA material. Furthermore, smooth PLA exhibited more labeling than smooth PS. Between the various grooved PS substrates no differences could be found. If the grooved PS substrates were compared with the grooved PLA substrates, it was seen that only on PLA with 1.0 μm deep grooves significantly more labeling was found. Between the grooved PLA substrates some differences were found, but only among the 1.0 μm deep grooves. Here, it was found that most mineralized ECM appeared to be deposited on the substrates with a groove width of 1 or 2 μm .

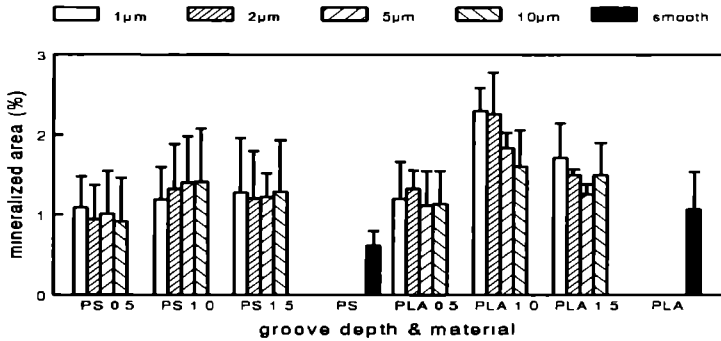


Figure 7: Diagram showing the results of the tetracycline assay, indicating the rate of ECM formation. The mineralized surface area is expressed as a percentage of the total surface area. The bars indicate the mean, intervals represent the standard deviation.

Measurement of alkaline phosphatase activity

Figure 8 and 9 show the results of the alkaline phosphatase activity (ALP) assay. Again statistical evaluation was performed using an ANOVA test, to reveal if significant differences existed between similar data groups. Because not all data groups contained the same number of measurements, post-ANOVA testing was performed using a Student-Newman-Keuls test instead of a Tukey test.

In Figure 8, results are presented for pooled data with as varying parameter groove depth. In general, the ALP activity of RBM cells on PLA and PS surfaces after 16 days of incubation was higher, compared to that after 8 days. After 8 days, it was observed that ALP activity on 0.5 and 1.5 µm deep textures in PS were higher compared to the smooth PS surfaces. Between the various PLA substrates no differences were found. When PS and PLA were compared, also no differences were found. After 16 days, it was observed that ALP activity on 1.0 and 1.5 µm deep textures in PS was higher, compared to the activity found on smooth surfaces. Also between the various PLA substrates some differences were found; here 0.5 and 1.5 µm deep textures showed more ALP activity than the smooth control substrates. When PS and PLA were compared, all groups were different. Cells cultured on PLA showed more ALP activity, except for 1.0 µm deep textures where activity on PS was higher.

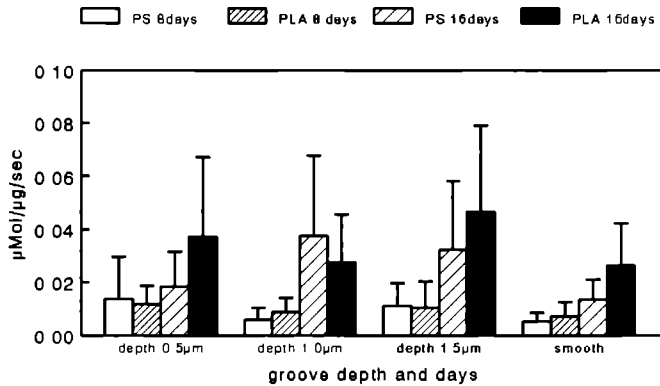


Figure 8: Diagram showing results of the alkaline phosphatase specific activity assay Results are pooled for each groove depth The bars indicate the mean, the intervals represent the standard deviation

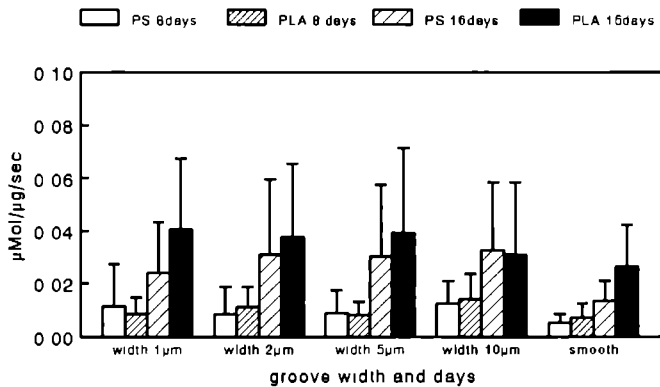


Figure 9: Diagram showing the results of the alkaline phosphatase specific activity assay Results are pooled for each groove width The bars indicate the mean, the intervals represent the standard deviation

In Figure 9, results are presented for pooled data with as varying parameter the groove width. Again, the ALP activity of RBM cells on PLA and PS surfaces after 16 days of incubation proved to be higher than on 8 days. After 8 days, it was observed that ALP activity on all grooved substrates was higher, compared to that on the smooth surfaces. This was found for both the PS as the PLA material. When PS and PLA were compared, no differences could be found. After 16 days, again it was observed that ALP activity on grooved substrates was higher, compared to that found on the smooth surfaces. And also again, this was found for both the PS as the PLA material. When PS and PLA were compared, only few differences were found. On 1 μm wide and on smooth PLA substrates, it was observed that cells showed more ALP activity, compared to their PS counterparts.

DISCUSSION

The biocompatibility of an implant-material is determined by various factors, including its surface topography. In this study we evaluated growth behaviour of osteoblast-like rat bone marrow cells on microgrooved polystyrene and poly-L-lactic acid substrates. Polystyrene was chosen because it is the most common material used in cell and tissue culturing. Poly-L-lactic acid was selected because it is biodegradable polymer, often used in implanted materials involved in bone tissue healing. Both types of substrates were made by solvent-casting. Solvent casting of PS has been described earlier by our group¹⁴ to be an accurate and easy way to produce large numbers of microgrooved substrata of high quality. The same was observed in this study for the production of the PLA substrates.

Scanning electron microscopy was performed to visualize the morphology of the cells. The fixation of the cells seems accurate, since delicate structures like the micropodiae of the cells are very well preserved. The RBM cells have a flattened appearance and, after eight days of incubation, are clearly oriented in the direction of the surface grooves on both materials. Independent on the groove depth, the cell extensions attached always to the surface ridge on the 1 and 2 μm wide patterns. On the other hand, on the 5 and 10 μm wide substrates they attached both to ridges and the bottom of the grooves. The observed morphology and alignment behaviour of the RBM cells is in agreement with previous studies of Walboomers *et al*¹⁴ in our group, in which similar texture dimensions were used. Although the rate of orientation was not measured in this study, this also seems to be comparable to earlier studies on fibroblasts in our group^{14, 16, 20}.

After 16 days of culturing the cells have formed a nearly confluent monolayer of cells, covering the entire substratum. Qualitatively in SEM we could not observe any differences in the formation of ECM between smooth or grooved surfaces, or between the two substrate materials. Nevertheless, we noticed that the globular accretions as well as the formed collagen bundles were aligned to the surface grooves. The forming of mineralized globuli has been described extensively in literature^{21, 24}. Our results closely resemble a recent report of osteoblast being cultured on nano- and microtextures by the groups of Brunette^{25, 26}, Chesmel²⁷, Boyan^{28, 31}, and Curtis^{32, 33}. Apparently, microtexture is not only capable of influencing the shape of the cells, but also in determining the deposition of extracellular matrix.

A tetracycline assay was performed to quantify the formation of calcified extracellular matrix³⁴. We observed that more calcification occurred on the smooth PLA substrates, compared to PS. When

PLA substrates were compared, especially the 1 μm deep and 1 or 2 μm wide grooves exhibited high calcification levels. Evidently, microtextured surfaces are capable of increasing calcification. Our results agree with *in vivo* reports by Chehroudi³⁵, who observed increased mineralization around micromachined surfaces, implanted in rats. These bonelike foci were also oriented with the applied microtexture. However, we think that quantification of fluorescent images remains a rather difficult process. Therefore, future research should also address to more accurate biochemical measurements on ECM formation and calcification.

An alkaline phosphatase assay was also performed. Alkaline phosphatase activity is a parameter of bone cell differentiation. Our results showed that after 16 days the alkaline phosphatase activity was greatly increased, compared to the situation after 8 days. This seems logical. After a longer incubation period the culture is gradually reaching confluency. More cells are differentiated and producing extracellular matrix, hence the higher alkaline phosphatase activity. After 16 days of culture, it is observed that the cells on smooth surfaces show less alkaline phosphatase activity than cells on microgrooved substrates. In general, alkaline phosphatase activity seems to be increased on PLA surfaces. This is in agreement with reports in literature. Generally, around bone-bonding implant materials the alkaline phosphatase activity is increased²⁸. Investigations on the effect of PLA wire on the proliferation and differentiation of primary bone cells *in vitro* showed also an increase in the alkaline phosphatase activity of osteoblasts³⁶. Further, the same group showed that bone formation took place around poly-L-lactic acid wires, in an *in vivo* model³⁷. Our results confirm that the application of PLA influences the differential stage of the cells. Apparently, the expression of the osteoblastic phenotype is upregulated by the PLA, resulting in an increased alkaline phosphatase activity.

Overall, the osteoblast-like RBM cells did respond better to PLA than to PS. Although at the moment no explicit reasons for this phenomenon can be given, various explanations can be suggested. First, we know that PLA is a bio-degradable material. Released degradation products of the PLA, a lower pH at the surface, and an increased surface roughness, can influence the final behaviour of cells on the material. Perhaps that in future experiments, atomic force microscopy (AFM) appears to be a suitable technique to visualize the degradation of the surface of PLA materials in time. Second, mineralized ECM formation on culture surfaces is the result of an adsorption/precipitation (protein and apatite) process, which can be influenced by the increased roughness after degradation. Previous studies already showed that changes in surface morphological structure can act as nucleation point for matrix formation and nodule production^{38,40}. Third, specific serum proteins, that act as initiators of mineralization, might be adsorbed differently on PS and PLA material. We cannot exclude that differences in surface chemistry between the substrates not only cause a different numerical and preferential adsorption of proteins, but also influence the conformational state of the adsorbed proteins. Hasegawa⁴¹ demonstrated that the conformational state of proteins can influence cell activity and consequently ECM formation. More research has to be performed to prove any of the above mentioned theories.

In the treatment of periodontitis or implantitis, the alveolar bone often needs to be regenerated. One of the treatment techniques involves guided tissue regeneration (GTR). The hereby used membranes are often made of PLA, because of the biocompatible, low cytotoxic, and biodegradable properties^{6,7}. Our results show, that application of microtexture could possibly increase the bone

regeneration around such devices. Microtextured surfaces are able of influencing the deposition of mineralized matrix, and the stage of differentiation of osteoblast like cells. Despite these promising *in vitro* cell culture studies, the final efficacy of surface microtextured GTR membranes has to be proven in animal experiments.

REFERENCES

- 1 Nyman, S., Lindhe, J. and Karring, T. Reattachment - new attachment In : Lindhe, J. (ed) . Textbook of clinical periodontology. Copenhagen: Munksgaard, 1988, pp409-429
- 2 Gottlow, J., Nyman, S. and Karring, T.: Maintenance of new attachment gained through guided tissue regeneration. J Clin Periodontol, 1992; 19: 315-317
- 3 Selvig, K.A., Kersten, B.G, Chamberlain, A.D, Wikesjo, U.M. and Nilveus, R.E.: Regenerative surgery of intrabony periodontal defects using ePTFE barrier membranes: scanning electron microscopic evaluation of retrieved membranes versus clinical healing J Periodontol, 1992; 63 974-978
- 4 Buser, D, Dahlin, C. And Schenk, R.K. · Bone regeneration, Biologic basis. Guided Bone Regeneration in Implant Dentistry (Schenk, R.B.) Publishing Quintessence Co Inc, USA, 1992, pp49-100
- 5 Tempro, P J and Nalbandian, J · Colonization of retrieved polytetrafluoroethylene membranes. Morphological and microbiological observations. J Periodontol, 1993; 64. 162-168
- 6 Chung, C.P., Kim, D.K., Park, Y J., Nam, K H. and Lee, S H. · Biological effects of drugloaded biodegradable membranes for guided bone regeneration. J Periodont Res, 1997; 32:172-175
- 7 Lundgren, D., Laurell, L., Gottlow, J., Rylander, H , Mathisen, T., Nyman, S and Rask, M. : The influence of the design of two different bioresorbable barriers on the results of guided tissue regeneration therapy an individual comparative study in the monkey J Periodontol, 1995; 66· 605-612
- 8 Greenstein, G and Caton, J · Biodegradable barriers and guided tissue regeneration. Periodontol regeneration. Periodontol, 1993; 2000. 36-45
- 9 Schakenraad, J.M., Busscher, H J, Wildevuur, C R H. and Arends, J : The influence of substratum surface free energy on growth and spreading of human fibroblasts in the presence and absence of serum proteins J Biomed Mater Res, 1986; 20: 773-784
- 10 von Recum, A.F. and Van Kooten, T G . The influence of micro-topography on cellular response and the implications for silicone implants. J Biomat Sci, Polymer Edn. 1995; 7: 181-198
- 11 Harris, A. : Behaviour of cultured cells on substrata of variable adhesiveness. Exp. Cell Res, 1973, 77: 285-297
- 12 Shinghvi, R., Stephanopoulos, G. and Wang, D I C · Review: Effect of substratum morphology on cell physiology Biotechnology and bioengineering, 1994, 43 764-771
- 13 Walboomers, X F , Croes, H J.E., Ginsel, L.A , and Jansen, J.A. : Growth behaviour of fibroblasts on microgrooved polystyrene. Biomaterials, 1998, 19 1861-1868.
- 14 Walboomers, X F , Croes, H J.E , Ginsel, L.A., and Jansen, J.A.: Contact guidance of rat fibroblasts on various implant materials J. Biomed Mater Res, 1999, 47. 204-212.
- 15 Maniatopoulos, C , Sodek, J and Melcher, A.H · Bone formation *in vitro* by stromal cells obtained from bone marrow of young adult rats. Cell Tiss Res, 1988; 254: 317-330
- 16 den Braber, E.T, de Ruijter, J.E., Smits, H T.J., Ginsel, L A , von Recum, A.F and Jansen, J.A. : Quantitative analysis of cell proliferation and orientation on substrata with uniform parallel surface micro grooves Biomaterials, 1996; 17 1093-1099
- 17 den Braber, E.T., de Ruijter, J E , Smits, H.T.J., Ginsel, L.A., von Recum, A.F. and Jansen, J.A. · Effect of parallel surface micro grooves and surface energy on cell growth J Biomed Mater Res, 1995; 29:511-518
- 18 den Braber, E T., de Ruijter, J.E , Ginsel, L.A , von Recum, A F and Jansen, J.A. : Quantitative analysis of fibroblasts morphology on microgrooved surfaces with various groove and ridge dimension. Biomaterials, 1996;17· 2037-2044

Chapter 6

- 19 den Braber, E.T., de Ruijter, J.E., Ginsel, L.A., von Recum, A.F. and Jansen, J.A.: Orientation of ECM protein deposition, fibroblast cytoskeleton, and attachment complex components on silicone microgrooved surfaces *J Biomed Mater Res*, 1998; 40, 291-300.
- 20 den Braber, E.T., de Ruijter, J.E., Croes, H.J.E., Ginsel, L.A. and Jansen, J.A.: Transmission electron microscopical study of fibroblast attachment to microtextured silicone rubber surfaces *Cell and Materials*, 1997; 7, 31-39
- 21 Davies, J.E. In vitro modeling of the bone/implant interface. *Anat-Rec*, 1996; 245, 426-45
- 22 De Bruijn, J.D., van Blitterswijk, C.A. and Davies, J.E.: Initial bone matrix formation at the hydroxyapatite interface in vivo *J Biomed Mater. Res.*, 1995, 29, 89-99
- 23 Itakura, Y., Kosugi, A., Sudo, H. and Yamamoto, S.: Development of a new system for evaluating the biocompatibility of implant materials using an osteogenic cell line (MC3T3-E1). *J Biomed. Mater. Res.*, 1988, 22, 613-622
- 24 Gomi, K. and Davies, J.E.: Guided bone tissue elaboration by osteogenic cells *in vitro*. *J Biomed. Mater. Res.*, 1993, 27, 429-431
- 25 Brunette, J.E. the bone- biomaterial interface, in Davies, J.E. ed. University of Toronto Press, 1991: 170-180
- 26 Qu, J., Chehroudi, B. and Brunette, D.M.: The use of micromachined surfaces to investigate the cell behavioural factors essential to osseointegration. *Oral Diseases*, 1996; 2, 102-115
- 27 Chesmel, K.D., Clark, C.C., Brighton, C.T. and Black, J.: Cellular responses to chemical and morphologic aspects of biomaterial surfaces. II. The biosynthetic and migratory response of bone cell populations. *J Biomed. Mater Res.*, 1995; 29, 1101-1110
- 28 Boyan, B.D., Schwartz, Z. and Hambleton, J.C.: Response of bone and cartilage cells to biomaterials *in vivo* and *in vitro* *J Oral Implantol*, 1993, 19: 116-22
- 29 Martin, J.Y., Schwartz, Z., Hummert, T.W., Schraub, D.M., Simpson, J., Lankford, J., Dean, D.D., Cochran, D.L. and Boyan, B.D.: Effect of titanium surface roughness on proliferation, differentiation, and protein synthesis of human osteoblast-like cells (MG63) *J. Biomed. Mater. Res.*, 1995; 29: 389-401
- 30 Schwartz, Z., Martin, J.Y., Dean, D.D., Simpson, J., Cochran, D.L. and Boyan, B.D.: Effect of titanium surface roughness on chondrocyte proliferation, matrix production, and differentiation depends on the state of cell maturation. *J. Biomed. Mater. Res.*, 1996; 30: 145-155
- 31 Hambleton, J., Schwartz, Z., Khare, A., Windeler, S.W., Luna, M., Brooks, B.P., Dean, D.D. and Boyan, B.D.: Culture surface coated with various implant materials affect chondrocyte growth and metabolism *J. Orthopaedic Res.* 1994, 12, 542-552
- 32 Ferris, D.M., Curtis, A.S.G., Monaghan, W. and Wilkinson, C.W.: The influence of grooved surfaces on osteoblast extracellular matrix production. Abstract Soc. for Biomaterials, 24th Annual Meeting, 1998, 469
- 33 Curtis, A. and Wilkinson, C.: Review, Topographical control of cells. *Biomaterials* 1997, 18, 1573-1583
- 34 Todescan, R., Lowenberg, B.F., Hosseini, M.M. and Davies, J.E.: Tetracycline fluorescence; a new method to quantify bone produced *in vitro*. Abstract Fifth World Biomaterials Congress, 1996; 721
- 35 Chehroudi, B., McDonnell, D. and Brunette, D.M.: The effects of micromachined surfaces on formation of bone-like tissue on subcutaneous implants as assessed by radiography and computer image processing, *J Biomed Mater Res*, 1997; 34: 279-290
- 36 Otto, T.E., Klein Nulend, J., Patka, P., Burger, E.H. and Haarman, H.J.Th.M.: Effect of poly-L-lactic acid on the proliferation and differentiation of primary bone cells *in vitro* *J Biomed Mater Res*, 1996, 32 513-518
- 37 Otto, T.E., Klein, C.P.A.T., Patka, P., Vriesde, R. and Haarman, H.J.Th.M.: Intramedullary bone formation after poly-lactic acid wire implantation *J Mater Sci Mater Med*, 1994; 5: 407-410
- 38 Cooper, L.F., Masuda, T., Yliheikkilä, P.K. and Felton, D.A.: Generalization regarding the process and phenomenon of osseointegration. Part II. In vitro studies *Int J. Oral Maxillofac. Implants*, 1998; 13: 163-174
- 39 Kieswetter, K., Schwartz, Z., Dean, D.D. and Boyan, B.D.: The role of implant surface characteristic in the healing of bone. *Crit. Rev. Oral Biol. Med.*, 1996; 7: 329-345
- 40 Stanford, C.M., Keller, J.C. and Solursh, M.: Bone cell expression on titanium surfaces is altered by sterilization treatments *J Dent. Res.*, 1994; 73: 1061-1071
- 41 Hasegawa, T., Oguchi, H., Mizuno, M. and Kuboki, Y.: The effect of the extracellular matrix on differentiation of bone marrow stromal cells to osteoblasts. *Jpn J Oral Biol*, 1994; 36 383-394

Microgrooved subcutaneous implants in the goat

Walboomers, X F , Croes, H J E , Ginsel, L A and Jansen, J A
Journal of Biomedical Materials Research **42**, 634-641 (1998)

INTRODUCTION

Microtexturing of a substrate-surface has been shown to influence the behaviour of cells growing on such substrates *in vitro*^{1,2}. Cells, especially fibroblasts, recognize the micrometer-sized dimensions of surface configurations. They react accordingly, probably by reshaping the actin filaments in their surface-probing structures like filopodia^{3,5}. The result is a cell which is lying in the same direction as the surface grooves. This phenomenon is known as 'contact guidance'⁶.

Because of the evident influence of microgrooves on fibroblasts in culture, it has been suggested in literature that they could also affect capsule formation after implantation in soft tissue. Microtexture might influence the number of inflammatory cells, capsule thickness, capsule organization, capsule quality and the number of blood vessels present around the implant^{7,8}.

Previous *in vivo* studies on microtextured implants are limited in number. The group of Cheroudi and Brunette^{8,13}, when studying percutaneous implants, found that micro-machined implants were able to impede epithelial downgrowth around the implant. This could greatly improve implant performance. It was found that the reactions of fibroblasts to microtexture differed greatly with the size of the applied texture. Fibroblasts orient along 3 and 10 μm deep grooves, whereas they seem to insert obliquely into 22 μm deep grooves. In this group also a better osseo-integration¹⁴ and induction of mineralized tissue¹⁵ caused by microtextures was described. Von Recum and coworkers studied the implantation of porous implants surfaces in dogs¹⁶. Here it was found that topography of 1 to 2 μm allowed direct fibroblast attachment, which diminished the presence of inflammatory cells. In our group¹⁷ *in vivo* experiments were done with silicone microgrooved implants in rabbits. From this study, it was concluded that the applied texture did not affect the thickness of fibrous capsule around the implant. On the other hand, both the presence of immunological cells as well as the number of blood vessels around implants were markedly influenced by the grooves. A similar experiment, was done by Picha and Drake¹⁸. However, they used silicone implants provided with micropillars much larger than used by Den Braber¹⁷ (100 μm diameter, 500 μm high). They found that this surface texture reduced fibrosis and improved blood vessel proximity around the implants.

A disadvantage of the use of silicone in implant studies is, that this material limits the histological evaluation, since it cannot be easily sectioned for light or transmission electron microscopy. We therefore looked for a way to produce an implant, not subjected to such disadvantages. The production of silicon wafers provided with microgrooves allows also the possibility of solvent casting other polymers than silicone, like polystyrene (PS)¹⁹. Implants made of this material can be subjected to different kinds of histological techniques, to obtain information about the effect of surface microtexture on the tissue reaction.

We hypothesize that an optimal surface topography exists, that can be recognized by the cells, and minimizes tissue reaction *in vivo*. The objective of this study therefore is to quantify the influence of microgrooves on capsule formation, around subcutaneous PS implants, in an animal experiment.

MATERIALS AND METHODS

Substrata

The PS substrates were solvent-cast¹⁹ on molds from a solution of 25 g tissue culture PS (Greiner, Germany) in 150 ml chloroform (LabScan, UK). As molds we used a smooth glass plate, or a silicon wafer provided with parallel microgrooves (MESA institute, University of Twente, Enschede, the Netherlands). The groove-depth always was 1.0 μm ; the ridge- and groove-width was 1.0, 2.0, 5.0, or 10.0 μm (Table 1).

Table 1: Types of implants placed subcutaneously, with the sizes of grooves (μm)

type	groove width	ridge with	groove depth
0	0	0	0
1	1	1	1
2	2	2	1
5	5	5	1
10	10	10	1

The PS replicas were cut to appropriate size: round discs with a diameter of 18 mm. These discs were glued back to back so that an implant was produced, textured at both sides. The total implant was approximately 0.2 mm thick. For the glueing, a small drop of Sycomet 8400 (Henkel, the Netherlands), a medical-grade cyanoacrylate glue, was used. At both sides of the implant the groove orientation was kept similar. The glue was allowed to dry. Then, the produced implants were washed by ultrasonical rinse (10 min.) in milliQ water, and kept in 70% EtOH for at least two days. Just before use, they were dried to air in a sterile environment and given a radiofrequency glow discharge (RFGD) treatment²⁰⁻²².

Implant characterization

To observe the quality of the pattern-reproduction on the implant surface implants were observed by scanning electron microscopy (SEM). For this purpose specimens were washed in 100% EtOH, dried to air, and coated with gold. Subsequently they were examined with a JEOL 6310 SEM.

To test any cytotoxic effect²³ of the implants, discs were positioned on the bottom of a 6 wells plate. Rat dermal fibroblasts (RDF) was obtained from the ventral skin of male Wistar rats as described before³. A suspension of these RDF was added to the wells, at $5 \cdot 10^5$ cells/ 3 ml. Cells were cultured for 24 hours in MEM- α medium, containing Earle's salts, L-glutamine, 15% FCS, and gentamicin (50 $\mu\text{g}/\text{ml}$). Subsequently, the possible formation of an inhibition zone around the discs was observed by phase contrast microscopy.

Animal

In this study one healthy mature female Saanen goat was used. The animal was housed in a stable. The various samples were inserted subcutaneously into the flanks of the goat for either 1, 4 or 12 weeks. For each period, three specimens with identical surface texture were used. A total of 45 implants was placed.

Surgery was performed under general anaesthesia induced by intravenous pentobarbital (25 mg/kg¹) and atropine (0.5 mg). After oro-tracheal intubation, anaesthesia was maintained by ethrane (2-3%) with a constant volume ventilator.

For the insertion of the discs, the dorso-lateral skin was shaved, washed and disinfected with iodine. Implantation of the 1, 4 and 12 week implants was performed in three separate surgical sessions. In each session fifteen longitudinal incisions of about 3 cm were made through the full thickness of the skin. Subsequently, lateral to the incisions subcutaneous pockets were created by blunt dissection with scissors. One implant was inserted in each pocket. Finally the wounds were carefully closed. The position of the implants is shown in Figure 1. To reduce the postoperative infection risk, prophylactic antibiotic Albipen[®] was administered for three days, starting one hour postoperatively.

Histological evaluation techniques

At the end of all implantation periods the goat was killed by an overdose of Nembutal[®] *iv*. Then the implanted PS discs were removed including all surrounding tissues. For histological analysis the capsule-covered implants were fixed in 2% glutaraldehyde in 0.1 M sodium cacodylate buffer, dehydrated in a series of ethanol and embedded in LR White acrylic resin (Polysciences, Warrington). Sections of about 10 µm were cut using a modified diamond blade sawing microtome technique^{24,25}. These were stained with methylene blue and basic fuchsin. Subsequently, the sections were examined with a Leica DM RBE light microscope at a magnification of 40x.

Since the groove direction is not visible when the implant is covered with tissue, all embedded blocks were cut in two directions, perpendicular to each other. In this way large and small sections were produced (Figure 2). Of each direction at least three sections suitable for evaluation were made.

Histomorphometrical evaluation

To assess the soft tissue response to the implants, histomorphometric evaluations were performed. In these measurements the thickness of the fibrous capsule was measured in the sections of 1, 4, and 12 week implants. Also the presence of inflammatory cells after 4 weeks, and the presence of bloodvessels after 4 and 12 weeks were quantified. For this purpose, the microscopic images were projected with a total magnification of 400x on a color monitor using a CCD/RGB camera (Sony DXC151P) attached to the light microscope. Subsequently, measurements were performed in 4 (small sections) or 8 (large sections) predetermined fields. The fields were positioned at regular 2 mm intervals, in the capsule surrounding the implant (Figure 3).

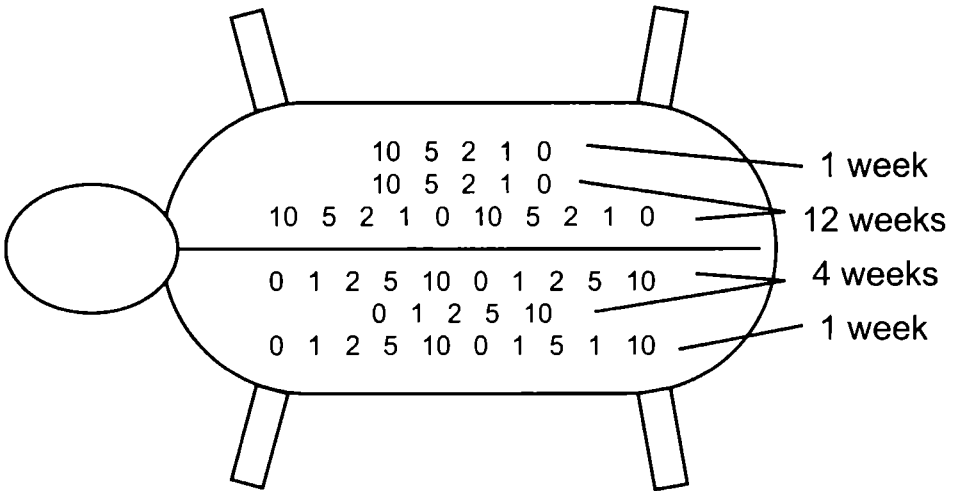


Figure 1: Schematic representation of the goat, with the positions and healing times of the implants. On both flanks three rows of implants were placed. The numbers 0, 1, 2, 5, and 10 in Table 1 indicate the groove- and ridge widths (0 is the smooth control surface)

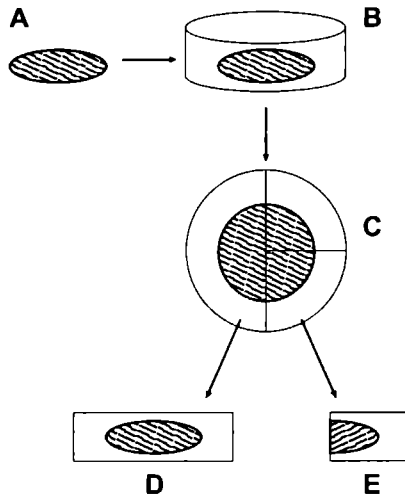


Figure 2: Embedding and sectioning. Implants covered with tissue (A) were embedded in LR White resin (B) and cut in two directions perpendicular to each other (C). After sectioning, large sections (D) and smaller ones (E) are available for histologic evaluation.

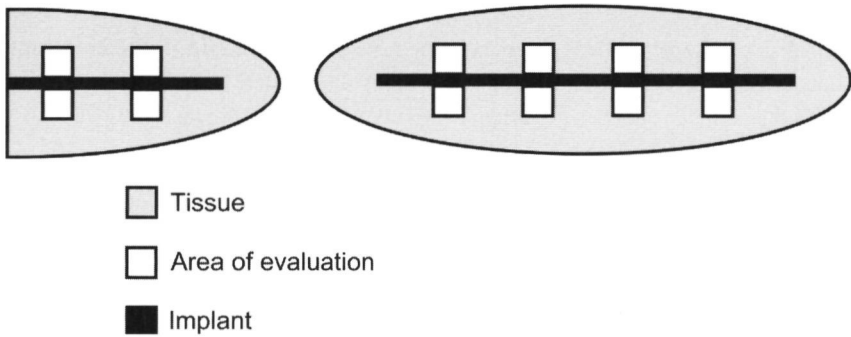


Figure 3: Schematic drawing of the sections of the subcutaneous implant, showing the fields of evaluation used in the histomorphometric analysis.

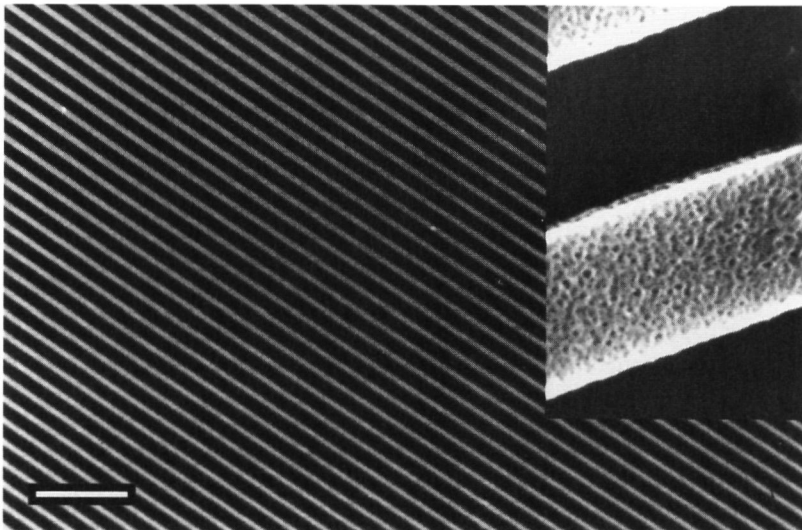


Figure 4: Scanning electron micrograph of the implant surface, showing the groove pattern. In the inset, an additional nano-roughness can be observed on the ridges (Bar= 25 μm).

Statistical analysis

Of each implant 3 microscopical slides were examined histomorphometrically. Subsequently, the averages and standard deviations were calculated and compared with StatMost (DataMost corporation, Salt Lake City, USA), using an analysis of variance (ANOVA) and a non-parametric Kruskal-Wallis test.

Transmission electron microscopy

Embedded tissue blocks, used for the production of light microscopical sections, were further cut for transmission electron microscopy (TEM). First, semi-thin sections were cut of these specimens. After determining the right position for evaluation, the embedded tissue block was trimmed to desired size and cut further into ultrathin sections for TEM analysis. The sections were stained with uranylacetate and leadcitrate. No osmiumtetroxide was used. Finally, specimens were observed with a JEOL 1210 transmission electron microscope.

RESULTS

Implant characterization

SEM evaluation of the implant surface revealed that the microgrooved pattern was reproduced perfectly from the molds. However, at large magnifications an additional nano-roughness can be observed on the ridges (Figure 4). This is the result of the etching process of the grooves. In the replicas the roughness then will appear on the ridges.

The cytotoxicity testing revealed that fibroblasts were growing around, and adhering to the implantable discs (Figure 5). Nowhere an inhibition zone could be observed, which indicates no toxic effect of the produced polystyrene, or leached cyanoacrylate glue.

Macroscopic findings

During the post-implantation period, the animal showed an unevoked healing without any disturbance of the wound healing process. All removed implants were surrounded by a thin fibrous capsule. There was no sign of an inflammatory reaction. Some implants did show the presence of a haematoma. Further, we observed that also some of the discs were bent or broken. Table 2 summarizes all macroscopic findings. It has to be emphasized that haematoma only occurred in the short implantation periods. Bending or breaking of implants could not be correlated to a difference in implant texture, but was observed more frequently at the longer implantation times. Broken implants were not further evaluated. Three implants were damaged during recovery or subsequent embedding, and therefore not further analyzed (labeled not available in Table 2).

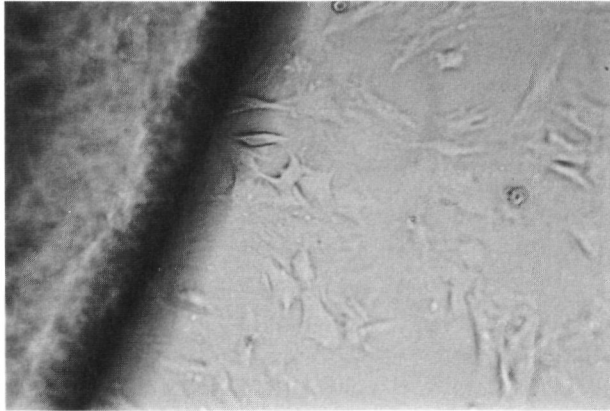


Figure 5: Phase-contrast micrograph of fibroblasts growing around and adhering to an implantable PS disc. Original magnification 20x.

Table 2: The macroscopic quality of the implants after implantation. + =implant intact and suitable for evaluation; - =implant broken; H =haematoma; NA =not available.

weeks	0 µm	1 µm	2 µm	5 µm	10 µm
1	+	+	+	NA	+
	-	+	+	NA	H
	H	+	-	+	+
4	+	+	-	H	+
	-	+	+	+	+
	+	+	+	+	+
12	+	-	+	+	+
	+	+	+	+	-
	-	+	+	NA	-

Light microscopy

Examination of the histological sections revealed a fairly uniform tissue response for all tested materials. At all implantation periods, the PS discs were surrounded by a fibrous capsule containing over 30 layers of fibroblasts.

After one week (Figure 6a), the tissue around the implants was still at the beginning of wound healing. The matrix of the capsule was loose, and contained fibrocytes and many inflammatory cells (macrophages, granulocytes, monocytes).

After 4 weeks (Figure 6b), the matrix of the capsule had matured, and contained fibrocytes and many newly formed blood vessels, recognizable by their large lumen. Inflammatory cells were also present in the capsule, but to much lesser extent than after 1 week of implantation. However, at the implant surface a multilayer of mainly inflammatory cells was present.

After 12 weeks (Figure 6c) fibrocytes had flattened very much compared with 4 weeks, and immunological cells were hardly present in the capsule. We observed that the fibrous capsule was still separated from the implants by a single layer of mono- and multinucleated phagocytotic cells. Compared to 4 weeks, the observed blood vessels in general had much smaller lumen.

Histomorphometrical evaluation

Figure 7 shows the data of the thickness measurements of the capsule layer surrounding the implant. The capsule thickness after 1, 4 or 12 weeks was about 80 μm . No decrease in capsule thickness was observed in time. Also no significant differences ($p>0.05$) were seen in relation to the reaction towards the various textures.

In Figure 8 the thickness of the inflammatory layer surrounding 4 week old implants is listed. This layer was relatively thin, about 10 μm . No significant differences were present ($p>0.05$) between the smooth and various textured surfaces. The thickness of the layer of inflammatory cells, present at 12 weeks of implantation, was not quantified since it was a single layer.

Figure 9, finally, shows the numerical appearance of the blood vessels in the examined fields. In each examined field of evaluation about 2 vessels were present. Again, no significant differences were apparent between the numbers of vessels in the fibrous tissue capsule, surrounding either smooth or grooved implants.

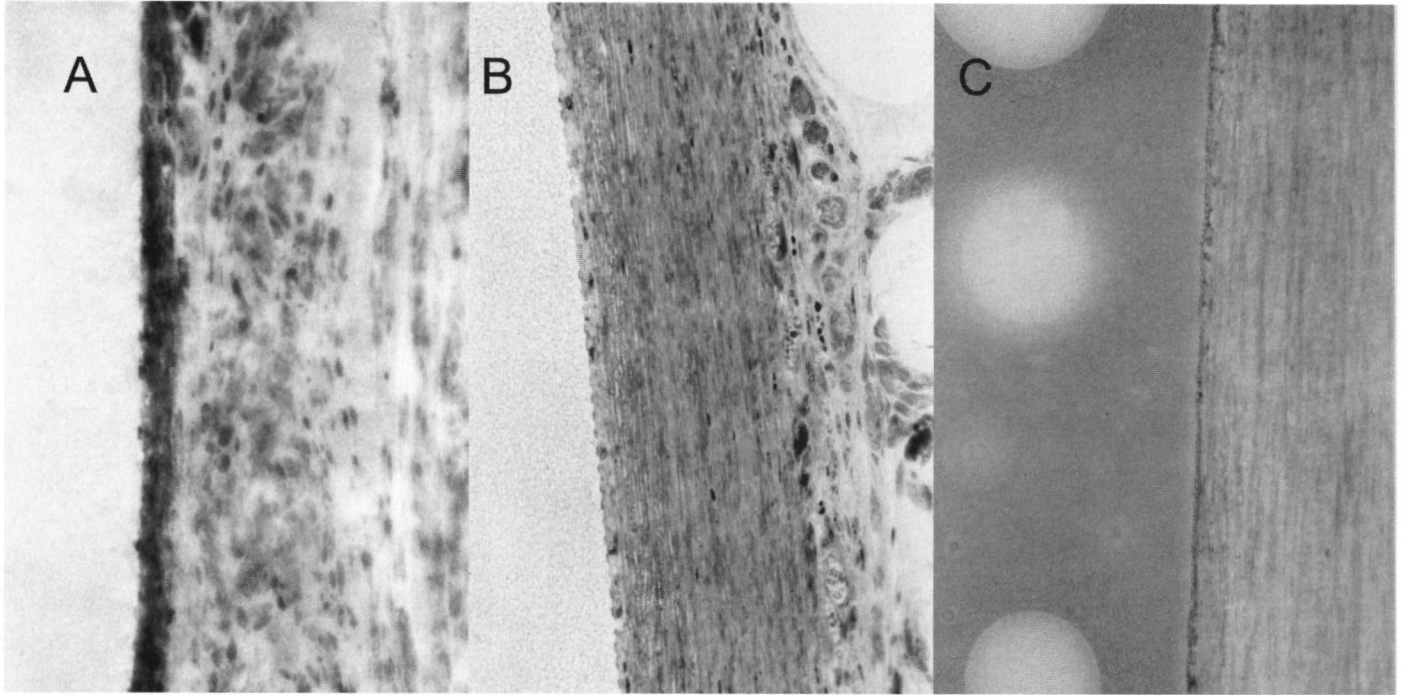


Figure 6: A) The capsule around a smooth implant after 1 week contains fibrocytes and many inflammatory cells; B) Histological picture of the fibrous capsule around a microgrooved (1 µm deep, 5 µm wide) implant, 4 weeks after implantation. Note the newly formed blood vessels and the layer of mainly inflammatory cells at the implant surface; C) After 12 weeks fibrocytes have flattened very much compared with 4 weeks. Still the fibrous capsule is separated from the implants by a single layer of mono- and multinucleated phagocytotic cells (methylene blue/ basic fuchsin staining; original magnification 40x).

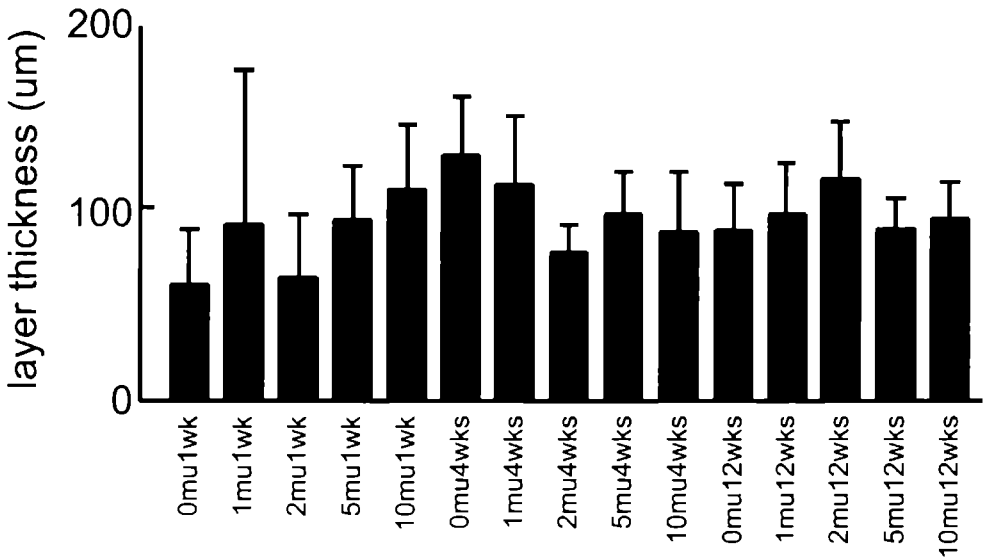


Figure 7: Thickness measurements of the fibrous capsule surrounding the various implants
 0mu 1wk= smooth implant, 1 week of implantation 1mu 1wk= 1 μ m wide grooves, 1 week of implantation, etc

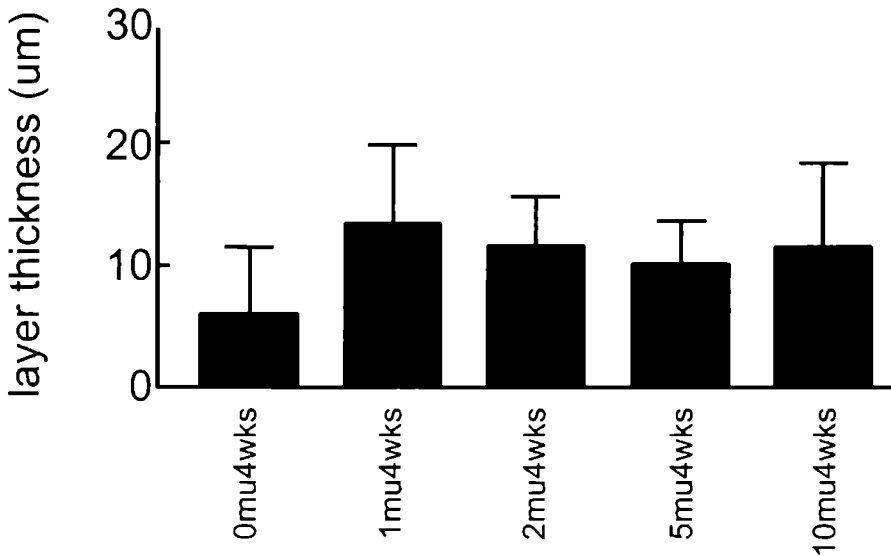


Figure 8: Thickness measurements of the layer of inflammatory cells, surrounding the implant after 4 weeks of implantation

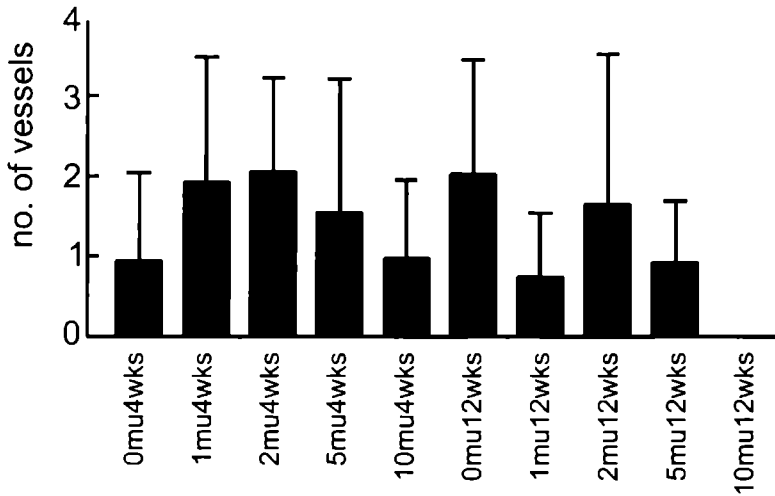


Figure 9: Representation of the number of blood vessels, present in the fibrous capsule, surrounding the subcutaneous implants

Transmission electron microscopy

Transmission electron microscopy showed that the microgrooved patterns had been conserved well during implantation. Although the tissue layer on the implants was relatively thick (about 2 to 3 mm), and no osmium was used, fixation proved to be successful. Nuclei and organelles of all cells were conserved well. The absence of osmium accounts for the somewhat lower contrast of cellular and organelle membranes. In all TEM images dark structures appeared in the PS.

After 4 weeks (Figure 10a) the interfacial tissue layer surrounding implants showed normal wound healing. Prominent structures like the nucleus, mitochondria, ribosomes and rough endoplasmic reticulum were well preserved in all cells. When observing the cytoplasm and shape of the nucleus, fibrocytes and inflammatory cells can be distinguished. Inflammatory cells were present, directly at the implant surface. The inflammatory cells filled the groove cavities totally, and touched the bottom of the grooves. After 12 weeks (Figure 10b) inflammatory cells were still present at the implant surface. The surrounding layer consisted of flattened fibroblasts. Occasionally, collagenous bundles could be observed.

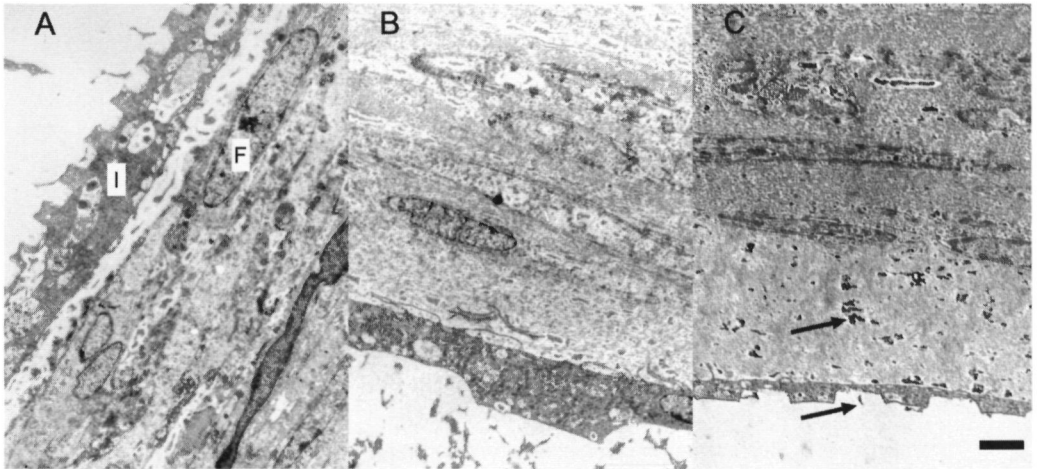


Figure 10: A) Transmission electron micrograph of the tissue surrounding implants after 4 weeks. Note that the microgrooved pattern (1 μm deep, 1 μm wide) has been conserved well. F=fibrocyte; I=inflammatory cells; B) The microgrooved implant (1 μm deep, 5 μm wide) after 12 weeks still is surrounded by inflammatory cells; C) Dark structures (arrows) appear in the polystyrene. These structures are also present in this seroma cavity (bar= 2 μm ; original magnification 3000x).

DISCUSSION

In the last few years, most researchers have focused on contact guidance on microgrooved substrata *in vitro*, but little *in vivo* work has been undertaken. Our goal was to determine the behaviour of microgrooved implants, in subcutaneous tissue. In our study, the overall tissue reaction around the implants was characterized by fibrous encapsulation. No obvious effects of microtexturing on capsule formation was found. This is not in agreement with previous research^{17,18}.

In the 1950s, cancer researchers investigated implantation of polymers in mice and rats. In this research, also PS implants were thoroughly studied²⁶⁻²⁹. It was shown that PS, after implantation is covered by a capsule with generalized reactive fibroblastic activity, that in time becomes almost inactive. PS therefore seems a suitable implant material to study fibrous capsule formation. The glueing of polystyrene with cyanoacrylate is not expected to cause any negative effects. Implants were dried and cleaned carefully. No inhibition zone, indicating cytotoxicity, could be observed in the performed *in vitro* test.

In our study, a goat was chosen as experimental model, so that multiple substrates could be placed in the same goat, without animal to animal variability. Besides, the data obtained from big animals are more comparable to human wound healing processes, than if rats or other small laboratory animals had been used.

We observed that after 4 and 12 weeks of implantation, several implants were bent or broken. We suppose that this is due to the mechanical properties of the PS discs, which showed a brittle behaviour, even when casted into thin films (our implants were approximately 0.2 mm thick). During implantation, the discs are subjected to mechanical stress present in a free-moving animal. Further, capsule contraction evokes additional mechanical stress. For this reason, fracture occurs especially after longer implantation periods. In addition, this fracturing emphasizes again that also around soft tissue-implants the influence of interfacial mechanical stresses on the final wound healing process cannot be neglected.

When examining the tissue reaction histomorphometrically, we were unable to determine any effect of microstructured surfaces on wound healing. The inflammatory response, capsule thickness, and formation of blood vessels, all were not markedly affected. We propose two explanations for this finding.

First there is a difference of Young's modulus of elasticity between the implants and the surrounding tissue. When implanting a material, caution should be taken that the implanted material has about the same mechanical properties as the surrounding tissue^{30,31}. This mismatch could be the cause for the formation of a relatively thick capsule. Apparently, this discrepancy overrules the effect of the microgrooves on the capsule formation process. Studies by Picha¹⁸ and den Braber¹⁷, as mentioned in the introduction, used silicone implants, did not have this problem, or to lesser extent.

Secondly, our grooves were relatively shallow (1 μm), compared to the pillars used by Picha (500 μm)¹⁸. If the effect of microtexture is based on stabilizing implants by mechanical retention, our grooves might have been too shallow to induce such an effect. On the other hand we have to emphasize that den Braber¹⁷ also used shallow (0.5 μm deep) grooves and still found an effect on inflammation and vascularization. We assume that the use of a material with the appropriate mechanical properties is a very important additional parameter.

In TEM it was observed that the microgrooved patterns and adherent tissue had been conserved well during implantation and subsequent processing. In all TEM images dark structures were visible in the PS (Figure 10c), which seems to be a result of embedding PS in LR White resin. The same structures sometimes appeared in the tissue. The presence of these structures in the tissue probably is not the result of phagocytosis of PS during the implantation period. Namely, these structures also appeared in places where no phagocytosis could have occurred, for instance in seroma cavities (Figure 10c). Probably, the LR White has accumulated in empty spaces in the tissue, and shows the same dark structures there.

Subjectively, in TEM there seemed to be no difference in tissue reaction at the interfacial layer between smooth or textured implants at any of the implantation times. As seen in light microscopy, in time the presence of inflammatory cells decreases, but no contact between fibrous tissue and the implant is accomplished. This might have been caused by a phenomenon known as rugophilia. *In vitro* and *in vivo* macrophages seem to be attracted to roughened surfaces^{32,33}. In the SEM evaluation it can be observed that part of our implant surfaces shows additional nano-roughness, caused by the etching procedure. This roughness is only present on ridges, and not in the grooves. Because implants are covered with inflammatory cells, it can also be argued that this might inhibit the effect of microgrooves. Namely, from previous *in vitro* research it is known that inflammatory cells hardly show contact

guidance, compared to fibroblasts³⁴. If at the implant surface a layer of cells is present, that are not affected by the texture, the cells outside that layer cannot sense the difference between textured and smooth surfaces.

From this experiment we conclude that the presence of 1 μm deep and 1-10 μm wide microgrooves does not affect the tissue response around polystyrene implants in soft tissue.

LITERATURE

- 1 R. Singhvi, G. Stephanopoulos, and D.I.C. Wang, "Review. effects of substratum morphology on cell physiology," *Biotechnol. Bioeng* , **43**, 764-771 (1994).
- 2 A.F. Von Recum, C E Shannon, E.C. Cannon, K.J. Long, T.G. Van Kooten, and J. Meyle, "Surface roughness, porosity, and texture as modifiers of cellular adhesion," *Tissue Engineering*, **2**, 241-253 (1996)
- 3 X F. Walboomers, H J.E Croes, L.A. Ginsel, and J.A Jansen, "Growth behaviour of fibroblasts on microgrooved polystyrene," *Biomaterials*, **19**, 1861-1868 (1998).
- 4 T J Mitchinson, and L P Cramer, "Actin-based cell motility and cell locomotion," *Cell*, **84**, 371-379 (1996)
- 5 J.V. Small, K. Anderson, and K. Rottner, "Actin and the coordination of protrusion, attachment and retraction in cell crawling," *Biosc Reports*, **16**, 351-368 (1996).
- 6 P. Weiss, "Experiments on cell and axon orientation in vitro: the role of colloidal exudates in tissue organization," *J Exp. Zool* , **100**, 353-386 (1945).
- 7 A.F. Von Recum, and T.G. van Kooten, "The influence of micro-topography on cellular response and the implications for silicone implants.," *Journal of Biomaterials Science - Polymer Edition*, **7**, 181-198 (1995).
- 8 D M. Brunette, "Effects of surface topography on cell behaviour in vitro and in vivo," in: *Nanofabrication and biosystems*, H.C. Hoch (ed.), Cambridge University Press, New York, 1996, 335-366
- 9 B Chehroudi, T R. Gould, and D M. Brunette, "Effects of a grooved epoxy substratum on epithelial cell behaviour in vitro and in vivo," *J Biomed Mater Res* , **22**, 459-473 (1988).
- 10 B. Chehroudi, T.R. Gould, and D.M. Brunette, "Effects of a grooved titanium-coated implant surface on epithelial cell behaviour in vitro and in vivo," *J Biomed Mater Res* , **23**, 1067-1085 (1989).
- 11 B. Chehroudi, T R. Gould, and D.M. Brunette, "Titanium-coated micromachined grooves of different dimensions affect epithelial and connective-tissue cells differently in vivo," *J. Biomed Mater Res* , **24**, 1203-1219 (1990).
- 12 B. Chehroudi, T R. Gould, and D.M Brunette, "A light and electron microscopic study of the effects of surface topography on the behaviour of cells attached to titanium-coated percutaneous implants," *J Biomed Mater Res* , **25**, 387-405 (1991).
- 13 B. Chehroudi, T.R. Gould, and D.M Brunette, "The role of connective tissue in inhibiting epithelial downgrowth on titanium-coated percutaneous implants," *J Biomed Mater Res* , **25**, 387-405 (1991).
- 14 J. Qu, B. Chehroudi, T.R. Gould, and D.M Brunette, "The use of micromachined surfaces to investigate the cell behavioural factors essential to osseointegration," *Oral Dis* , **2**, 102-115 (1996)
- 15 B. Chehroudi, D McDonnel, and D.M. Brunette, "The effects of micromachined surfaces on formation of bonelike tissue on subcutaneous implants as assessed by radiography and computer image processing" *J Biomed Mater Res* , **34**, 279-290 (1997)
- 16 C.E. Campbell, and A.F Von Recum, "Microtopography and soft tissue response," *J Invest Surg* , **2**, 51-74 (1989)
- 17 E T. den Braber, J E. de Ruijter, and J A Jansen, "The effect of a subcutaneous silicone rubber implant with shallow surface micro grooves on the surrounding tissue in rabbits," *J Biomed Mater Res* , **37**, 539-547 (1997)
- 18 G J Picha, and R.F. Drake, "Pillared-surface microstructure and soft-tissue implants Effect of implant site and fixation," *J Biomed Mater Res* , **30**, 305-312 (1996).
- 19 K Chesmel, and J. Black, "Cellular responses to chemical and morphologic aspects of biomaterial surfaces I A novel in vitro model system" *J Biomed Mat Res* , **29**, 1089-1099 (1995)

- 20 R E Baier, and V.A. DePalma, "Electrodeless glow discharge cleaning and activation of high-energy substrates to insure their freedom from organic contamination and their receptivity for adhesives and coatings," *Calspan Report*, **176** (1970).
- 21 C.F. Amstein, and P A. Hartman, "Adaptation of plastic surfaces for tissue culture by glowdischarge," *J Clin Microbiol.*, **2**, 46-54 (1975).
- 22 J.A. Chinn, T.A. Horbett, and B.D Ratner, "Laboratory preparation of plasticware to support cell culture," *J. Tiss Culture Meth* , **16**, 155-159 (1994).
- 23 S J Northup, "Mammalian cell culture methods," in: *Handbook of biomaterials evaluation*, A.F. Von Recum (ed.), Macmillan publishing Company, New York, 1986, 209-225.
- 24 H.B M. van der Lubbe, C.P.A.T. Klein, and K de Groot, "A simple method for preparing thin (10 μ m) histological sections of undecalcified plastic embedded bone with implants," *Stain Technology*, **63**, 171-177 (1988).
- 25 C.P.A T. Klein, Y.M H F Sauren, W.E Modderman, and J P.C.M van der Waerden, "A new saw technique improves preparation of bone sections for light and electron microscopy," *Journal of Applied Biomaterials*, **5**, 369-373 (1994)
- 26 B S Oppenheimer, E T Oppenheimer, I Danishefsky, A.P. Stout, and F R. Eirich, "Further studies of polymers as carcinogenic agents in animals," *Cancer Research*, **15**, 333-345 (1955).
- 27 B S Oppenheimer, E T. Oppenheimer, A.P. Stout, M. Willhite, and I. Danishefsky, "The latent period in carcinogenesis by plastics in rats and its relation to the presarcomatous stage," *Cancer*, **111**, 204-213 (1958).
- 28 E.T Oppenheimer, M.M. Fishman, A.P. Stout, M. Willhite, and I Danishefsky, "Autoradiographic studies on the connective tissue pocket formed around imbedded plastics," *Cancer Research* , **20**, 654-657 (1960).
- 29 E T. Oppenheimer, M. Willhite, A P Stout, I Danishefsky, and M.M Fishman, "A comparative study of the effects of imbedding cellophane and polystyrene films in rats," *Cancer Research*, **24**, 379-387 (1964).
- 30 J.F.V. Vincent, *Structural biomaterials-revisited edition*, Princeton University Press, New Jersey, USA, 1990
- 31 D F. Williams, and R Roaf, *Implants in surgery*. W.B Saunders Company Ltd., London, United Kingdom, 1973.
- 32 A.K Harris, and A Rich, "Anomalous preferences of cultured macrophages for hydrophobic and roughened substrata," *J Cell Sci* , **50**, 1-7 (1981).
- 33 T N Salthouse, "Some aspects of macrophage behaviour at the implant interface," *J Biomed Mater Res* , **18**, 395-401 (1984).
- 34 J Meyle, K Gultig, and W. Nisch, "Variation in contact guidance by human cells on a microstructured surface," *J Biomed Mater Res* , **29**, 81-88 (1995).

Microgrooved silicone subcutaneous implants in guinea pigs

Walboomers, X F , and Jansen, J A
Biomaterials, in press (1999)

INTRODUCTION

In vitro experiments have shown that providing a substrate surface with micrometer-sized parallel grooves, influences the behaviour of cells growing on such substrates¹⁻³ Cells elongate in the direction of the groove and migrate guided by the grooves This phenomenon is known as 'contact guidance'^{4,5} Next to contact guidance, microgrooves are known to evoke a number of other responses in cell culture, like the expression of certain enzymes that in normal tissue are involved in remodeling⁶

Because of the evident influence of microgrooves on fibroblasts in culture, it has been suggested in literature that this phenomenon can also be used to affect the wound healing or tissue repair around medical implants For soft tissue devices, microtexturing might influence the number of inflammatory cells, capsule thickness, capsule organization, and the number of blood vessels present around the implant^{7,9} Despite this supposed effect of microtexture on soft tissue response, *in vivo* studies on microtextured implants are limited in number, and remain rather inconclusive For instance, in our group two *in vivo* experiments were done with microgrooved implants The first study¹⁰ investigated the connective tissue response to silicone implants, provided at one side with 0.5 µm deep microgrooves, in rabbits The implants were left for implantation periods from 2-12 weeks It was observed that the applied texture did not affect the thickness of the fibrous capsule around the implant On the other hand, both the presence of immunological cells as well as the number of blood vessels around implants were markedly influenced at the grooved side The second study¹¹ considered similar, but now two-sided microgrooved polystyrene implants in goats The implants were left for 1-14 weeks In this study no evident effects of the applied texture was found The results of both studies lead to the suggestion that the applied texture might have been too shallow to induce significant effects Consequently, in the current research we intend to further determine the extent with which tissue behaviour can be influenced and directed by surface microgeometry, and how this interferes with wound healing phenomena around implants

We hypothesize that an optimal surface topography exists, that can be recognized by the cells surrounding the implant, and minimizes tissue reaction *in vivo* Therefore we qualified and quantified the influence of 2 µm wide microgrooves, with various depths (0.5-6 µm), on capsule formation around subcutaneous silicone implants, in an animal experiment

MATERIALS AND METHODS

Implant production

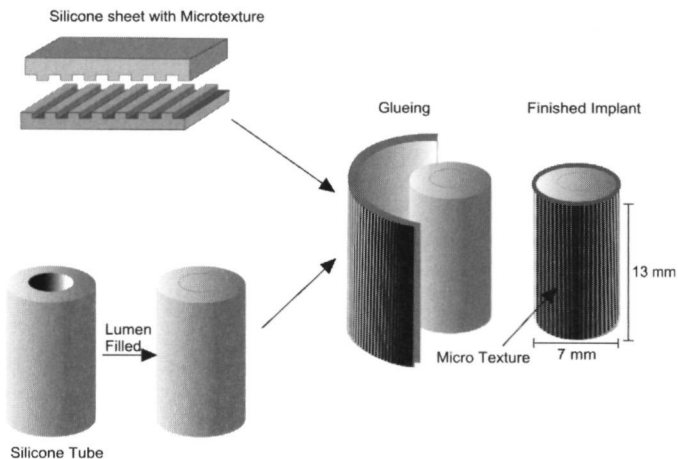
Using photo lithographic techniques, four different micro grooved patterns were made in molds of silicon (Twente Microproducts, Enschede, the Netherlands), or fused silica (dept of Electronics and Electrical Engineering, University of Glasgow, UK) The molds were covered with silicone (polydimethylsiloxane, NuSil MED-4211, NuSil Technology, Carpinteria, California) After polymerization, the silicone rubber sheets were removed from the molds Also smooth silicone sheets were produced, using a non-textured mold

Table 1: Summary of the used types of implant

implant type	groove depth (μm)	groove width (μm)	ridge width (μm)
control	0	0	0
smooth	0	0	0
0.5	0.5	2	2
1	1	2	2
1.5	1.5	2	2
6	6	2.5	2.5

The lumen of a silicone tube (SiR tube, Baxter Healthcare, Mirandola, Italy) was filled with silicone, and left to polymerize. Subsequently, the silicone sheets were glued around the silicone tubes, using adhesive silicone (NuSil MED-1137). The groove direction was longitudinal to the tube. Finally, they were cut to the desired size, i.e. a length of 13 mm and diameter of 7 mm. This resulted in a tube shaped implant. The production process is visualized in Figure 1. Also control implants were made, without a silicone sheet glued onto it. The surface topographical dimensions of the prepared implants are summarized in Table 1.

After drying of the glue, the finished implants were washed in 10% liquinox solution (Alconox, New York, NY), cleaned ultrasonically in 1% liquinox, rinsed thoroughly, and given an overnight Soxhlet rinse in distilled, de-ionized water. They were dried to air in a sterile environment and, just before use, given a radiofrequency glow discharge treatment (RFGD, 5 min, 150 mTorr), for sterilization¹²⁻¹⁶, and to ensure proper surface wettability for cell adhesion¹⁷.

**Figure 1:** Schematic representation of the production of the implants

Characterization of materials

To test any cytotoxic effect¹⁸ of the implants, disc shaped test samples were cut from an implant. These samples were positioned on the bottom of a 6 wells plate. Primary rat dermal fibroblasts (RDF) were obtained from the ventral skin of male Wistar rats as described before^{5,19}. A suspension of these RDF was added to the wells, at 5×10^5 cells/ 3 ml. Cells were cultured for 4 days in MEM- α medium, containing Earle's salts, L-glutamine, 15% FCS, and gentamicin (50 μ g/ml). Subsequently, the possible formation of an inhibition zone around the discs was observed by phase contrast microscopy.

Animals

In this study eight healthy mature female albino guinea pigs were used, 12-14 weeks of age. The animals were housed according to standard regulations at the central animal facility (CDL) of the University of Nijmegen, the Netherlands.

Surgery was performed under general anaesthesia induced by a combination of fluanisone 6.75 mg/kg body weight, fentanyl citrate 0.2133 mg/kg body weight (Hypnorm®) and midazolam 3.375 mg/kg body weight (Dormicum®). Anaesthesia was maintained by ethrane (2-3%) with a constant volume ventilator. For the insertion of the tubes, the dorsal skin was shaved, washed and disinfected with iodine. Then, on both sides of the vertebral column three longitudinal incisions of about 2 cm were made through the full thickness of the skin. Subsequently, lateral to the incisions subcutaneous pockets were created by blunt dissection with scissors. One implant was inserted in each pocket. Finally the wounds were carefully closed with two Vicryl sutures. Of each type of implant, eight specimens were used. A total of 48 implants was placed. Randomization was achieved with a Latin square implantation schedule. Each animal received all types of implant. The implants were left in place for 10 weeks. Three weeks after implantation the sutures were removed. During the entire experiment, animal health was inspected weekly.

Histological evaluation techniques

At the end of the implantation period, the animals were sacrificed by suffocation in CO₂. Then the implanted tubes were removed including all surrounding tissues. For histological analysis the tissue-covered implants were fixed in 4% buffered formalin for one week, dehydrated in a series of ethanol and embedded in LR White resin (Polysciences, Warrington, USA) for two days at 45°C. LR White was chosen because its viscosity properties allows excellent penetration into the tissue. On the other hand, LR White does not penetrate into, or otherwise affects the silicone. After polymerization of the resin, the silicone implants were removed. The created opening in the specimens was then filled with LR White, that was cured with LR White accelerator. Subsequently, perpendicular to the groove direction, sections were cut of about 10 μ m in thickness, using a modified diamond blade sawing microtome technique^{20,21}. These were stained with methylene blue and basic fuchsin. Of each implant at least 3 sections suitable for evaluation were made, at different parts of the specimen. Thereafter, from the same tissue blocks, sections were cut of 8 μ m in thickness using a Leica RM 2165 Microtome equipped with a D knife. Three sections suitable for evaluation were made, and stained with a Van Gieson connective tissue staining. The advantage of Van Gieson staining is that it clearly discriminates the newly formed fibrous tissue in the capsule, from the older fibrous tissue.

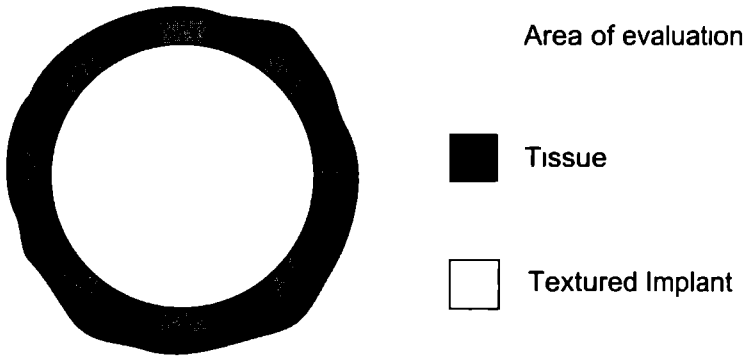


Figure 2: Schematic representation of a section used for the histomorphometrical evaluation, showing the predetermined areas of evaluation

Scanning electron microscopy

Scanning electron microscopy (SEM) was performed on silicone tube implants removed from the tissue after polymerization of the LR White. In this way, the quality of the substrates after explantation could be observed, and the possibility of tissue remaining on the implant surface could be determined. For this purpose, removed implant tubes were dried to air from EtOH 100%. Subsequently, specimens were sputter-coated with a thin layer of gold, and examined in a JEOL 6310 scanning electron microscope.

Qualitative histology

To assess the tissue reaction qualitatively, all sections were examined with a Leica DM RBE light microscope at a magnification of 40x.

Histomorphometrical evaluation

To quantify the soft tissue response to the implants, histomorphometric evaluations were performed on the 10 μm thick methylene blue/basic fuchsin sections. For this purpose, the microscopic images were projected with a total magnification of 400x on a color monitor using a CCD/RGB camera (Sony DXC151P) attached to the microscope. Subsequently, measurements were performed in 8 predetermined fields, using a computer, equipped with digital image analysis software (ArcImage, v 1.43, Foster Findlay Associates). The fields were positioned at regular intervals, in the capsule surrounding the implant (Figure 2). The used method of evaluation was adapted from an earlier publication of our group²². For each histological section we assessed four parameters, i.e. capsule thickness (quantitatively, in μm), capsule quality (in arbitrary points 0-4), interface thickness (quantitatively, in μm), and interface quality (in arbitrary points 0-4). A complete description of the arbitrary point scale is shown in Table 2.

Table 2: Histological grading scale for soft-tissue implants.

Score	Reaction Zone Response
Capsule Qualitatively:	
4	Capsule tissue is fibrous, mature, not dense, resembling connective or fat tissue in the non-injured regions
3	Capsule tissue is fibrous but immature, showing fibroblasts and little collagen
2	Capsule tissue is granious and dense, containing both fibroblasts and many inflammatory cells
1	Capsule consists of masses of inflammatory cells with little or no signs of connective tissue organization
0	Cannot be evaluated because of infection or other factors not necessarily related to the material
Interface Qualitatively	
4	Fibroblasts contact the implant surface without the presence of macrophages or foreign body giant cells
3	Scattered foci of macrophages and foreign body cells are present
2	One layer of macrophages and foreign body cells is present
1	Multiple layers of macrophages and foreign body cells are present
0	Cannot be evaluated because of infection or other factors not necessarily related to the material

Statistical analysis

After histomorphometrical evaluation, averages and standard deviations of all obtained data were calculated. Data were compared with an analysis of variance (ANOVA). If this revealed that statistical differences were present, post ANOVA testing was performed with a Student-Newman-Keuls test. All statistics were executed using StatMost (v.2.01 DataMost Co, Salt Lake City, USA).

RESULTS

Implant characterization

The cytotoxicity testing revealed that fibroblasts were growing around, and adhering to the discs *in vitro*. Fibroblasts were observed to exhibit normal cell morphology. Nowhere around the specimens an inhibition zone could be observed.

Macroscopic findings

During the post-implantation period, all animals showed an unevoked healing without any disturbance of the wound healing process. At implant retrieval, all removed implants were observed to be surrounded by a thin fibrous capsule. There were no macroscopic signs of an inflammatory reaction. The implants did not deteriorate. Unfortunately, one control-type implant was damaged during implant removal. In addition, another one could not be found during recovery. Consequently, only 6 controls were left for histological evaluation.

Scanning electron microscopy

SEM observation showed that the quality of the substrates after explantation was comparable to that before implantation. On all retrieved implants, surface microgrooves were clearly maintained. Hardly any tissue, or cellular debris, was found to be left on the explanted surface. This confirmed that during removal of the silicone implants from the polymerized LR-White blocks, separation occurred at the interface tissue-implanted surface.

Light microscopy

Examination of the histological sections revealed a fairly uniform tissue response for all tested materials. In all sections, normal skin and underlying tissues could be determined; i.e. epidermis, dermis, fibrous tissue, musculature, and fat. Sometimes a hair vesicle, blood vessel, or nerve bundle was seen. All implants were observed to be encapsulated in a fibrous layer, which could be clearly discerned from the original connective tissue like muscle fascia (Figure 3a). This capsule was about seven to eight layers of cells in thickness. The fibrocytes had flattened very much, indicating a matured capsule formation. Furthermore, a difference in capsule appearance existed between the median and skin side of the implants. At the skin side the capsule was always thicker (Figure 3b,c). Very occasionally, in the capsules small newly formed blood vessels were observed. Also, inflammatory cells were hardly seen in the capsule. On the other hand, in almost all sections, the fibrous capsule was found to be separated from the implant surface by a thin, single layer of mono- and multinucleated phagocytotic cells (Figure 3d). This layer was almost continuous, and only very occasionally a direct attachment of fibrous tissue to the implant was observed. For the microtextured surface, at the interface, the microgrooved pattern could be clearly seen. This again showed that the removal of the implants had not resulted in disruption of the tissue capsule. No gross differences in tissue response were observed between the various implant surfaces. Nevertheless, we noticed that on implants with the 6 μm deep surface microgrooves, the nuclei of the interfacial cells were frequently located in the grooves (Figure 3d). Finally, we found that the seam of the implant, where the edges of the sheets had been glued together, was always clearly visible. The non-uniform implant surface at these sites, gave rise to a local accumulation of fluid (Figure 3e). At these sites the fibrous capsule had a somewhat altered appearance. Therefore, these areas were therefore excluded from the histomorphometrical evaluation.

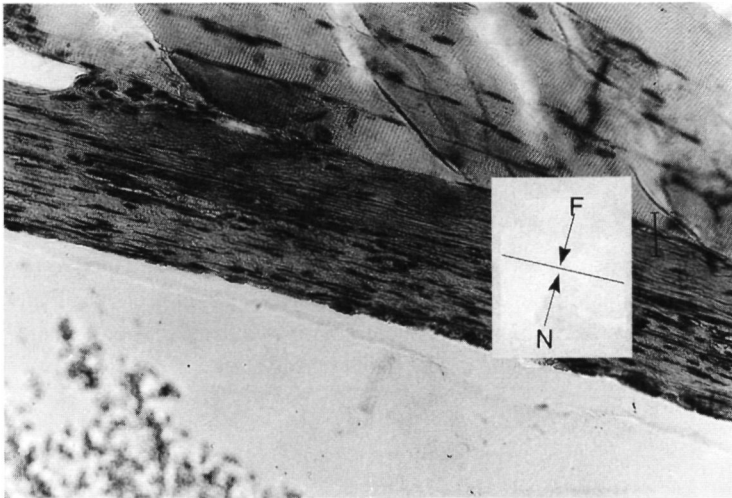


Figure 3a: Light micrograph of the tissue surrounding an implant, equipped with 0.5 μm deep microgrooves. Van Gieson staining enables clear distinction between new-formed fibrous tissue (N), and old fibrous tissue (F), original magnification 40x.



Figure 3b: Light micrograph of the tissue surrounding a 'control'-type implants. Implants are covered with a fibrous tissue capsule. Methylene blue/ basic fuchsin staining, original magnification 20x.

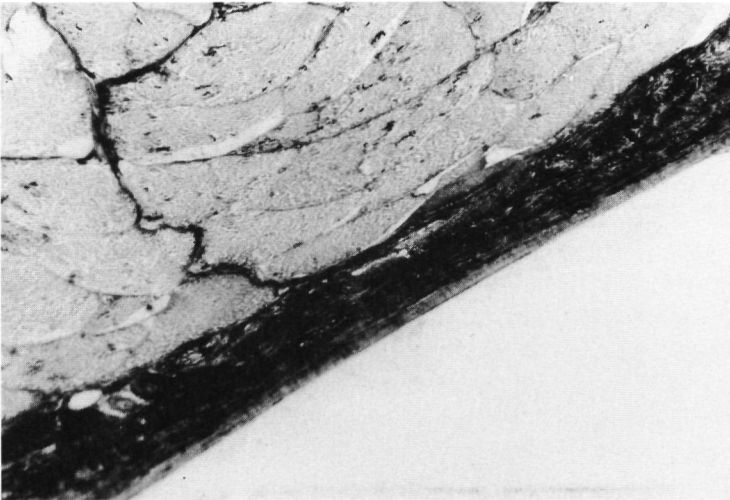


Figure 3c: Light micrograph of the tissue surrounding an implant, at the median side. Note that capsule quality is remarkably less than on the skin side, in Figure 3b. Methylene blue/ basic fuchsin staining, original magnification 20x.

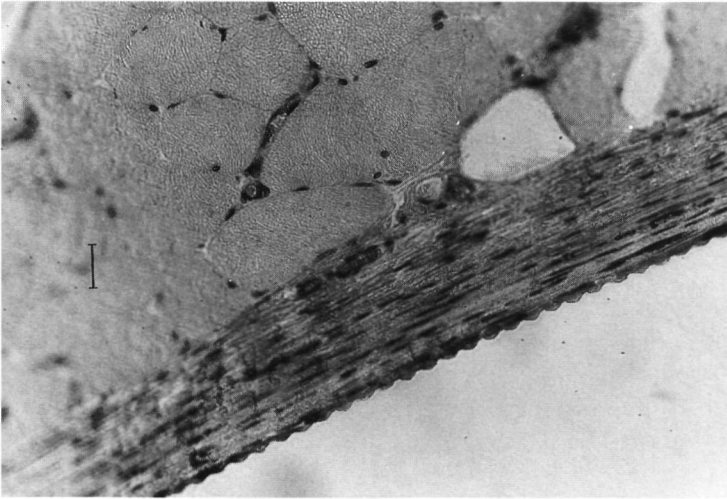


Figure 3d: Light micrograph of the tissue surrounding an implant, equipped with 6 μm deep microgrooves. A layer of inflammatory cells can be observed at the implant surface. Note that nuclei of these cells are mostly located in the grooves. Van Gieson staining, original magnification 40x.

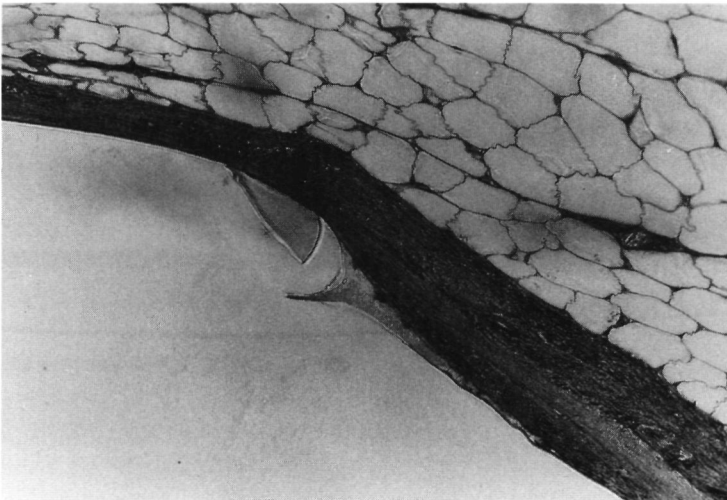


Figure 3e: At the seam of the implant, where the edges of the sheets had been glued together, a disruption in implant surface occurs (see also Figure 1). At these sites locally fluid accumulated. These areas were therefore excluded from the histomorphometrical evaluation. Methylene blue/ basic fuchsin staining, original magnification 20x.

Histomorphometrical evaluation

All histomorphometrical findings are listed in Table 3. The data show that around all types of implants, the capsule thickness was about 20 μm . No significant differences ($p>0.05$) were seen in relation to the various applied textures. The results of the qualitative assessment of the fibrous capsule indicates that after 10 weeks of implantation the capsule had not matured fully yet. Again, no significant differences ($p>0.05$) were seen between the different implant surfaces.

Further, measurement of the layer of inflammatory cells surrounding the implants revealed that this interfacial layer was about 3.5-4.5 μm thick. Although the data suggest that this layer around the 6 μm deep textures was somewhat thicker, statistical analysis revealed no significant difference between the smooth and various textured surfaces. Also, in the histomorphometric rating of the interfacial layer quality no differences in response towards the surface grooves were found ($p>0.05$).

DISCUSSION

In the last few years, many researchers have focused on microgrooved substrata. Though most researchers suggest possible clinical applications in implantology, most of the studies deal with *in vitro* phenomena. Our goal was to determine the behaviour of microgrooved implants, placed in the subcutaneous tissue of guinea pigs.

The guinea pig is often used as a model system for human skin²³. We choose to use it as our experimental model, because of the structural resemblance of also its subcutaneous tissue with the human analogue. Besides, multiple substrates can be placed in the same animal, which is favorable above smaller animals like rats or mice, and reduces intra-animal variability.

As implants, we used microgrooved silicone. Silicone is, despite several disadvantages, still a common used implant material for incorporation in soft tissue. The overall design of our implant was tube-like. In this way a completely textured surface could be achieved. Supported by our cytotoxicity *in vitro* test, our production process including the glueing of the textured silicone sheets is not expected to cause any negative effects. On the other hand, we know that the mechanical properties of an implant have a definitive influence on the wound healing process. Implants of the same material and surface configuration, but with different shape, exert different mechanical stresses on the surrounding tissue. Subsequently, this can affect capsule formation and contraction. Therefore tubular, or at least rounded implant designs are preferable²⁴. Despite these favorable characteristics of our implant design, there is also a disadvantage. Silicone rubber is a very flexible material. We know that irrespective their shape, implants will always be subjected to some mechanical stress in a free-moving animal. This can be enhanced by capsule contraction. In view of this, recent *in vitro* studies showed that fibroblasts are capable to deform silicone microfeatures by cytoskeletal contraction of the adhering cells¹⁷. SEM observation did not reveal any distortion of the surface patterns as applied on our implants during implantation. Still, the occurrence of a similar deformation effect as *in vitro* cannot completely be excluded. Consequently, we have to notice that the final 'controllability' of silicone rubber is perhaps not optimal. Nevertheless, based again on our *in vitro* results, we think that the used surface patterns were discriminating enough to induce a biological effect, even when some deformation occurs.

Table 3: Results of the histomorphometrical evaluations.

<i>Fibrous capsule thickness (µm (±standard deviation))</i>	
control	20.8 (5.1)
smooth	18.9 (4.3)
0.5	20.7 (5.5)
1	19.2 (4.3)
1.5	19.0 (4.0)
6	21.4 (4.8)
<i>Fibrous capsule quality (arbitrary points, see Table 2)</i>	
control	2.9 (0.2)
smooth	2.9 (0.2)
0.5	2.9 (0.2)
1	2.9 (0.2)
1.5	2.9 (0.2)
6	3.0 (0.1)
<i>Interfacial layer thickness (µm (±standard deviation))</i>	
control	3.6 (2.1)
smooth	3.7 (2.1)
0.5	3.7 (1.5)
1	3.7 (1.6)
1.5	3.9 (1.5)
6	4.5 (1.5)
<i>Interfacial layer quality (arbitrary points, see Table 2)</i>	
control	2.1 (0.2)
smooth	2.2 (0.3)
0.5	2.1 (0.2)
1.0	2.1 (0.2)
1.5	2.0 (0.1)
6	2.0 (0.1)

Corroborating our previous study, here we have found again no beneficial effect of all applied microtextures on the subcutaneous tissue healing response. Even despite the fact that we also implanted surfaces with a significantly increased groove depth. The overall tissue reaction was characterized by a fibrous encapsulation associated with an interfacial layer of inflammatory cells. There are some indications that the number of inflammatory cells on the deeper microtextures are enhanced. We suppose that the mechanical forces applied on an implant during movement, have caused an accumulation of inflammatory cells onto the implant surface. Furthermore, we know that both *in vitro* and *in vivo* macrophages are attracted to roughened surfaces, a phenomenon known as rugophilia^{25,26}. When comparing the different textures in this study, and those in our previous investigation¹¹, we only conclude that an increase of groove depth inevitably will lead to a further increase of this accumulation. This is confirmed by data from other investigators, who used micro-pillared surfaces with dimensions up to 500 μm ²⁷. As soon as implants are covered with inflammatory cells, these inhibit any effect of microgrooves on the fibrous capsule architecture. Inflammatory cells are subject to contact guidance, compared to fibroblasts²⁸. When at the implant surface a layer of inflammatory cells is present, the connective tissue cells outside that layer cannot sense the difference between textured and smooth surfaces.

In summary, we conclude that parallel surface microgrooves do not have an effect on capsule formation around silicone implants in soft tissue. However, we cannot exclude that this type of surface microfeatures has effects on other tissue healing responses. For example, it has been described extensively that microtextures can inhibit epithelial downgrowth around percutaneous implants²⁹⁻³¹. Further, because of their enlarged surface, microgrooves can also be applied as a carrier for tissue-repairing proteins, such as growth factors³².

LITERATURE

- 1 Singhvi R, Stephanopoulos G, and Wang DIC Review effects of substratum morphology on cell physiology. *Biotechnol Bioeng* 1994, 43, 764-771.
- 2 Von Recum AF, Shannon CE, Cannon EC, Long KJ, Van Kooten TG, and Meyle J Surface roughness, porosity, and texture as modifiers of cellular adhesion *Tissue Engineering* 1996, 2, 241-253
- 3 Curtis ASG, and Wilkinson C Topographical control of cells. *Biomaterials* 1997, 18, 1573-83.
- 4 Weiss P Experiments on cell and axon orientation in vitro: the role of colloidal exudates in tissue organization. *J Exp Zool* 1945, 100, 353-386
- 5 Walboomers XF, Croes HJE, Ginsel LA, and Jansen JA Growth behaviour of fibroblasts on microgrooved polystyrene. *Biomaterials* 1998, 19, 1861-1868
- 6 Chou L, Furth JD, Uitto V-J, and Brunette DM Effects of titanium substratum and grooved surface topography on metalloproteinase-2 expression in human fibroblasts *J Biomed Mater Res* 1998, 39, 437-445
- 7 Von Recum AF, and Van Kooten TG. The influence of micro-topography on cellular response and the implications for silicone implants *Journal of Biomaterials Science - Polymer Edition* 1995, 7, 181-198.
- 8 Brunette DM. Effects of surface topography on cell behaviour in vitro and in vivo. in: *Nanofabrication and biosystems* Hoch HC (ed.), Cambridge University Press, New York, 1996, 335-366.
- 9 Taylor SR, and Gibbons DF Effect of surface texture on the soft tissue response to polymer implants. *J Biomed Mater Res* 1983, 17, 205-227
- 10 Den Braber ET, De Ruijter JE, and Jansen JA. The effect of a subcutaneous silicone rubber implant with shallow surface micro grooves on the surrounding tissue in rabbits *J Biomed Mater Res* 1997, 37, 539-547

Chapter 8

- 11 Walboomers XF, Croes HJE, Ginsel LA, and Jansen JA Microgrooved subcutaneous implants in the goat. *J Biomed Mater Res* 1998, 42, 634-641.
- 12 Baier RE, and DePalma VA. Electrodeless glow discharge cleaning and activation of high-energy substrates to insure their freedom from organic contamination and their receptivity for adhesives and coatings. Calspan Report 1970, 176.
- 13 Amstein CF, and Hartman PA. Adaptation of plastic surfaces for tissue culture by glowdischarge. *J Clin Microbiol* 1975, 2, 46-54.
- 14 Chinn JA, Horbett TA, and Ratner BD Laboratory preparation of plasticware to support cell culture. *J Tiss Culture Meth* 1994, 16, 155-159.
- 15 Hill D Design engineering of biomaterials for medical devices. John Wiley & Sons, Chichester, UK, 1998
- 16 Chamberlain VC, Lambert B, and Tang FW. Sterilization effects. in: *Handbook of biomaterials evaluation, second edition* Von Recum AF (ed.), Taylor and Francis, Philadelphia, 1999, 253-261.
- 17 Walboomers XF, Croes HJE, Ginsel LA, and Jansen JA. Contact guidance of rat fibroblasts on various implant materials. *J Biomed Mat Res* 1999, 47, 204-212.
- 18 Northup SJ, and Cammack JN. Mammalian cell culture methods. in: *Handbook of biomaterials evaluation, second edition* Von Recum AF (ed.), Taylor and Francis, Philadelphia, 1999, 325-339.
- 19 Freshney RI. Culture of animal cells. a manual of basic technique. New York, Alan R. Liss Inc., 1987.
- 20 Van der Lubbe HBM, Klein CPAT, and De Groot K. A simple method for preparing thin (10 µm) histological sections of undecalcified plastic embedded bone with implants. *Stain Technology* 1988, 63, 171-177.
- 21 Klein CPAT, Sauren YMHF, Modderman WE, and Van der Waerden JPCM. A new saw technique improves preparation of bone sections for light and electron microscopy. *J Appl Biomater* 1994, 5, 369-373.
- 22 Jansen JA, and Van 't Hof MA. Histological assessment of sintered metal-fibre-web materials", *J of Biomaterials applications* 1994, 9, 30-54.
- 23 Mendenhall HV. Animal selection in: *Handbook of biomaterials evaluation, second edition* Von Recum AF (ed.), Taylor and Francis, Philadelphia, 1999, 475-479.
- 24 Cholvin NR, and Bayne NR General compatibility in: *Handbook of biomaterials evaluation, second edition* Von Recum AF (ed.), Taylor and Francis, Philadelphia, 1999, 507-521.
- 25 Harris AK, and Rich A. Anomalous preferences of cultured macrophages for hydrophobic and roughened substrata. *J Cell Sci* 1981, 50, 1-7.
- 26 Salthouse TN. Some aspects of macrophage behaviour at the implant interface. *J Biomed Mater Res* 1984, 18, 395-401.
- 27 Picha GJ, and Drake RF. Pillared-surface microtexture and soft-tissue implants: effect of implant site and fixation. *J Biomed Mat Res* 1996, 30, 305-312.
- 28 Meyle J, Gultig K, and Nisch W. Variation in contact guidance by human cells on a microtextured surface *J Biomed Mat Res* 1995, 29, 81-88.
- 29 Chehroudi B, Gould TR, and Brunette DM. Effects of a grooved titanium-coated implant surface on epithelial cell behaviour in vitro and in vivo. *J Biomed Mater Res* 1989, 23, 1067-1085.
- 30 Chehroudi B, Gould TR, and Brunette DM. Titanium-coated micromachined grooves of different dimensions affect epithelial and connective-tissue cells differently in vivo *J Biomed Mater Res* 1990, 24, 1203-1219.
- 31 Chehroudi B, Gould TR, and Brunette DM. A light and electron microscopic study of the effects of surface topography on the behaviour of cells attached to titanium-coated percutaneous implants *J Biomed Mater Res* 1991, 25, 387-405.
- 32 Kapur R, Calvert JM, and Rudolph AS. Electrical, chemical, and topological addressing of mammalian cells with microfabricated systems. *J Biomech Eng* 1999, 121, 65-72

Summary, address to the aims, and closing remarks

Samenvatting, evaluatie van de doelstellingen, en afsluitende opmerkingen

SUMMARY, ADDRESS TO THE AIMS, AND CLOSING REMARKS

Epidemiologic research still indicates that medical and dental implants are inclined to occasional early and more frequent late “failures”, meaning that the implantation did not result in lasting and/or permanent clinical performance. It is supposed that the initial reaction of cells is an important factor in the final tissue-reaction towards an implanted device. Many studies performed during the last two decades have focused on understanding the interactions between different cells and tissues of the body, and implant materials. All studies in the current thesis deal with the potential use of microgrooved surfaces for application onto implant materials. Therefore, a general introduction into the cells’ cytoskeleton, and current knowledge of cell reaction towards microtextures, is presented in **chapter 1**. Each subsequent chapter discusses a separate study. In this summary, the aims as described in the first chapter are addressed on a point-by-point basis.

- 1 Does the cellular growth behaviour *in vitro* to standardized, well characterized surfaces relate to the microgeometrical properties of these surfaces?
- 2 Does the orientation of intra-cellular cytoskeletal components differ between cells cultured on smooth and microtextured surfaces?
- 3 Several scientific publications propose mechanisms for the occurrence of contact guidance. Can any of these theories be proven true or rejected?

In **chapter 2**, a study is presented investigating the contact guidance phenomenon of rat dermal fibroblasts (RDF) on microgrooved polystyrene substrates. Polystyrene (PS) microgrooved substrates were produced by solvent casting on molds produced by photo lithographic techniques. The grooves were 1 μm deep, and between 1 and 10 μm wide. Light microscopy and digital image analysis (DIA) showed that RDF were oriented on all microgrooved substrates. Scanning electron microscopy (SEM) showed that RDF cultured on 1 or 2 μm wide grooves were positioned on top of the ridges. On wider 5 and 10 μm grooves cells were able to descend into the grooves. In confocal laser scanning microscopy (CLSM), focal adhesions were lying in the same direction as the actin filament where they attached to DIA confirmed an orientational behaviour of focal adhesions and actin filaments on microgrooves. There were no differences in the measured orientation between the different grooves. Besides, no obvious preference was found for focal adhesions to lie along edges of the surface ridges. Transmission electron microscopy (TEM) showed that focal adhesions were able to bend along the edges of ridges. On basis of our observations we suggest that the breakdown and formation of fibrous cellular components, especially in the filopodium, is influenced by the microgrooves. The microgrooves create a pattern of mechanical stress, which influences cell spreading and cause the cell to be aligned with surface microgrooves.

- 4 What is the influence of the groove-depth on the response of the cells? Is groove depth an important factor in the alignment and maximal attachment of cells?

In **chapter 3**, RDF cells were cultured on smooth or microgrooved (1-20 μm wide, 0.5-5.4 μm deep)

substrates We investigated the attachment of RDF with various analytical techniques Light microscopy and image analysis showed that RDF were oriented on most microgrooves The rate of orientation was effectively increased by an increase of groove depth Analysis of confluent layers of RDF showed that at confluency microgrooves were able to support greater numbers of cells However, the largest numbers of cells were not found on the narrowest and deepest microgrooves, though these have the largest total surface and induce strongest alignment Interference reflection microscopy (IRM) showed that the RDF form focal adhesions, where the cell membrane is only 10 nm from the substrate IRM also showed that RDF follow the contours of shallow and wide microgrooves, but bridge the grooves on deeper and narrower ones This could explain why such grooves are not able to increase the numerical cell adhesion more The absence of contact between cells and bottom of the grooves is a very important factor in establishing contact guidance

5 Is the cellular response to microtextures the same if different substrate materials are compared?

In literature, it has been suggested that cellular alignment on microgrooves is predominantly dependent on groove dimensions, and that surface chemical variation of the substrate material has little effect Therefore, in **chapter 4** we seeded RDF on smooth and microgrooved (grooves 1-10 μm , depth 0.5 μm) PS, poly-L-lactic acid (PLA), silicone (SIL), and titanium (Ti) substrates The production process was found to be more accurate for PS and PLA, than for SIL and Ti substrates A proliferation study, and scanning electron microscopy, confocal laser scanning microscopy, and transmission electron microscopy revealed differences between RDF behaviour on the materials Our conclusions are, that 1) the accuracy of microtexture production by casting depends greatly on the used material, 2) even if no sharp discontinuities are present, microtextures are still potent of inducing contact guidance, and 3) besides surface texture, surface chemistry has a definitive influence on cell morphology

6 How is the initial attachment behaviour of cells towards the substrate influenced by the application of microgrooves?

Before, we suggested that the contact guidance phenomenon is based on mechanical clues, and that it is expected to occur from the earliest phases of cell spreading Therefore, in **chapter 5** we investigated the 'contact guidance' phenomenon, shortly after cell attachment For this purpose PS substrates were produced, either smooth, or equipped with microgrooves (depth 0.5 μm , width 1-10 μm) On these substrates, fibroblasts were cultured in standard culture medium, and in cytochalasin-B (an actin polymerization inhibitor) supplemented medium Cells were fixed at 15, 30, 45, 60, 120, and 240 minutes and studied with light microscopy, SEM, CLSM, and DIA We found that up to 1 hour, cell attachment on the grooved substrates was impaired Further, cells oriented to the direction of the microgrooves This orientation was established fastest on the narrow grooves SEM showed that cells form membrane extensions in all directions after 30 minutes CLSM showed that well-formed actin filaments were not present in the cell body at timepoints before 4 hours, and that cells on smooth surfaces exhibited less filaments Cytochalasin-B caused a delay of cell attachment and spreading From these experiments, we conclude that a well formed cellular actin cytoskeleton is no prerequisite for the occurrence of

contact guidance The interplay between the filopodium and extracellular matrix (ECM) molecules seems to be the determining factor in the establishment of contact guidance

7 Is the response to microgrooves in the substrate dependent on cell-type?

To be compared with the previous studies on fibroblasts, the study presented in **chapter 6** evaluated the behaviour of rat bone marrow (RBM) cells RBM were cultured on microgrooved PLA and PS surfaces The applied groove depth was 0.5, 1.0 or 1.5 μm , with a groove and ridge width of 1, 2, 5 or 10 μm SEM examination showed a collagen rich mineralized layer of ECM was deposited Alignment of the cells and matrix to the surface grooves, was observed as described before Quantitative evaluation, using a tetracycline labeling assay, revealed that more mineralized ECM was formed on the PLA than on the PS Further, PLA surfaces with a groove depth of 1.0 μm and groove widths of 1 and 2 μm induced most mineralized ECM Finally, alkaline phosphatase activity was also higher on most microgrooved PLA surfaces, compared with the other materials On basis of these observations, we concluded that microtextured surfaces are able to influence the differentiation of osteoblast-like cells and the deposition of mineralized matrix Probably, this phenomenon can be used to increase the bone regeneration around oral implants

8 Does the application of microgrooves on implant surfaces influence the healing of these implants?

In this thesis, 2 *in vivo* studies are presented, where we investigated the behaviour of microgrooved implants in soft subcutaneous tissue

In **chapter 7**, we used PS implantable discs, either smooth or microgrooved (1-10 μm) at both sides Implants were placed subcutaneously for 1, 4 or 12 weeks, in a goat Light and TEM showed that fibrous capsule formation around implants was fairly uniform After 1 week implants were covered with a fibrous capsule, about 80 μm thick The collagen matrix was loose, and many inflammatory cells were present After four weeks, the matrix was more dense and contained many newly formed blood vessels At the implant surface a layer of inflammatory cells, about 10 μm in thickness, had accumulated Finally, after 12 weeks, the matrix had densified One cellular layer of inflammatory cells was present at the implant surface We carried out histomorphometric measurements, concerning capsule thickness, inflammatory layer thickness and number of blood vessels Capsule thickness appeared not to decrease in time Further, these measurements showed that there were no differences in tissue reaction between smooth and microgrooved implants On the basis of our observations, we suggest that 1 μm deep, and 1-10 μm wide, microgrooves do not influence the tissue response around polystyrene implants in soft tissue

In **chapter 8**, we studied the influence of 2 μm wide microgrooves, with various depths (0.5-6 μm), on capsule formation around subcutaneous silicone implants, in an animal experiment Silicone sheets with microtexture were glued around silicone tubes These implants were placed subcutaneously in eight guinea pigs for 10 weeks The implanted tubes were removed including all surrounding tissues, and processed for light microscopy and subsequent histomorphometrical evaluation All removed

implants were surrounded by a thin fibrous capsule, and it was observed that this capsule was separated from the implants by a thin, single layer of mono- and multinucleated phagocytotic cells. In histomorphometry no significant differences were seen in relation to the reaction towards the various textures. We again conclude that microtextures do not have an effect on the morphological characteristics of capsule formation around silicone implants in soft tissue.

Closing remarks, and future perspectives

The current investigations have provided further insight on the contact guidance phenomenon. Based on all cell-culturing experiments, a new explanation for the occurrence of contact guidance is postulated. We suggest that cellular actin cytoskeleton is no prerequisite for the occurrence of contact guidance. The interplay between the filopodium and ECM molecules seems to be the determining factor in the establishment of contact guidance. Of course, further investigations to the properties of both cells and substratum are necessary to prove our assumptions. The role of the filopodium should be investigated more extensively, for instance with high-resolution optics. For investigating the physico-chemical surface properties and related ECM adsorption, atomic force microscopy (AFM) seems a valuable technique.

In our *in vivo* experiments we could not determine an evident effect of microtextures on the formation of fibrous capsules around subcutaneous implants. Implant parameters in the soft tissue response to implants are the design and mechanical properties of the used implant material. Various tissue layers slid over each other during movements of the animal. This, in combination with a discrepancy in E-modulus between implant and surrounding tissue is a stronger determinant of capsule formation than the applied textures. Though no influence of microtexture on capsule formation could be determined, on basis of the cell-culturing experiments, and *in vivo* results of other groups, we still think that other possible applications for the microtexturing phenomenon in implantology have to be explored. Perhaps microgrooved surfaces can be applied on membranes as used for guided tissue regeneration (GTR) techniques. Further, since microgrooves orient the migration of cells they might also be useful to support healing of large tissue defects, like cleft palates, burn wounds, and to enhance repair of highly orientated structures like nerve bundles, and tendon. In these regenerative processes additional benefit can be obtained from the use of microtextured surfaces as a carrier for growth factors.

Besides soft-tissue applications, the use of surface texturing can be interesting for hard tissue implants. Our and other recent studies indicated that microtextures can have an effect on bone cells. Unfortunately, at the moment no *in vivo* data are available.

Finally, an additional point of interest remains the production of differently shaped, microgrooved surfaces. Usually, implants are not planar. Therefore, to study the possible beneficial effect of microtexturing for implants, development of new microfabrication techniques to manufacture microstructures on non-planar surfaces is imperative. Development of these techniques will not only benefit biomaterial research, but also the production of microelectronic, mechanical, and optical devices and subsystems.

SAMENVATTING, EVALUATIE VAN DE DOELSTELLINGEN, EN AFSLUITENDE OPMERKINGEN

Epidemiologisch onderzoek toont aan, dat medische en tandheelkundige implantaties kunnen eindigen in een “mislukking” Hiermee wordt bedoeld dat de procedure niet heeft geleid tot een blijvend klinisch resultaat. Af en toe tredt dit falen vroeg na implantatie op, frequenter op latere tijdstippen. Algemeen wordt aangenomen dat de initiële weefsel-reactie ten opzichte van een implantaat mede bepalend is voor het uiteindelijke succes. Daarom zijn er in de laatste twee decennia vele studies uitgevoerd die zich richten op het ontrafelen van interacties tussen de verschillende cellen en weefsels van het lichaam, en implantatie materialen. De studies die in dit proefschrift besproken worden hebben betrekking op het gebruik van microgroeven, als mogelijk oppervlak voor implantatie materialen. In **hoofdstuk 1** wordt eerst een algemene introductie gegeven, over het cel cytoskelet, en huidige kennis van microtexturen. De volgende hoofdstukken bespreken elk een bijzonder onderzoek. Deze samenvatting behandelt puntsgewijs de in het eerste hoofdstuk aangegeven doelstellingen.

- 1 Is het groei gedrag *in vitro* op gestandaardiseerde, en goed gekarakteriseerde, celkweek oppervlakken gerelateerd aan de micro-geometrische afmetingen van deze oppervlakken?
- 2 Is de orientatie van intra-cellulaire cytoskelet componenten verschillend bij cellen gekweekt op gladde oppervlakken versus oppervlakken voorzien van een microtextuur?
- 3 Een aantal wetenschappelijke publicaties stellen mechanismen voor, ter verklaring van het verschijnsel contact geleiding. Kan een van deze theorieën bewezen, of ontkend worden?

In **hoofdstuk 2** wordt een studie beschreven naar contact geleiding van ratte huid fibroblasten (RDF) op polystyreen (PS) substraten met microgroeven. Deze substraten werden gegoten op mallen, die gemaakt werden met behulp van een foto- lithografische techniek. De groeven waren 1 μm diep, en tussen 1 en 10 μm breed. Licht microscopie, en digitale beeld analyse (DIA) lieten zien dat RDF cellen georiënteerd groeiden op alle substraten die voorzien waren van microgroeven. Scanning elektronen microscopie (SEM) liet zien dat RDF cellen op 1 of 2 μm brede groeven boven op de richeltjes van het oppervlak gepositioneerd waren. Op de bredere 5 en 10 μm brede groeven daarentegen, waren de cellen ook in staat af te dalen in de groeven. Met behulp van confocale laser scanning microscopie (CLSM), werden de focale adhesiepunten van de cellen afgebeeld. Deze lagen in dezelfde richting als de actine filamenten waaraan zij verbonden waren. DIA bevestigde het georiënteerde gedrag van de focale adhesies, en de actine filamenten. Tussen de verschillende groef types, werden geen verschillen gevonden in de gemeten orientaties. Daarnaast kon geen voorkeur vastgesteld worden van de focale adhesies voor een positie op de randen van de richeltjes. Transmissie elektronen microscopie (TEM) liet zien dat focale adhesies in staat waren om te buigen rond de randen van de richeltjes. Gebaseerd op deze observaties stellen we voor dat de afbraak en vorming van fibreuze cellulaire componenten, vooral in het filopodium, beïnvloed wordt door de microgroeven. De microgroeven veroorzaken zo een patroon van mechanische stress, dat op zijn beurt cel spreiding beïnvloed, en het cel uitrichtings-gedrag veroorzaakt.

4. Wat is de invloed van de toegepaste groefdiepte op de respons van de cellen? Is groefdiepte een belangrijke factor voor cel uitrichting en maximale celhechting?

In **hoofdstuk 3**, werden RDF cellen gekweekt op gladde en gegroefde (1-20 μm breed, 0.5-5.4 μm diep) substraten. We onderzochten de hechting van RDF met verschillende technieken. Lichtmicroscopie en DIA liet zien dat RDF zich oriënteerde op de meeste soorten microgroeven. De mate van oriëntatie werd zeer effectief verhoogd wanneer de groefdiepte toenam. Bij analyse van confluente lagen RDF cellen, bleek dat substraten voorzien van microgroeven in staat waren om meer cellen te dragen, dan gladde substraten. Echter, de grootste hoeveelheden cellen werden niet gevonden op de smalste en diepste microgroeven, terwijl deze wel het grootste totale oppervlak hebben, en bovendien het sterkst celoriëntatie induceren. Interferentie reflectie microscopie (IRM) liet zien dat de RDF focale adhesies vormen. Op deze punten is de cel membraan slechts 10 nm van het substraat verwijderd. IRM toonde verder aan dat RDF de contouren van ondiepe en brede microgroeven volgen, terwijl de diepere en nauwere groeven overbrugd werden. Dit zou kunnen verklaren waarom deze laatste groeven niet in staat bleken de cel adhesie te vermeerderen. De afwezigheid van contacten tussen de cellen en de bodem van de groeven lijkt een erg belangrijke factor in het optreden van contact geleiding.

5. Is de cellulaire reactie ten opzichte van microtexturen vergelijkbaar wanneer naar verschillende substraat materialen worden vergeleken?

In de vakliteratuur wordt beweerd dat cellulaire uitlijning op micro-groefpatronen voornamelijk afhankelijk is van de groef dimensies, en dat oppervlakte chemische veranderingen van het substraat materiaal weinig effect zal hebben. In het onderzoek beschreven in **hoofdstuk 4**, werden daarom RDF cellen uitgezet op gladde en gegroefde (groeven 1-10 μm , diepte 0.5 μm) PS, poly-l-melkzuur (PLA), siliconen rubber (SIL), en titanium (Ti) substraten. Het gebruikte productie proces bleek veel accurater voor het maken van PS en PLA, dan voor SIL and Ti substraten. Een proliferatie studie, SEM, CLSM, en TEM onthulde een aantal verschillen tussen het gedrag van RDF cellen op de vier materialen. Onze conclusies waren dat 1) de accuratesse van microtextuur fabricage is grotendeels afhankelijk van het gebruikte materiaal, 2) zelfs als er geen scherpe oneffenheden aanwezig zijn, zijn microtexturen nog in staat contact geleiding te veroorzaken, en 3) naast oppervlakte textuur, hebben ook de oppervlakte chemische eigenschappen van een materiaal een beduidende invloed op cel morfologie.

6. Hoe wordt het initiële hechtings gedrag van cellen aan substraten beïnvloed door de toepassing van microgroeven?

Eerder beweerden we dat contact geleiding gebaseerd is op mechanische stimulansen, en waarschijnlijk optreedt vanaf de allereerste fasen van cel spreiding. Daarom was het onderzoek gepresenteerd in **hoofdstuk 5** gericht op het verder onderzoeken van de invloed van microgroeven op de celvorm, vlak na celhechting. Hiertoe werden PS substraten gemaakt, die glad waren, of voorzien van microgroeven (diepte 0.5 μm , breedte 1-10 μm). Op deze substraten, werden fibroblasten gekweekt in standaard kweekmedium, en in medium waaraan cytochalasine-B (een actine polymerisatie remmer) was

toegevoegd De cellen werden gefixeerd na 15, 30, 45, 60, 120, en 240 minuten, en bestudeerd met licht microscopie, SEM, CLSM, en DIA Gezien werd dat tot een uur het aantal cellen op gegroefde substraten lager was, dan op gladde oppervlakken Cel orientatie trad het eerst op bij de smalste groefpatronen Geen verschillen in cel oppervlak konden worden aangetoond tussen de verschillende substraten SEM liet zien dat cellen vanaf 30 minuten in alle richtingen membraan-uitstulpingen maakten, om het oppervlak af te zoeken CLSM liet zien dat volledig gevormde actine filamenten in het cellichaam pas na 4 uur ontstonden, en dat cellen op gladde oppervlakken een minder filamenten bezaten Cytochalasine-B veroorzaakte een vertraging van cel hechting en spreiding Uit deze experimenten, leiden we af dat een volledig gevormd cellulair actine cytoskelet geen voorwaarde is voor het optreden van contact geleiding De interactie tussen het filopodium en extracellulaire matrix (ECM) moleculen lijkt de beslissende factor te zijn in het optreden van contact geleiding

7 Is de respons ten aanzien van substraat microgroeven afhankelijk van het celtype?

Ter vergelijking met eerdere studies aan fibroblasten, werd in het onderzoek gepresenteerd in **hoofdstuk 6**, het gedrag van ratte beenmerg cellen (RBM) geëvalueerd Deze werden gekweekt op PLA en PS oppervlakken voorzien van microgroeven De aangebrachte groefdiepte was 0,5, 1,0 of 1,5 μm , met een groefbreedte van 1, 2, 5 of 10 μm SEM onderzoek wees uit dat door deze cellen een collageen rijke laag van gemineraliseerde matrix werd afgezet De uitlijning van cellen in de richting van de oppervlakte groeven, was vergelijkbaar met eerdere onderzoeken aan fibroblasten Kwantitatieve evaluatie, met een tetracycline labeling assay, liet zien dat meer gemineraliseerde ECM gevormd werd op PLA dan op PS PLA oppervlakken met een groefpatroon van 1,0 μm diep en 1 of 2 μm breed induceren mineralisatie van de ECM het sterkst Tenslotte was ook de alkaline fosfatase activiteit hoger op de meeste gegroefde PLA substraten Op basis van deze observaties concluderen we dat microstructuren in staat zijn om de differentiatie van osteoblast-achtige cellen, en de depositie van gemineraliseerde matrix, te beïnvloeden Waarschijnlijk kan dit fenomeen gebruikt worden om de botregeneratie te bevorderen rond bijvoorbeeld orale implantaten

8 Kunnen microgroeven op implantaat oppervlakken de wondheling rond die implantaten beïnvloeden?

In dit proefschrift, worden 2 *in vivo* studies gepresenteerd, waarbij gekeken werd naar het gedrag van gegroefde implantaten in zacht weefsel

In **hoofdstuk 7**, werden implanteerbare PS schijfjes gebruikt, die glad waren of aan beide kanten voorzien van microgroeven (1-10 μm) Deze implantaten werden subcutaan in een geit geplaatst gedurende 1, 4 of 12 weken Licht microscopie en TEM lieten zien dat de vorming van een fibreus kapsel rond de implantaten redelijk uniform optrad Na 1 week waren de implantaten bedekt met een fibreus kapsel, van ongeveer 80 μm dik De collageen matrix was weinig georganiseerd, en er waren vele ontstekingscellen aanwezig Na 4 weken, had de matrix zich sterk verdicht, en bevatte het kapsel vele nieuwgevormde bloedvaatjes Op het implantaat oppervlak had zich een laag van ontstekingscellen gevormd, die ongeveer 10 μm dik was Tenslotte, na 12 weken, was de matrix zeer verdicht Een enkele

laag van onstekingscellen was aanwezig op het implantaat oppervlak. Met behulp van histomorfometrie werden de dikte van het kapsel, de dikte van de laag ontstekingscellen, en het aantal bloedvaten bepaald. De kapseldikte bleek niet af te nemen met de tijd. Verder lieten de metingen zien dat er geen verschillen bestonden in de weefselreactie tussen gladde implantaten, en implantaten voorzien van microgroeven. Daarom nemen we aan dat 1 μm diepe, en 1-10 μm brede, microgroeven de weefsel respons rond polystyreen implantaten in zacht weefsel niet beïnvloeden.

In hoofdstuk 8, bestudeerden we de invloed van 2 μm brede microgroeven met verschillende diepten (0.5-6 μm), op kapsel vorming rond subcutane siliconen implantaten. Siliconen films met een microtextuur werden rond siliconen slangetjes gelijmd. Deze implantaten werden subcutaan geplaatst in acht cavia's, gedurende 10 weken. De geïmplanteerde slangetjes werden verwijderd inclusief al het omliggende weefsel, en bewerkt voor licht microscopie en daaropvolgende histomorfometrische evaluatie. Alle verwijderde implantaten waren omgeven met een dun fibreus kapsel. Dit kapsel was gescheiden van het implantaat oppervlak door een dunne enkele laag van mono- en multinucleaire fagocytotische cellen. In de histomorfometrie werden geen significante verschillen gezien, in relatie tot de reactie op verschillende texturen. We concluderen dat microtexturen geen effect hebben op de morfologische karakteristieken van kapsel vorming rond siliconen implantaten in zacht weefsel.

Afsluitende opmerkingen en toekomstperspectief

De studies in dit proefschrift hebben geleid tot nieuwe inzichten in het fenomeen contact geleiding. Gebaseerd op alle celkweek experimenten is een nieuwe theorie geformuleerd ter verklaring van dit verschijnsel. We nemen aan dat een cellulair actine cytoskelet geen vereiste is, maar dat interactie tussen het filopodium en ECM eiwitten de belangrijkste factor in het ontstaan van contact geleiding lijkt. Natuurlijk zijn vervolg studies nodig, die verder ingaan op de eigenschappen van zowel de cellen als het substraat, om onze aannames te bevestigen. De rol van het filopodium zou bijvoorbeeld beter bestudeerd moeten worden op een hogere resolutie dan voorheen. Voor de bestudering van de physico-chemische oppervlakte eigenschappen van het substraat en de daaraan gerelateerde ECM adsorptie, lijkt atomic force microscopy (AFM) een veelbelovende techniek.

In onze *in vivo* experimenten konden we geen duidelijke effecten van microtexturen vaststellen op de vorming van fibreuze weefsel kapsels rond subcutane implantaten. De parameters die de zacht weefsel reactie ten opzichte van een implantaat bepalen zijn ten eerste de vorm, en ten tweede de mechanische eigenschappen van het gebruikte materiaal. De verschillende lagen weefsel bewegen over elkaar bij bewegingen van het dier. Dit, in combinatie met de discrepantie van E-modulus tussen het implantaat en het omliggende weefsel, blijkt een sterkere determinant van kapsel vorming dan de aangebrachte texturen. Alhoewel geen invloed van microtextuur vastgesteld kon worden lijkt het op basis van de celkweek experimenten, en *in vivo* resultaten van andere onderzoeksgroepen, dat er wel andere mogelijke applicaties van micro textuur techniek in implantologie onderzocht dienen te worden. Microgroeven kunnen bijvoorbeeld toegepast worden op membranen zoals die in de tandheelkunde toegepast worden, voor geleide weefsel regeneratie (GTR). Omdat microgroeven de migratie richting van cellen bepalen, zouden ze ook waardevol kunnen blijken ter ondersteuning van de reparatie van grote weefsel defecten zoals een gespleten verhemelte en brandwonden, en van sterk georiënteerde structuren zoals zenuwbanen en pezen. Bij deze regeneratieve processen zou bovendien microtextuur

van additionele waarde kunnen blijken als drager voor groeifactoren

Naast een toepassing in zachte weefsels, zou oppervlakte textuur gebruikt kunnen worden voor implantaten die geplaatst worden in harde weefsels. Onze, en andere recente celkweek studies hebben bewezen dat microtexturen ook bruikbaar zijn om botcellen te beïnvloeden. Helaas zijn er op dit moment nog geen *in vivo* data beschikbaar.

Tenslotte blijft een laatste punt van interesse de ontwikkeling van andersvormige micro-gegroefde oppervlakken. Normaliter zijn implantaten niet vlak. Voor het bestuderen van mogelijke positieve effecten van microtextuur op implantaten, is het noodzakelijk nieuwe microfabricage technieken te ontwikkelen om microtexturen te kunnen produceren op niet-gladde oppervlakken. De ontwikkeling van zulke technieken zal niet alleen een stimulans zijn voor het biomaterialen onderzoek, maar ook voor het onderzoek aan micro-elektronische, mechanische, en optische apparatuur en deelsystemen.

DANKWOORD

Bij het uitvoeren van de experimenten, en schrijven van dit proefschrift ben ik natuurlijk gesteund door een groot aantal mensen, die ik hierbij wil bedanken

Allereerst prof dr John Jansen, hoofd van de afdeling Biomaterialen, mijn begeleider en promotor Zijn deskundigheid en enthousiasme waren de basis van het onderzoek Op een begeleider met zijn snelheid en accuratesse bij het correctiewerk zullen veel promovendi jaloers zijn

Daarnaast wil ik de mensen van het Trigon bedanken Prof dr Leo Ginsel was mijn tweede promotor Vooral tijdens de 'maandag-praatjes' en werkoverleggen heeft hij me regelmatig van bruikbaar commentaar voorzien Voor het TEM werk dat in de diverse hoofdstukken staat beschreven heeft Huib Croes de coupes gemaakt Huib, hardstikke bedankt Daarnaast wil ik in het bijzonder Hans Smits noemen Hans is zonder meer een van de vriendelijkste mensen die ik ooit ben tegengekomen! Hij was altijd bereid om me te helpen met allerlei microscopie-problemen en het maken van dia's

Twee analisten hebben bijzonder veel bijgedragen aan de experimenten Anja de Ruijter heeft geholpen met alles wat met celkweek en histologie te maken heeft, met een grote no-nonsense aanpak Jan-Paul van der Waerden heeft op vele manieren zijn steentje bijgedragen, vooral op het gebied van histologie en microscopie Daarnaast weet JP (bijna) alles van computers, fotografie, en heeft hij vele mooie tekeningen voor me gemaakt

Verder wil ik mijn kamergenoot Martijn Gerritsen bedanken Eigenlijk had ik een eigen kamertje op de afdeling, maar door 'duistere krachten' werd ik al na een half jaar verdreven naar 671 Vaak hebben we gediscussieerd over het onderzoek en vele andere zaken En dan zijn stimulerende opmerkingen ("hé, kan je niet gewoon naar huis gaan ofzo ")

Ook een dankjewel voor alle medewerkers van Biomaterialen van vroeger en nu Gonnie, Piet, Kitty, Hilde, Suzy, Yvonne, Anne-Gitte, Edwin, Frank, Joop, Suzanne, Harry, Kenichi Matsuzaka ('the crazy man from Japan'), Edwin, Jack, Juliette, Johan, Petra, Bas, Olga en Marianne Ook mogen de 'masters-studenten' parodontologie met wie ik heb samengewerkt niet onvermeld blijven Roberto, Tjil, en Thorsten

De mensen van het CDL wil ik bedanken voor alle deskundige hulp Fred, Ton en Theo voor de studie beschreven in hoofdstuk 7, en Alex en Henk voor het werk uit hoofdstuk 8

Also I would like to express my gratitude to the people of the Centre for Cell Engineering in Glasgow First of all prof Adam Curtis, who was so kind to have me on his lab for a while, and who showed me the Highlands during the weekend Dr Mathis Riehle and Graham Tobiasnick helped me a lot in the lab with cell culturing and the IRM microscopy And finally Douglas Hamilton, who showed me the pubs of Glasgow

Tenslotte wil ik mijn familie, en Jenneke bedanken voor hun liefde, steun, en vertrouwen in de afgelopen jaren Zonder jullie was dit proefschrift nooit tot stand gekomen

CURRICULUM VITAE

Xaverius Franciscus (Frank) Walboomers werd op 15 juni 1971 geboren in Apeldoorn. In 1989 behaalde hij het diploma Atheneum-B aan het Katholiek Veluws College te Apeldoorn. Hetzelfde jaar begon hij een studie biologie aan de Katholieke Universiteit Nijmegen. In september 1995 werd het doctoraal examen afgelegd, in de medisch-biologische richting, met als hoofdvakken Celbiologie (prof. dr. E.J.J. van Zoelen) en Experimentele Gynaecologie (dr. H. Goverde), en als bijvak Vergelijkende en Fysiologische Psychologie (prof. dr. A.M.L. Coenen en dr. W.H.I.M. Drinkenburg). Hierna werd hij aangesteld als onderzoeker-in-opleiding (OIO) om microtexturen te bestuderen op de afdeling Biomaterialen, vakgroep Orale Functieeler, Faculteit der Medische Wetenschappen van de Katholieke Universiteit Nijmegen (prof. dr. J.A. Jansen). Het onderzoek resulteerde in dit proefschrift. De studies werden uitgevoerd in samenwerking met de vakgroep Celbiologie en Histologie (prof. dr. L.A. Ginsel), en werden gesubsidieerd door de Nederlandse Organisatie voor Wetenschappelijk Onderzoek (NWO). Tijdens de onderzoeksperiode werden geregeld presentaties verzorgd op diverse binnenlandse en buitenlandse congressen, onder andere twee maal op de *Annual Meeting of the Society for Biomaterials*. Dit werd mede mogelijk gemaakt door een aan hem toegekende subsidie in het kader van het Van Walree Fonds. Daarnaast werd een werkbezoek van enkele weken gebracht aan het Centre for Cell Engineering (prof. dr. A.S.G. Curtis), van de Universiteit van Glasgow, UK. Momenteel is hij werkzaam als onderzoeker ('post-doc') op de afdeling Biomaterialen.

